

WestminsterResearch

<http://www.westminster.ac.uk/westminsterresearch>

**Investigation of the Effect of Static Magnetic Field on Production
of Industrially Viable Microbial Products**

Mohtasham, P.

This is an electronic version of a PhD thesis awarded by the University of Westminster.
© Miss Parya Mohtasham, 2017.

The WestminsterResearch online digital archive at the University of Westminster aims to make the research output of the University available to a wider audience. Copyright and Moral Rights remain with the authors and/or copyright owners.

Whilst further distribution of specific materials from within this archive is forbidden, you may freely distribute the URL of WestminsterResearch: (<http://westminsterresearch.wmin.ac.uk/>).

In case of abuse or copyright appearing without permission e-mail repository@westminster.ac.uk

Investigation of the Effect of Static Magnetic Field
on Production of Industrially Viable Microbial
Products

Parya Mohtasham

A thesis submitted in partial fulfilment of the requirements
of the University of Westminster for the degree of Doctor
of Philosophy

September 2017

ABSTRACT

Static magnetic field (MF) has a range of applications in pharmaceutical and biotechnology industries from medical devices and tissue engineering to wastewater treatment. The effect of MF on microbial cultures has been investigated by some researchers. However, the findings have been inconsistent. Extensive, systematic and comprehensive investigations are needed before potential application of MF in the industry.

The aim of this research was to investigate the effect of MF on Gram-positive and Gram-negative bacterial strains for production of industrially viable products. To this end, an MF generator (MFG) was coupled with small-scale 100 mL shaken flasks (SFs) and bench-top 2 L stirred tank bioreactors (STRs). The effect of MF on two Gram-positive (*Bacillus licheniformis* NCIMB 8874 and *Bacillus subtilis* NCTC 3610) and one Gram-negative (*Pseudomonas putida* KT2440) bacterial strains was investigated with focus on production of two industrially viable products (bacitracin A and polyhydroxybutyrate (P(3HB))). P(3HB) was chosen as a valuable product of recent interest, produced by both Gram-negative and Gram-positive bacteria, making it a good candidate for this research. Bacitracin A was chosen as a model antibiotic produced by *B. licheniformis*.

Experiments were carried out in SF cultures of *B. licheniformis* with circulation rate of 10 mL. min⁻¹ through MFG producing 28 mT static MF. While there was no notable difference in the specific growth rate between the test and the control cultures, a decrease in the highest concentration of bacitracin A by 23% was observed. Subsequently, the experiment was extended to 2 L STRs with the same circulation rate (10 mL. min⁻¹), but at two MF intensities of 28 mT and 10 mT. The former, showed no notable effect on bacitracin A production or cell growth. The latter experiment, however, resulted in 27% increase in the highest bacitracin A concentration. As bacitracin A concentration in the culture medium started to decrease due to unfavourable alkaline conditions, the next fermentation was carried out under pH control at 6-7. In this fermentation, bacitracin A concentration continued to increase in both MF exposed and control cultures without a notable difference between the two. However, substrate uptake, growth profile and total carbohydrate concentrations changed considerably. These changes suggest a shift in cellular metabolism leading possibly to biosynthesis of other products including extracellular polymeric substances.

The STR system was then coupled with MFG of 18 and 28 mT intensities at a circulation rate of 10 mL. min⁻¹, and used for production of P(3HB) by *B. subtilis* and *P. putida*. Neither of the two MF intensities led to any considerable changes in growth profile, cell morphology or P(3HB) production in *B. subtilis* STR system. On the other hand, a considerable change in morphology was observed in *P. putida* cultures. Also, P(3HB) concentration in the culture exposed to MF increased by 15% under 18 mT and by 29% under 28 mT. These novel findings suggest a great scope for further investigations of this system for potential industrial applications.

Contents

List of Figures	v
List of Tables.....	xi
1. Introduction.....	2
1.1. Bacteria.....	2
1.1.1. <i>Bacillus spp. and their applications</i>	4
1.1.1. <i>Pseudomonas spp. and their applications</i>	8
1.2. Bacterial products	9
1.2.1. <i>Plastics</i>	10
1.2.2. <i>Biopolymers</i>	11
1.2.3. <i>Bacitracin</i>	17
1.3. Magnetic field	20
1.3.1. <i>Use of Magnetic field in biotechnology and biomedical sciences</i>	22
1.3.2. <i>Effect of magnetic field on microorganisms</i>	24
1.4. Hypothesis	34
1.5. Aim.....	34
1.6. Objectives	34
2. Materials and Methods	37
2.1. Materials.....	38
2.1.1. <i>Chemicals</i>	38
2.1.2. <i>Microorganisms</i>	42
2.1.3. <i>Equipment</i>	42
2.2. Methods	46
2.2.1. <i>Maintenance and preparations</i>	46
2.2.2. <i>Processes</i>	48
2.2.3. <i>Procedures</i>	52
2.2.4. <i>Calculations</i>	58
3. Results.....	63
3.1. Studies on the effect of magnetic field on <i>Bacillus licheniformis</i>	66
3.1.1. <i>SF fermentation of B. licheniformis with 28 mT magnetic field</i>	66
3.1.2. <i>STR Batch fermentation of B. licheniformis with 28 mT magnetic field</i>	73

3.1.3.	<i>STR Batch Fermentation of B. licheniformis with 10 mT magnetic field</i>	80
3.1.4.	<i>STR Batch Fermentation of B. licheniformis with 10 mT magnetic field and pH control</i>	85
3.2.	Studies on the effect of magnetic field on <i>Bacillus Subtilis</i>	95
3.2.1.	<i>STR Batch fermentation of B. subtilis with magnetic field intensity of 18 mT</i>	96
3.2.2.	<i>STR Batch fermentation of B. subtilis with magnetic field intensity of 28 mT</i>	101
3.3.	Studies on the effect of magnetic field on <i>Pseudomonas putida</i>	107
3.3.1.	<i>STR Batch fermentation of P. putida with magnetic field intensity of 18 mT</i>	107
3.3.2.	<i>STR Batch fermentation of P. putida with magnetic field intensity of 28 mT</i>	114
4.	Discussion	123
4.1.	Effect of magnetic field on <i>Bacillus licheniformis</i> NCIMB 8874	124
4.1.1.	<i>Effect of magnetic field on growth profile of B. licheniformis</i>	125
4.1.2.	<i>Effect of magnetic field on morphology of B. licheniformis</i>	128
4.1.3.	<i>Effect of magnetic field on substrate uptake of B. licheniformis</i>	128
4.1.4.	<i>Effect of magnetic field on bacitracin production</i>	131
4.2.	Effect of magnetic field on <i>Bacillus subtilis</i> NCTC 3610	137
4.2.1.	<i>Effect of magnetic field on cell growth and morphology of B. subtilis</i>	138
4.2.2.	<i>Effect of magnetic field on P(3HB) production</i>	139
4.2.3.	<i>Confirmation of chemical structure of P(3HB)</i>	140
4.3.	Effect of magnetic field on <i>Pseudomonas putida</i> KT 2440	142
4.3.1.	<i>Effect of magnetic field on cell morphology of P. putida KT 2440</i>	143
4.3.2.	<i>Effect of magnetic field on cell growth and P(3HB) production</i>	144
5.	Conclusion	150
5.1.	Investigation of the effect of magnetic field on <i>Bacillus licheniformis</i> NCIMB8874	150

5.2.	Investigation of the effect of magnetic field on <i>Bacillus subtilis</i> NCTC 3610.....	151
5.3.	Investigation of the effect of magnetic field on <i>P. putida</i> KT2440....	151
6.	Future Work.....	154
6.1.	Short term future work focus recommendations.....	154
6.1.1.	<i>Different intensities of MF</i>	155
6.1.2.	<i>Different types of MF</i>	155
6.1.3.	<i>Different circulation rates through the MFG</i>	155
6.2.	Long term future work recommendations.....	155
6.2.1.	<i>Investigation of the effect of MF on product structure</i>	157
6.2.2.	<i>Investigation of the effect of MF on cells at a steady state physiological condition</i>	157
6.2.3.	<i>Investigation of the effect of MF on diauxic growth, protein secretion and EPS composition</i>	157
6.2.4.	<i>Investigation of the effect of MF on ionic channels of cell membrane</i>	158
6.2.5.	<i>Investigation of the effect of MF on production of by-products.</i>	158
7.	References	160
8.	Appendices	180
8.1.	Appendix 1	180
8.1.1.	<i>Bacitracin concentration standard curve</i>	180
8.1.2.	<i>P(3HB) concentration standard curve</i>	181
8.1.3.	<i>Glutamic acid assay calibration curve</i>	181
8.1.4.	<i>Total carbohydrate concentration calibration curve</i>	182
8.1.5.	<i>Glucose concentration of glucose assay calibration curve</i>	182
8.1.6.	<i>Flow rate calibration curve of peristaltic pump</i>	183
8.2.	Appendix 2	183
8.3.	Appendix 3	184

List of Figures

Figure 1. Schematic diagram of A) Gram-negative and B) Gram-positive bacterial structures (Bhat et al., 2012)	3
Figure 2. Plastics consumption in the UK by application, reprinted from (British plastics federation, 2016).....	10
Figure 3. PHB production process (Varsha and Savitha, 2011).....	15
Figure 4. Bacitracin A structure. Arrows show C-N bonds. Thiazole ring is formed from L-isoleucine and L-cysteine and the cyclic heptapeptide ring is formed by the amino group of L-lysine reaction with the β -carboxyl group of D-asparagine (Stone and Strominger, 1971)	18
Figure 5. Classical demonstration of iron fillings around a bar magnet.....	20
Figure 6. Examples of medical devices that utilize permanent magnets for operation include: (A) a magnetic retraction and triangulation device for single-port laparoscopic surgery, (B) a laparoscopic tissue retractor, (C) a magnetic camera system for single-port laparoscopic surgery, (D) magnetic tilt control for a laparoscopic camera, (E) a remotely triggered capsule for controlled colonic insufflation, (F) a magnetic field-guided capsule endoscope control system for navigation in the gastrointestinal tract, (G) a magnetic air capsule robotic system for colonoscopy , (H) a magnetically controlled compliant capsule endoscope with a magnetically actuated drug delivery mechanism and (I) a magnetic sphincter for treatment of gastroesophageal reflux disease. Reprinted from (Sliker et al., 2015).....	23
Figure 7. Schematic presentation of MFG setup used by Alvarez et. al (2006). (1) STR, (2) <i>Lactococcus lactis</i> cell suspension, (3) three-way valve, (4) peristaltic pump, (5) Stainless steel tube, (6) MFG. Reprinted from (Alvarez et al., 2006).....	25
Figure 8. Schematic presentation of MFG setup used by Perez et. al (2007). (1) STR, (2) <i>S. cerevisiae</i> cell suspension, (3) three-way valve, (4) peristaltic pump, (5) solenoid coupled with current source of 2 A, (6) stainless steel tube, (7) main MFG. Reprinted from (Perez et al., 2007)	26

Figure 9. Schematic of the magnetic device system used in the study of effect of MF on <i>A. niger</i> for production of citric acid and cellulase (reprinted from Gao et al., 2011).....	27
Figure 10. Schematic design of MFG.....	44
Figure 11. Schematic design of MFG coupled with bioreactor process system	44
Figure 12. Complete process set-ups. The test shaken flask (back) is attached to the MFG, with circulation of microbial culture via the pump. The control shaken flask (front) is attached to a peristaltic pump to mimic the effects of outside circulation.....	50
Figure 13. Complete process set-ups. The test bioreactor (right) is attached to the MFG, with circulation of microbial culture via the pump. The control bioreactor (on the left) is attached to a peristaltic pump to mimic the effects of outside circulation.....	52
Figure 14. Growth profile of <i>B. licheniformis</i> in shaken flasks. The test was exposed to 28 mT MF.....	67
Figure 15. Logarithmic scale growth profile of <i>B. licheniformis</i> in shaken flasks. The test was exposed to 28 mT MF.....	67
Figure 16. pH profile of <i>B. licheniformis</i> in 20 mL SFs. The test was exposed to 28 mT MF	68
Figure 17. Bacitracin profile of <i>B.licheniformis</i> in 20 mL SFs based on average of three repeats. The test was exposed to 28 mT MF.....	69
Figure 18. Glutamic acid consumption profile of <i>B. licheniformis</i> in 20 mL SFs. The test was exposed to 28 mT	71
Figure 19. Total carbohydrate concentration of <i>B. licheniformis</i> in 20 mL SFs. The test was exposed to 28 mT.....	72
Figure 20. Growth profile of <i>B. licheniformis</i> in 2 L STRs. The test was exposed to 28 mT MF	74
Figure 21. Growth profile of <i>B. licheniformis</i> in 2 L fermenters in logarithmic The test was exposed to 28 mT MF.....	74
Figure 22. pH profile of the two STRs of <i>B. licheniformis</i> in 2 L STRs. The test was exposed to 28 mT MF	76
Figure 23. Bacitracin production profile of <i>B. licheniformis</i> in 2 L STRs. The test was exposed to 28 mT MF	77

Figure 24. Glutamic acid concentration profile of <i>B. licheniformis</i> in 2 L STRs. The test was exposed to 28 mT MF.....	78
Figure 25. Carbohydrate production profile of <i>B. licheniformis</i> in 2 L STRs. The test was exposed to 28 mT MF.....	79
Figure 26. SEM images of a) the control and b) the test (exposed to 28 mT MF) samples of <i>B. licheniformis</i> in 2 L STRs with 60k magnification. The images were taken from samples after 64 h of incubation.....	79
Figure 27. Growth profile of <i>B. licheniformis</i> in 2 L STRs. The test was exposed to 10 mT MF.....	81
Figure 28. Logarithmic scale growth profile of <i>B. licheniformis</i> in 2 L STRs. The control and the test with outside circulation and 10 mT MF are shown.	81
Figure 29. pH values of the cultures during the fermentation of <i>B. licheniformis</i> in 2 L STRs. The control and the test under 10 mT MF are shown.	82
Figure 30. Bacitracin concentration of <i>B. licheniformis</i> culture in 2 L STRs. The control and the test under 10 mT MF are shown.	83
Figure 31. Glutamic acid concentration profile of <i>B. licheniformis</i> in 2 L STRs. The test was exposed to 10 mT MF.....	84
Figure 32. Total carbohydrate concentration profile in 2 L STRs including control and test STR exposed to 10 mT MF.....	85
Figure 33. Growth profile of <i>B. licheniformis</i> in 2 L STRs with controlled pH. The test was exposed to 10 mT MF.....	86
Figure 34. Logarithmic scale growth profile of <i>B. licheniformis</i> in 2 L STRs with controlled pH. The test was exposed to 10 mT MF.....	87
Figure 35. pH profile of <i>B. licheniformis</i> culture in 2 L STRs with controlled pH. The test was exposed to 10 mT MF.....	89
Figure 36. Bacitracin production profile of <i>B. licheniformis</i> in pH-controlled STRs. The test STR was exposed to 10 mT MF.....	90
Figure 37. Glutamic acid concentration in the culture medium of <i>B. licheniformis</i> in 2 L STRs with controlled pH. The test was exposed to 10 mT MF.....	91
Figure 38. Total carbohydrate concentration profile in pH-controlled STRs of <i>B. licheniformis</i> with 10 mT MF exposure of the test STR.	92

Figure 39. SEM images of <i>B. licheniformis</i> cells at the end of 2 L STR runs with pH control below 7. a) <i>B. licheniformis</i> cells in the control STR with 60K (top image) and 30K (bottom image) magnifications. b) <i>B. licheniformis</i> cells in the test STR under 10 mT magnetic field with 60k (top image) and 30k (bottom image). Arrows indicate the morphology changes to cells.	95
Figure 40. Growth profile of <i>B. subtilis</i> in the two 2 L STRs with test under 18 mT MF.	97
Figure 41. Growth profile of <i>B. subtilis</i> in 2 L bioreactors in logarithmic scale with test under 18 mT MF	98
Figure 42. Microscopic image of <i>B. subtilis</i> culture taken from the control STR under 10 X magnification. The P(3HB) present as inclusion bodies inside the cells, were observed by their fluorescence. Arrows indicate these inclusion bodies.	99
Figure 43. FTIR results of the control and the test P(3HB) from <i>B. subtilis</i> under 18 mT MF. Chemical structure of the polymer in both gave the same peaks. This confirms the structural similarity of the product between the two reactors.....	100
Figure 44. P(3HB) concentration change in <i>B. subtilis</i> STRs throughout the fermentation period in 2 L STRs with the test under 18 mT MF.....	100
Figure 45. Growth profile of <i>B. subtilis</i> in 2 L STRs. The control and the test under 28 mT MF are shown.....	102
Figure 46. Growth profile of <i>B. subtilis</i> in two 2 L STRs in logarithmic scale. The control and the test under 28 mT are shown	102
Figure 47. SEM images of <i>B. subtilis</i> cells. a) <i>B. subtilis</i> cells in the control STR with 60K (top image) and 30K (bottom image) magnifications. b) <i>B. subtilis</i> cells in the test STR exposed to 28 mT MF) with 60k (top image) and 30k (bottom image).....	104
Figure 48. Microscopic image of <i>B. subtilis</i> in the control STR. P(3HB) present as inclusion bodies inside the cells was observed by fluorescence. The arrow indicates some of these inclusion bodies. ...	105
Figure 49. FTIR results of the control and the test P(3HB) by <i>B. subtilis</i> under 28 mT MF. Chemical structure of the polymer in both gave the same	

peaks. This confirms the structural similarity of the product between the two reactors.	106
Figure 50. Concentration of P(3HB) during 2 L STR fermentation of <i>B. subtilis</i> with the test under 28 mT MF	106
Figure 51. Growth profile of <i>P. putida</i> in 2 L STRs. The test was exposed to 18 mT MF	108
Figure 52. Growth profile of <i>P. putida</i> in 2 L STRs on logarithmic scale. The test was exposed to 18 mT MF.....	109
Figure 53. SEM images of cultures of <i>P. putida</i> (a) Control and (b) Test (18 mT). Top images were taken at 60k magnification; bottom images were taken at 30k magnification. Arrows on (a) images indicate web formation and the chain-like organisation of the cells. Arrows on the right images indicate morphological changes to the control culture's cells. Arrows on (b) images indicate the de-shaped cells of the test.....	110
Figure 54. Image visualisation of <i>P. putida</i> cells containing P(3HB). These cells were stained with Nile red and visualised under fluorescence microscope. P(3HB) retains the Nile red colour, which was then observed under the microscope with 10 x magnification. Arrow indicates a floc of cells with inclusion bodies of P(3HB).....	111
Figure 55. FTIR results of the control and the test (18 mT) PHAs from <i>P. putida</i> STR cultures. Chemical structure of the polymer in both gave the same peaks. This confirms the structural similarity of the product between the two reactors.....	112
Figure 56. P(3HB) concentration profile during fermentation of <i>P. putida</i> under 18 mT magnetic field	113
Figure 57. Glucose consumption profile in the control and test cultures of <i>P. putida</i> in 2 L STRs. The test was exposed to 18 mT MF	114
Figure 58. Growth profile of <i>P. putida</i> in 2 L STRs under 28 mT MF	115
Figure 59. Growth profile of <i>P. putida</i> in 2 L STRs under 28 mT magnetic field on logarithmic scale.....	116
Figure 60. SEM images of samples of a: Control; b: The test culture of <i>P. putida</i> with 28 mT MF taken after 98 h of incubation. Top images were taken at 60k magnification; bottom images were taken at 30k magnification. Arrows indicate the de-shaped cells.	117

Figure 61. Sudan Black test on diluted samples (2×10^7 fold) of the control and the test (28 mT MF) STRs of <i>P. putida</i> . Arrows indicate the colonies containing P(3HB), which retained the black stain.....	118
Figure 62. Confirmation of type of P(3HB) produced by <i>P. putida</i> in 2 L STRs . The test was exposed to 28 mT magnetic field.....	119
Figure 63. P(3HB) concentration profile at different time points of fermentation of <i>P. putida</i> in 2 L STRs . The test was exposed to 28 mT magnetic field.....	119
Figure 64. Glucose consumption of by <i>P. putida</i> in 2 L STRs. The test was exposed to 28 mT magnetic field	120
Figure 65. Molecular structure of P(3HB).....	141
Figure 66. FTIR peaks obtained from STR 4	142
Figure 67. FTIR peaks obtained from STR 5	142
Figure 68. Growth profiles of the controls in STR 6 and STR 7	145
Figure 69. Growth profiles of the MF-exposed cultures in STR 6 and STR 7	146
Figure 70. Standard bacitracin concentration against peak area obtained from HPLC used for measurement of bacitracin concentration in <i>B. licheniformis</i> experiments	180
Figure 71. Standard curve obtained from crotonic acid assay on P(3HB) standards	181
Figure 72. Glutamic acid assay standard curve. The curve was obtained from absorbance reading of assayed glutamic acid standards at 570 nm. .	181
Figure 73. Total carbohydrate assay standard curve. The curve was obtained by reading absorbance of assayed glucose standards at 490 nm	182
Figure 74. Standard glucose concentration against peak area obtained from HPLC used for measurement of bacitracin concentration in <i>B. licheniformis</i> experiments	182
Figure 75. Calibration curve for flow rate of liquid circulation through the MFG	183
Figure 76. Growth profile of <i>B. licheniformis</i> in a 2 L STR without outside circulation.....	183
Figure 77. Growth profile of <i>Pseudomonas putida</i> 2 L STRs. The control and the test STR under 28 mT magnetic field are shown. Data points are	

average values of biological replicate runs with error bars showing standard deviations.....	184
--	-----

List of Tables

Table 1. Manufacturers and the microorganisms, raw materials used for the production of biodegradable plastics taken from (Wong et al., 2016). ...	16
Table 2. Summary of available literature on the effect of magnetic field on microorganisms	29
Table 3. Summary of materials and methods chapter.....	37
Table 4. Nutrient agar composition and concentration.....	39
Table 5. Nutrient broth composition and concentration.....	39
Table 6. M20 composition and concentration	39
Table 7. MGM composition and concentration.....	40
Table 8. Modified E2 medium composition and concentrations	40
Table 9. Composition and concentration of ninhydrin solution used for glutamic acid assay.....	41
Table 10. An outline of the results presented in this thesis	65
Table 11. Percentage differences of growth rate and doubling time between the test (exposed to 28 mT MF) and the control SFs.....	68
Table 12. Summary of bacitracin production rate of <i>B. licheniformis</i> in SFs at various stages of the runs. The test culture was exposed to 28 mT MF	69
Table 13. Bacitracin yield of <i>B. licheniformis</i> in 20 mL SFs. The test was exposed to 28 mT MF	70
Table 14. Summary of total carbohydrate production rates at two stages of growth of <i>B. licheniformis</i> in 20 mL SFs. The test was exposed to 28 mT	72
Table 15. Growth rate and doubling time of <i>B. licheniformis</i> in 2 L STRs. The test was exposed to 28 mT MF	75
Table 16. Colony forming unit counts in the samples taken from the two STRs of <i>B. licheniformis</i> in 2 L STRs. The test was exposed to 28 mT MF	75
Table 17. Bacitracin production rates of <i>B. licheniformis</i> in 2 L STRs. The test was exposed to 28 mT MF.....	77

Table 18. Summary of bacitracin production rate in Control and test (10 mT MF) 2 L STR cultures of <i>B. licheniformis</i>	83
Table 19. Percentage differences of doubling time and maximum growth rate between the control and the test cultures of <i>B. licheniformis</i> in 2 L STRs with controlled pH. The test was exposed to 10 mT MF	87
Table 20. Colony forming unit counts in the samples taken from the two 2 L STRs of <i>B. licheniformis</i> with controlled pH. The test was exposed to 10 mT MF	88
Table 21. Bacitracin production rate in the two pH-controlled 2 L STRs after the application of 10 mT MF (16-84 h).....	90
Table 22. Glutamic acid consumption rate in the pH-controlled 2 L STRs of <i>B. licheniformis</i> with 10 mT MF exposure of the test STR.	92
Table 23. Total carbohydrate production rate in <i>B. licheniformis</i> 2 L STRs after the first logarithmic stage. The test was exposed to 10 mT MF.	93
Table 24. Colony counts in the Control and the Test STRs of <i>B. subtilis</i> under 18 mT MF	98
Table 25. mg P(3HB)/g CDW in the control and test (18 mT) STRs of <i>B. subtilis</i>	101
Table 26. mg P(3HB)/g CDW in 2 L STRs of <i>B. subtilis</i> under 28 mT MF .	103
Table 27. Colony count of <i>B. subtilis</i> in 2 L STRs with test under 28 mT MF	103
Table 28. CFU percentage change at different time points after the application of 18 mT magnetic field to 2 L STR of <i>P. putida</i>	109
Table 29. P(3HB) production rate at different time intervals in <i>P. putida</i> 2 L STRs. The test was exposed to 18 mT MF	113
Table 30. Colony Forming Units per mL of <i>P. putida</i> culture in 2 L STRs. The test was exposed to 28 mT magnetic field	116
Table 31. P(3HB) concentration and the percentage difference between the control and the test STRs of <i>P. putida</i> under 28 mT MF at different time points	120
Table 32. Glucose consumption rate between different time points in <i>P. putida</i> cultures in 2 L STRs . The test was exposed to 28 mT magnetic field	121
Table 33. Specification of designs used for studies on the effect of magnetic field on <i>B. licheniformis</i>	124

Table 34. Doubling time of <i>B. licheniformis</i> in the experiments carried out in this research	125
Table 35. Summary of glutamic acid consumption rates in <i>B. licheniformis</i> experiments	130
Table 36. Specification of designs used for studies on the effect of magnetic field on <i>B. subtilis</i>	138
Table 37- doubling time of <i>B. subtilis</i> in STR 18 and STR 28 cultures.....	139
Table 38. Maximum P(3HB) content in STR cultures of <i>B. subtilis</i>	140
Table 39. FTIR expected readings for different functional groups and results obtained from the control and the test STR 4 and STR 5	141
Table 40. Specification of designs used for studies on the effect of magnetic field on <i>P. putida</i> KT 2440.....	143
Table 41. Doubling time of <i>P. putida</i> in STR 6 and STR 7 cultures.....	144
Table 42. Maximum P(3HB) concentrations in STR 6 and STR 7 systems	147

Chapter 1

Introduction

1. Introduction

1.1. Bacteria

Bacteria are unicellular microorganisms, which encompass a wide domain of prokaryotes. The bacterial cell has different shapes (i.e. spherical (cocci), rod-shape (bacilli) and spiral (spirilla); is few (0.5-5) micrometre in length and is covered by a cell wall. The shape and size of a bacterium is regarded as its morphology (Cabeen and Jacobs-Wagner, 2005). The cell morphology depends on the cell wall and affects bacterial behaviour and abilities such as nutrient intake, cell division rate, surface adherence, swimming in aqueous environments, shear resistance, biofilm formation, and so many more of bacterial functionalities (Young, 2006).

Bacteria are ubiquitous in nature and are inhabitants of a wide range of environments from soil and water to acidic high temperature climates and radioactive waste material. They also reside in/on other living organisms' bodies including plants, animals and humans.

Bacterial cell comprises of a cell envelope, which contains cell membrane and cell wall. Bacterial cell wall is made up of peptidoglycan (a polymer of polysaccharide and peptides which forms a 3-D mesh layer) (van Heijenoort, 2001).

Based on their cell-wall structures, bacterial cells are classified into two major categories; Gram-positive and Gram-negative. This terminology comes from the reaction of cells to the stain introduced by Danish bacteriologist Hans Christian Gram (Gram and Friedlaender, 1884). Fig. 1 shows the different structures of the two bacterial cell types.

Gram-positive bacteria consist of a single membrane covered by a thick, rigid peptidoglycan matrix (cell wall). They have a smaller volume of periplasm compared to Gram-negative bacteria (Madigan and Martinko, 2005). This type of bacteria retains the crystal violet dye used in Gram's method and when observed under a microscope, present a violet colour. Some Gram-positive

species include: *Bacillus* spp., *staphylococcus* spp., *Streptomyces*, *Clostridium* spp. and *Lactobacillus* spp.

Gram-negative bacteria consist of a thin peptidoglycan matrix (cell wall) placed between an inner (cytoplasmic) membrane and an outer cell membrane. The outer membrane consists of lipopolysaccharides and phospholipids. The space between the outer and cytoplasmic membranes in Gram-negative bacteria is filled with periplasm (Silhavy, 2016).

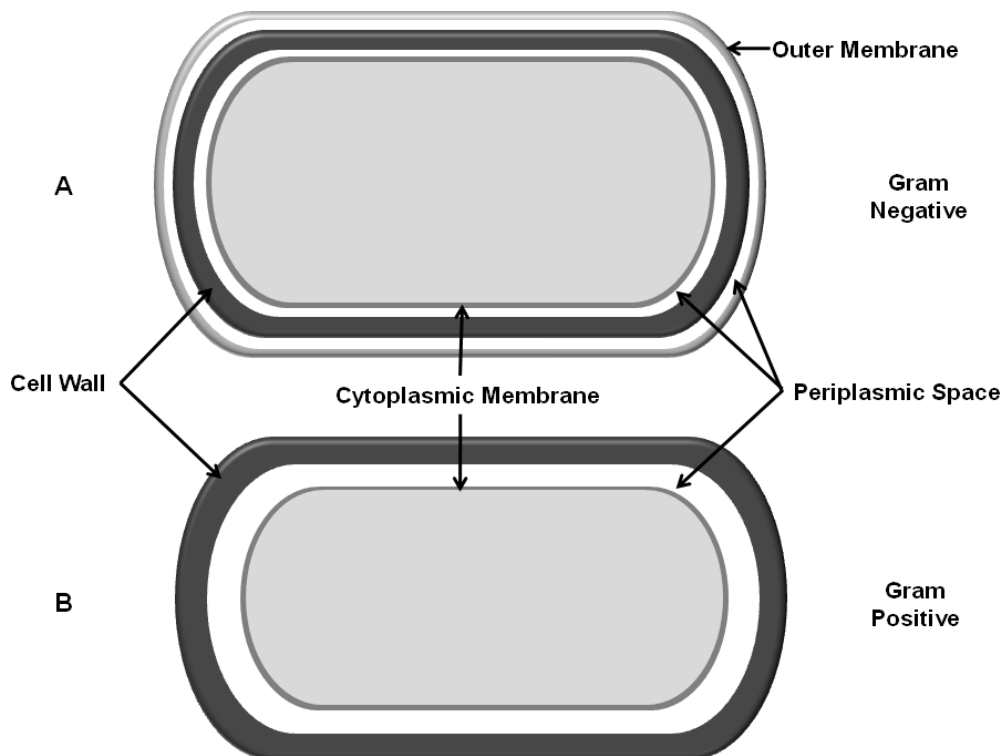


Figure 1. Schematic diagram of A) Gram-negative and B) Gram-positive bacterial structures (Bhat et al., 2012)

The outer membrane (OM) of Gram-negative bacteria is a bilayer of proteins. The inner layer of the outer membrane, consists of phospholipids similar to those in plasma membrane. The outer layer on the other hand, is formed by an amphiphilic molecule composed of lipopolysaccharide. This membrane, with a pore-like structure, acts as a barrier to the extracellular environment. The OM pore-like structural constituents through which the most nutrient uptake is accomplished, are called porins. Porins provide Gram-negative bacteria with a selective porous ability to block large charged toxic components and chemicals, helping with cell survival (Wiener and Horanyi, 2011).

Gram-negative bacteria do not retain the violet stain used in Gram's method and when counter washed with safranin, obtain a pink colour visible under a microscope. Some examples of Gram-negative bacteria include *Escherichia coli*, *Cyanobacteria*, *Pseudomonas* spp., *Chlamydia*, *salmonella* and *Helicobacter*.

In this study, a Gram-positive (*Bacillus subtilis* and *Bacillus licheniformis*) and a Gram-negative (*Pseudomonas putida*) bacterial species were used as model microorganisms in order to investigate the effect of magnetic field on bacterial cultures. These microorganisms were chosen due to their widespread availability in nature, extensive use in biotechnology industry and comprehensive information available on their mechanisms and metabolic activities. The experiments carried out here focus on two commercially viable products of these strains (Bacitracin and polyhydroxyalkanoates), as model target microbial products in order to investigate the effect of magnetic fields in a novel operation for production of the mentioned desirable industrial products.

1.1.1. *Bacillus* spp. and their applications

Bacillus spp. are Gram positive, rod shaped bacteria that belong to the Bacilli family consisting of different strains with numerous physio-chemical characteristics. The genera include more than 60 types of species differing in their genomic sequence and characteristics (Priest, 1993). They are endospore forming, aerobic or facultatively anaerobic. The genus is low in G+C content and consists of a variety of DNA and major amino acid compositions. *Bacillus* spp. are robust and can survive extreme environmental conditions. Endospores can resist extreme temperature changes, radiation, pH changes and many antibiotics. These species are characterised by their morphology and biochemical properties. Due to their robust nature, *Bacillus* spp. can be grown in different media compositions and a range of carbon and nitrogen sources.

These species are ubiquitous and are found in soil, water and airborne dust. They are the predominant bacteria present in soil and growing plants and

foods. They can compete with other microorganisms due to their antibacterial and antagonistic metabolites. Also, their robust nature (survival at extreme pH and temperature conditions) gives them an advantage over other microorganism (Amin et al., 2015)

Bacillus spp. are straight rods with round or square ends and usually appear as chains or pairs. Cells are usually between 0.5-1.2 µm by 2.5-10.0 µm depending on the strain. *Bacillus* colonies have different shapes depending on the strain and vary from large to very large in size, grey or white in colour, and dry or wet looking. Although several species of the genus are non-motile, most *Bacillus* species including *Bacillus subtilis* group are motile by peritrichous flagella (Doyle, 1989). *Bacillus* endospores have an oval, cylindrical or kidney shape depending on the strain. Each cell produces only one spore, which is located either in the centre of the cell (central), at the cell end (terminal), or close to the cell end (sub terminal) (Mehrotra, 2009).

Due to their resistant spores, *Bacillus* spp. create contamination problems in sterilisation processes and are key contaminants in food and agricultural industries (Baron, 1996a). *Bacillus* spp. include pathogenic and beneficial types; the pathogenic type includes only a minority of the genus. The cause of anthrax, *Bacillus anthracis*, is the only obligate pathogenic *Bacillus*, which causes the disease in livestock (Bauman, 2012). Other species of *Bacillus* that can cause infection in humans are *B. cereus*, *B. sphaericus*, *B. alvei*, *B. laterosporus*, *B. megaterium*, and *B. pumilus*. Some types such as *B. larvae*, *B. lentimorbus*, *B. popilliae*, *B. sphaericus*, and *B. thuringiensis* are pathogens of specific groups of insects (Baron, 1996a). *B. cereus* is the cause of the common fried rice syndrome, a foodborne disease to humans. Kefeli and Blum (2010) have identified *B. anthracis* and *B. cereus* as medically significant *Bacillus* spp. (Kefeli and Blum, 2010).

The beneficial types of *Bacillus* spp. are within the group of generally regarded as safe (GRAS) microorganisms by the Food and Drug Administration (FDA). This type of *Bacillus* spp. is comprised of two groups. One group of these species are used for studying bacterial cellular differentiation due to the

resistance of their spores against detergents and antibiotics (Zhang, 2011). Another group of important *Bacillus* spp. produce industrially viable metabolites. They are well known producers of different enzymes such as proteases for production of detergents and amylases for the starch industry. These species produce almost 60% of commercial enzymes. Most of these enzymes are homologous extracellular products released into the culture medium. *Bacillus* spp. are also used to produce antibiotics such as bacitracin, polymyxin and other industrially important products (Westers et al., 2004). *Bacillus* strains are also used to produce nucleotides, vitamin riboflavin and poly- γ -glutamic acid (Schallmey et al., 2004). They are also capable of producing fine chemicals in biotechnology such as carotenoid pigments and a range of biopolymers (e.g. poly glutamic acid, lactic acid, polyhydroxyalkanoates (PHAs), etc.) (Raddadi et al., 2012).

Bacillus subtilis, *Bacillus amyloliquefaciens* and *Bacillus licheniformis* are considered as bacterial super-secreting cell factories, since they have the capacity to secrete industrially important products including proteins in concentrations in ranges of gram per litre and non-toxic fermentation by-products (van Dijn and Hecker, 2013).

Bacillus subtilis (most strains) is harmless to humans, ubiquitous in natural habitats (upper layers of soil) and has a high capacity for producing enzymes used in detergents and food industry such as amylases, proteases and pesticides, and is also used in bioremediation and leather industries. Since they can produce these industrial products in high yields and in different ranges of substrates, and the fact that they secrete these enzymes into the culture medium, their fermentation process and downstream processing of the substrate tends to be cheap and makes them cost-effective strains for use in the mentioned industries. *B. subtilis* has been the most investigated Gram-positive bacteria in the industry, the main reason being its simple developmental programs and its high potential for genetic engineering and large-scale fermentation. It is used to study bacterium chromosome replication and cell differentiation (van Dijn and Hecker, 2013). It is also used as

sterilisation “indicator organism” for sterilisation checks in pharmaceuticals (The International Pharmacopoeia, Sixth Edition, 2016).

Other uses of *B. subtilis* include its application in gastrointestinal disorder therapy in the healthcare industry (Angioi et al., 1995; Green et al., 1999), speeding the growth of corn, improving biomass yields in agriculture (Sharaf-Eldin et al., 2008) and production of natural biopolymers, polyhydroxyalkanoates (PHAs) in biotechnology. *B. subtilis* includes two sub species: *B. subtilis* subsp. *Subtilis* and *B. subtilis* subsp. *Spizizenii*; with the latter being a natural producer of PHAs (Singh et al., 2009). Most of the PHA produced by these species is poly (3-hydroxybutyrate) (Keshavarz and Roy, 2010).

Bacillus licheniformis is another strain of *Bacillus* spp. found in soil and on bird feathers. *B. licheniformis* is a facultative anaerobe and can survive a wider range of environmental conditions than the obligate aerobe *B. subtilis* (Baron, 1996a). It is a mesophilic bacterium and is one of the bacterial enzyme producing factories used in the biotechnology industry (Parrado et al., 2014). *B. licheniformis* is used to produce alkaline serine proteases in high yields (Schallmey et al., 2004). Proteases produced by *B. licheniformis* are also used for dehairing and batting in the leather industry (Nadeem et al., 2010). Alpha-amylases are the other enzymes produced by *B. licheniformis* in large quantities through fermentation. They are used as desizing agents of textiles and for starch modification for sizing of paper (Souza, 2010). They are also used as bio-fungicide agents for treating plant fungal infections such as those causing leaf spot and blight diseases (Drahos and West, 2004; Mitoi et al., 2012). Another industrial use of *B. licheniformis* is the production of important biosurfactants such as lichenisin; and since it is considered as a probiotic strain, it is also used in food and veterinary feed stock industries (Madslien et al., 2013). Other industrial products of *B. licheniformis* include antimicrobial agents such as licheniformin and polypeptide antibiotic bacitracin. This bacterium is also reported amongst PHA-producing strains of *Bacillus* spp. (Shamala et al., 2003). It has been reported to have high PHA yield of 64-68% of CDW (Sangkharak and Prasertsan, 2013).

1.1.1. *Pseudomonas* spp. and their applications

Pseudomonas spp. are Gram-negative, rod-shaped bacteria belonging to Pseudomonad family consisting of numerous physio-chemical characteristics. The genera include over 150 species differing in their metabolic activities and genomic sequences. They do not form spores and are mostly strictly aerobic, except for a few anaerobic cells which use denitrification process as means of respiration and energy production. These species have motile cells with one or more polar flagella (Mandel, 1966; Stanier et al., 1966).

Like *Bacillus* spp. *Pseudomonas* spp. are abundant in nature due to their versatility. They inhabit in soil, water and living organisms such as plants and animals. Most species of the genus are beneficial and used in different industries as they are mostly non-pathogenic. However, strains such as *P. aeruginosa* and *P. maltophilia* are opportunistic human pathogens causing diseases in urinary tract, respiratory tract and wounds (Baron, 1996b).

These bacteria can live in a variety of conditions and are known for their metabolic versatility and genetic plasticity. They are fast growing organisms with simple nutritional requirements and can uptake a variety of substrates including toxic organic compounds (Moore et al., 2006). They can grow at temperature range of 4–42°C and pH range of 4-8 with complex or simple organic compounds. They are saprophytes and parasites. In general, *Pseudomonas* spp. cannot inhabit in anaerobic, thermophilic or acidophilic environmental conditions (Moore et al., 2006).

Pseudomonas spp. are the cause of meat, poultry and fish spoilage and can contaminate these products even under refrigerated conditions (Barrett et al., 1986; Moore et al., 2006). They can also form biofilms by producing exopolysaccharides, hard to remove from food production apparatuses (Mah et al., 2003).

Due to their simple medium requirements, *Pseudomonas* spp. can be used for production of a range of enzymes (e.g. enzymes used in leather industry for dehairing of products) and biocatalysts with various applications. They are used for production of bio surfactants, recombinant proteins and alginates in

the biotechnology industry. They are also used in environmental technologies as bioremediation and biocontrol agents to control disease severity in agriculture and to promote plant growth (Novik et al., 2015; Rehm, 2009). Other applications of Pseudomonads include production of monoacylglycerols and hydrocinnamic esters, manufacturing of detergents and production of biodiesel (Cheirsilp et al., 2009; Li and Yan, 2010; Priya and Chadha, 2003). Few strains of *Pseudomonas* spp. such as *P. putida*, *P. aeruginosa* (Silva-Queiroz et al., 2009), *P. extremaustralis* (Catone et al., 2014) and *P. cepacia* (Young et al., 1994) have been reported as PHA-producing strains.

One of Pseudomonads strains used in biotechnology is *Pseudomonas putida*. They have the ability to degrade hydrocarbon molecules and organic compounds and are used in bioremediation. They are also within the generally regarded as safe (GRAS) microorganisms (Anzai et al., 2000; Loeschcke and Thies, 2015). Other applications of *P. putida* in biotechnology include production of bio-based materials such as polyhydroxyalkanoates (PHAs), the strain's application in bio conversion and de novo synthesis of chemicals such as *p*-hydroxybenzoate and *p*-hydroxystyrene (Poblete-Castro et al., 2012). This bacterium is also used in industrial production of high-value products in pharmaceuticals industry such as paclitaxel (known as taxol used in chemotherapy) (Poblete-Castro et al., 2012).

1.2. Bacterial products

Bacteria are used as workhorses for production of many commercially viable products. These include pharmaceuticals, food and beverages, pesticides, polymers, fuels and detergent products.

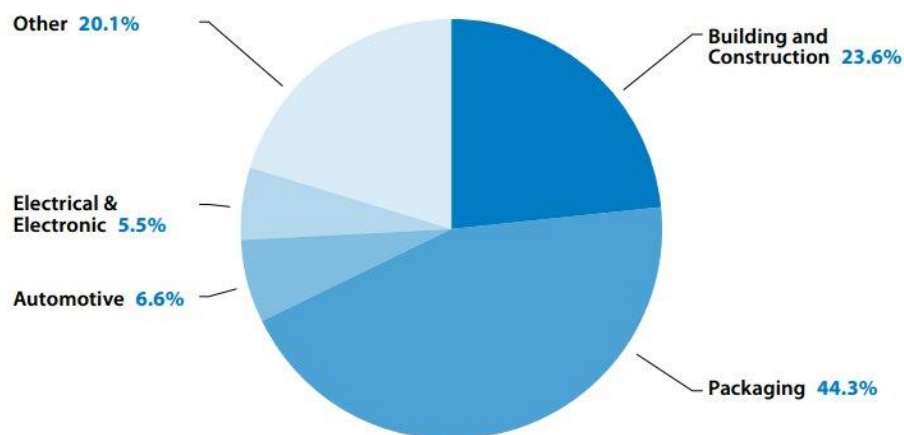
Pharmaceutical products include antibiotics such as bacitracin and neomycin (Bandyopadhyay and Majumdar, 1974), antitumor agents such as Rhizoxin (Tsuruo et al., 1986), enzymes such as lipases (Gupta et al., 2004), proteins (Terpe, 2006) and food supplements (Lancini and Demain, 2013). Bacteria are also used as factories in food industry for products such as proteases (used for brewing, baking and cheese processing), glucose isomerase, *beta*-galactosidase, dextran, yoghurt and vinegar.

This research focused on two bacterial products, polyhydroxyalkanoates and bacitracin as model microbial products. The processes for industrial production of these compounds are well-defined in biotechnology and their large-scale production makes them good candidates for the novel bioprocess design introduced here.

1.2.1. Plastics

Petroleum-based polymers (plastics) are widely used in almost all industries from food and packaging to car manufacturing, biotechnology and pharmaceuticals. The UK produces 2.5 million tonnes of plastics annually and is one of the top 5 processors of plastics in the EU with 4.8 million tonnes of materials consumed by plastic processors. Plastics are mostly used in packaging (44.3 %) and construction (23.6 %) (*UK plastics industry capability guide*, 2016). Fig. 2 below shows the percentage of plastics used in different industries.

Plastics consumption by application markets (%) in the UK



Plastics consumption by application - Source: PlasticsEurope Market Research Group (PEMRG) / Consultic Marketing und Industrieberatung GmbH

Figure 2. Plastics consumption in the UK by application, reprinted from (British plastics federation, 2016)

These useful products however, take decades to centuries to degrade. The plastic waste produced by different industries is discarded in landfill, incinerated or recycled for reuse. Landfill disposal causes a major environmental issue as it occupies thousands of square meters of land and disrupts animal and plant life in the surrounding areas. Incineration leads to the release of carcinogenic and hazardous molecules into air and soil not to mention its contribution to global warming. Although plastics are recycled and regulations have been applied to ban landfill disposal and encourage recycling of waste plastics, only one third of the plastic used by consumers in the UK is recycled and the rest goes to landfill (Plastics Europe, 2016).

On the other hand, while most petroleum based plastics are not biodegradable, there are some in this category that can be degraded by microorganisms. These include poly(ϵ -caprolactone) (PCL), poly(butylene succinate/adipate) (PBS/A), and poly(butylene adipate-co-terephthalate) (PBA/T) (Iwata, 2015; Tokiwa and Jarerat, 2003). These plastics however, are usually modified to obtain industrially desired characteristics. This modification is usually done through addition of non-biodegradable polymers, which have their own adverse effects on the environment since only the biodegradable part of the mixture is degraded and the remaining molecules can be toxic to the environment and cause environmental pollution (Iwata, 2015).

The mentioned issues arising from plastic waste and the ever-increasing oil prices have led to intense research on more environmental-friendly products of the same characteristics.

1.2.2. Biopolymers

Biodegradable bioplastics are environmental-friendly products with a potential for substitution of petroleum-based non-degradable plastics. Biodegradable products can be decomposed into carbon dioxide and water by microorganisms and are derived from either chemical (such as PCL, PBS/A and PBA/T) or biological matter (referred to as bioplastics).

Biodegradable bioplastics such as polylactic acid (PLA), succinic acid and 1,3-propanediol based polymers are made from natural resources (bio-based polymers) (Prieto, 2016). Their disposal does not have an adverse effect on the surrounding environment. They can be obtained from microorganisms and biomass including proteins, lipids and polysaccharides such as starch or through biotechnological processes (Bugnicourt et al., 2014). These polymers can be metabolised later by other microorganisms and therefore return to the ecosystem.

The first biodegradable polymer, poly-3-hydroxybuturate (P3HB), was discovered in 1920s. It was isolated from *Bacillus megaterium*. However, it took almost twenty years until it was recognised and discovered again independently in the late 1950s. Baptist and Werber at W.R. Grace & Co (U.S.A) published patents in 1960s, and the production of P(3HB) was initiated at a commercial scale. This was discontinued however, as they failed to decontaminate the product from bacterial residues and the price of the process was high (Baptist and Werber, 1963; Lenz and Marchessault, 2005; Philip et al., 2007).

When the 1970's oil crisis happened, oil prices rose from \$3 per barrel to \$12 between 1973-1974, followed by another rapid increase to \$39.5 in 1979 and continued until mid-1980s. The extent of research on biopolymers fluctuated with the price of oil since then until 1990s. It was only then that the application of biopolymers in biomedical industry was developed further and obtained economic viability, drawing more interest in research. Since then, PHAs were investigated extensively and a range of applications from packaging (e.g. cosmetic containers and food packaging) to pressure sensitive adhesives and fabrics (Keshavarz and Roy, 2010). Recent focus has been on the application of PHAs in healthcare industry including tissue engineering as scaffolds to replace and regenerate living tissue (Insomphun et al., 2016) and biologically active beads for the design of vaccines or disease diagnosis tools (Parlane et al., 2017). Other applications of PHAs in pharmaceuticals include their use in urology, wound management and cardiovascular products (Williams and Martin, 2005).

1.2.2.1. PHA types, characteristics and biosynthesis

Polyhydroxyalkanoates (PHAs) are biogenic polyesters of hydroxyalkanoates. Each monomer bonds to another through an ester bond from its carboxyl group to the hydroxyl group of the other (Rai, 2010). PHAs are produced by different types of Gram-negative and Gram-positive bacteria, algae or yeast. They are stored as a source of energy and carbon and are accumulated inside the cells at the presence of excess carbon and under limited nutrient availability (nutrients other than carbon) as well as physiological stress. PHAs are stored as insoluble granules in the cytoplasm of bacterial cells. They have thermoplastic and elastomeric properties (Philip et al., 2007).

PHAs fall into three categories: short-chain-length, which contain 3-5 carbon atoms such as poly-3-hydroxybutyrate (P3HB); medium-chain-length PHAs which contain 6-14 carbon atoms with alkyl side chains; and long-chain-length PHAs containing more than 14 carbon atoms (Anderson and Dawes, 1990; Visakh, 2014).

PHAs have different molecular structures based on the microorganism by which they are produced, media composition, fermentation conditions, mode of fermentation and purification methods used in downstream (Keshavarz and Roy, 2010; Varsha and Savitha, 2011). PHAs can be homo- polymers or hetero polymers. Homo-polymers are those with only one type of hydroxyalkanoate present in the monomer's structure, produced via utilisation of even-numbered normal alkanates and hetero polymers are those with more than one hydroxyalkanoate in the monomer (Sharma and Mudhoo, 2011).

The first and most studied form of PHA, poly-hydroxybutyrate (PHB), is a homo-polyester produced by different microbial species. Its characteristics are close to those of polypropylene or polyethylene except for fragility due to its high crystalline degree (Aremu et al., 2011; Visakh, 2014)

1.2.2.2. Polyhydroxybutyrate (PHB)

PHB is a right-handed helix with a similar structure to that of polypropylene with similar degrees of crystallinity and resistance to water and moisture,

despite their very different chemical properties. PHB is less resistant to solvents and more resistant to UV light compared to polypropylene. It is also stiffer and more brittle. Its biocompatibility makes PHB advantageous over polypropylene (Anderson and Dawes, 1990).

PHBs are linear polyesters accumulated as intracellular granules under nutrient limitation with molecular weights of 50k to over a million Da depending on the producer microorganism (Bugnicourt et al., 2014). They were first discovered by Maurice Lemoigne, a French researcher in late 1920s, while he was working with *B. megaterium* (Lemoigne, 1926; Reddy et al., 2003). Since then, over 90 genera of microbial species have been found to produce PHAs (Anjum et al., 2016; Rai, 2010; Zinn et al., 2001). Industrial producers of PHBs include *E. coli*, *Bacillus* spp., *Cupriavidus necator*, *Alcaligenes eutrophus* and *Pseudomonas* spp. (Reddy et al., 2003).

In terms of economic feasibility of PHB production, medium requirement is a key element with carbon source being the determining factor (Sukan, 2015). Possible carbon sources as substrate for PHB producing strains include glucose, sucrose, methanol, acetic acid, ethanol, cheese whey, cane molasses, cellulose and hemicellulose hydrolysate. PHBs can also be produced by microorganisms grown on petroleum-based substrate including alkenes, alkanes and aldehydes. Reddy et al. (2003) reported methanol and sucrose as the cheapest substrate for PHB production, with 43% and 40% PHB yield (g P(3HB)/ g substrate), respectively (Reddy et al., 2003).

Extensive research has been carried out on the use of industrial waste as cheap substrate for PHB production. Such examples include use of toxic chemical waste such as naphthalene as carbon source for fermentation of *P. putida* CA-3, use of malt wastes for the fermentation of *Alcaligenes latus* (Varsha and Savitha, 2011), use of starch-based waste such as potato starch and wheat for fermentation of *Ralstonia eutropha* and *Cupriavidus necator*, respectively, use of cellulose-based waste such as bagasse and soybean for fermentation of *Burkholderia sacchari* and recombinant *E. coli*, use of sugar cane for fermentation of *Pseudomonas fluorescens* and use of beet molasses for fermentation of *B. cereus* (Sukan, 2015).

PHB production can start at stationary phase of growth or during the log phase (Varsha and Savitha, 2011). This has been illustrated in Fig. 3.

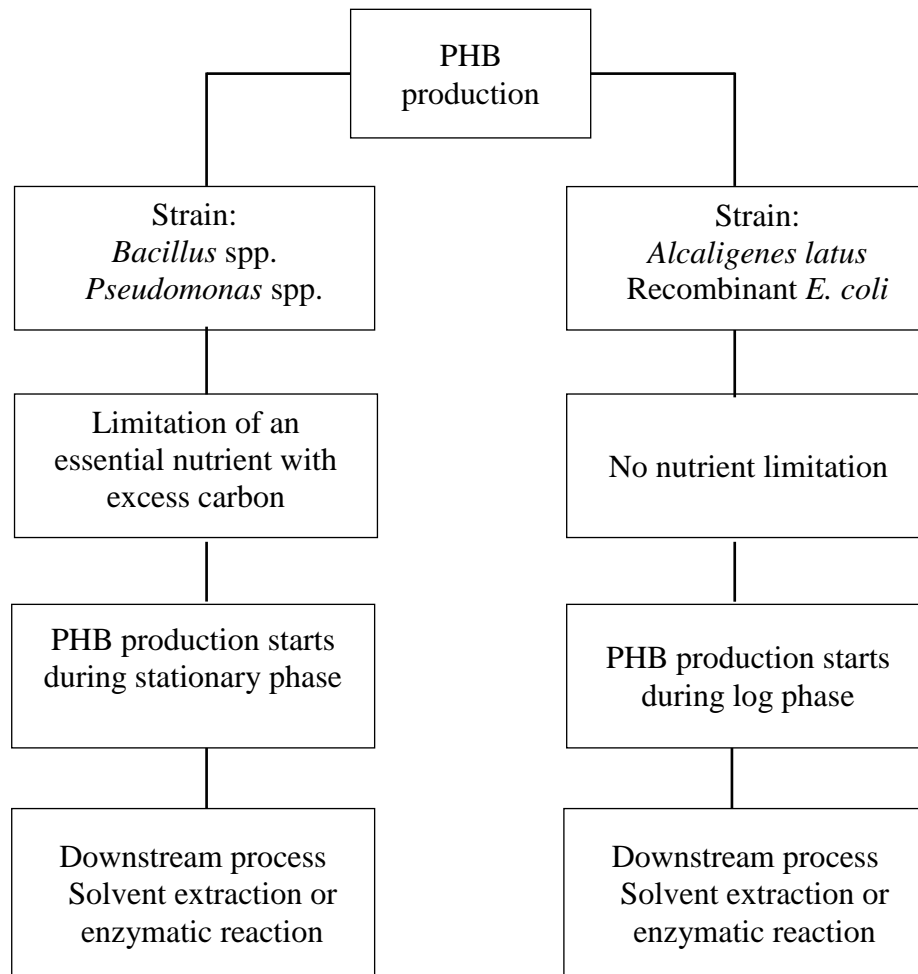


Figure 3. PHB production process (Varsha and Savitha, 2011)

Different companies have used PHBs in a wide range of products. These include: Metabolix (USA), who used PHB in a mixture as food additives and as a copolymer in BIOPOL, a product used in paper coating, film production and electronic packaging; Procter and Gamble (USA) with KAIST (Korea) and Tsinghua University (China) have used PHBs as flexible packaging products, medical equipment, thermos-formed articles and synthetic paper; Procter and Gamble who also developed NODAX from PHBs, which is used in production of hygienic wipes, surgical garments, compostable bags and thermo formed articles; Biomer (Germany), who use PHB in production of pens, combs and transformation process material; PHB industrial (Brazil), who use PHBs in manufacturing of bio plastic resins; Mitsubishi gas chemical company(Japan), who produce PHBs with the trade name Biogreen; Minerv-PHA (Italy), who

produce PHBs under the trade name Bio-on and many other chemical and medical companies (Anderson and Dawes, 1990; Rai, 2010). Table 1 shows a summary of manufacturers of PHAs from bacterial cultures, with their production substrate and commercial names.

Table 1. Manufacturers and the microorganisms, raw materials used for the production of biodegradable plastics taken from (Wong et al., 2016).

Company	Trade Name	Product	Location	Raw Material	Capacity (tons/year)	Price (€/kg)
Telles	Mirel	PHB copolymers	USA	Corn sugar	50,000	1.5 (2010)
Mitsubishi	Biogreen	P(3HB)	Japan	Methanol	10,000	2.5–3.0 (2010)
GreenBio/DSM	GreenBio	P(3HB-4HB)	China	Sugar	10,000	N/A
Bio-On	Minerv	PHB	Italy	N/A	10,000	N/A
TianAn Biopolymer	Enmat	PHBV	China	Dextrose/glucose	2000	4.1–4.3 (2012)
Kaneka	Kaneka	PHBH	Japan	Vegetable oil	1000	–
PHB Industrial	Biocycle	PHB	Brazil	Sugar cane	600	2.5–3.0 (2010)
MGH	Nodax	PHBH	USA	N/A	N/A	N/A
Biotechnology Co.	Biomer	N/A	Germany	Sucrose	50	3.0–5.0
Biomatera	Biomatera	PHBV	Canada	Sugar	N/A	N/A
Tianzhu	Tianzhu	PHBH	China	N/A	N/A	N/A
Tepha	N/A	N/A	USA	N/A	N/A	N/A
Tianjin Northern Food	N/A	N/A	China	N/A	10	N/A
Yikeman Shandong	N/A	N/A	China	N/A	3	N/A
Shenzen O'Bioer	N/A	N/A	China	N/A	N/A	N/A
Polyscience, Inc.	N/A	PHB	USA	N/A	N/A	N/A

PHB, polyhydroxybutyrate; *P(3HB)*, poly(3-hydroxybutyrate); *P(3HB-4HB)*, poly (3-hydroxybutyrate-4-hydroxybutyrate) *PHBV*, poly(3-hydroxybutyrate-co-3-hydroxyvalerate); *PHBH*, poly (3-hydroxybutyrate-co-3-hydroxyhexanoate).

PHBs are biodegradable and biocompatible. Their biocompatibility makes them appealing for medical purposes and drug delivery systems. They can be used as biomaterial in robust implants, as human immune system does not reject them. They are used in bone implants, wound dressings and scaffolds in tissue engineering (Rai, 2010). They are used as scaffolds to support tissue cell growth, which can provide an appropriate path for transfer of nutrients and wastes from their surface. After the formation of the tissue, the scaffold will degrade without the resulting in release of toxic degradation products into the body (Williams et al., 1999).

PHBs are also used in biomaterial production for nerve regeneration and bone tissue engineering and skin regeneration for wound healing (Rai, 2010).

Another application of PHBs is in drug delivery systems. They are used in matrices for scaffolds carrying antibiotics for internal infections such as bone infections known as osteomyelitis (Sivasubramanian, 2016; Rai, 2010) .

1.2.3. Bacitracin

Bacitracin is an antibiotic, which is commercially available in the form of its zinc salt. Zinc bacitracin is more stable in dry state than bacitracin. It is very soluble in water and Methanol, slightly soluble in acetone, benzene and ether and insoluble in chloroform. Its aqueous solution (both with and without buffer addition) is stable at pH range of 5-7 and rapidly loses its activity at pH values higher than 7. Additionally, it loses its activity at room temperature and can only be stored for up to four weeks at 4°C (Bond et al., 1949).

1.2.3.1. Bacitracin characteristics, molecular structure and biosynthesis

Bacitracin is a heat resistant (resists for 15 minutes at 100°C) branched polypeptide, stable at pH range of 5-7. There are several types of bacitracin based on the molecular structure of the polypeptide. These molecules are differentiated by one amino acid in their structure. The most common types of bacitracin formed during bioreactor production are bacitracin A and B, with bacitracin A being the most active. Other types of bacitracin include bacitracin C, D, E and F (Johnson et al., 1945; Konigsberg and Craig, 1962; Stone and Strominger, 1971).

Bacitracin A has a thiazoline ring in its molecular structure and an amino group attached to its N terminal (Fig. 4). To be active as an antibiotic against microorganisms, bacitracin A molecule needs the presence of metal ions. The nitrogen atom in the thiazoline ring and the adjacent amino group involve in the chelation process of the metal and contribute to the stability of the thiazoline ring, inhibiting its oxidation and thus keeping the antimicrobial activity of bacitracin A intact.

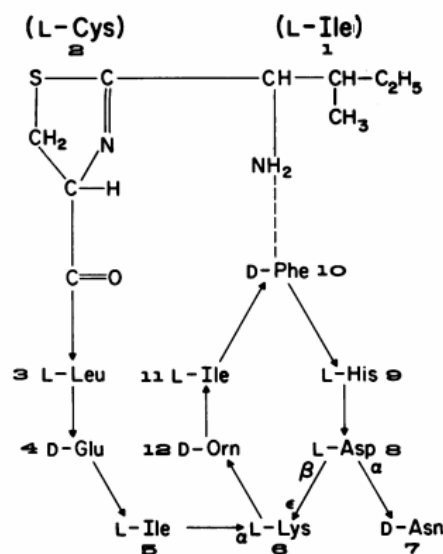


Figure 4. Bacitracin A structure. Arrows show C-N bonds. Thiazole ring is formed from L-isoleucine and L-cysteine and the cyclic heptapeptide ring is formed by the amino group of L-lysine reaction with the β -carboxyl group of D-asparagine (Stone and Strominger, 1971)

Bacitracin F is a by-product of fermentation under alkaline conditions. It is the product of deamination reaction of bacitracin A. It is formed when the thiazoline ring in bacitracin A molecule is converted into a ketothiazole ring (when the amino group is replaced by a carbonyl group). This reaction results in total loss of antibiotic activity and makes bacitracin F nephrotoxic and undesirable (Johnson et al., 1945; Murphy, 2008; Reffatti, 2012; Weinberg, 1967).

Bacitracin is mainly produced by *Bacillus* spp. including *B. licheniformis* and *B. subtilis* strains. It is synthesised non-ribosomally by a multi-enzyme complex termed bacitracin synthase ABC. The synthase follows a thiotemplate mechanism from a protein template pathway (Konz et al., 1997; Stone and Strominger, 1971).

1.2.3.2. Applications

Bacitracin is used in the pharmaceutical industry as medication for bacterial infections, such as minor skin and eye infections and as a constituent of antibiotic sprays along with other antibiotics, such as polymyxin and neomycin. It is widely used as animal food additive and acts as an important growth promoter in animal husbandry (Phillips, 1999; Reffatti, 2012).

1.2.3.3. Mechanisms of action

Bacitracin works primarily against Gram-positive bacteria, namely, *Staphylococcus* spp. and *Streptococcus* spp. and some Gram-negative bacteria (Brewer, 1981). This antimicrobial product acts as an antibiotic by disrupting bacterial cell wall. It inhibits the reaction required for dephosphorylation of C55-isoprenyl pyrophosphate. This reaction is essential for synthesis of the lipid carrier responsible for peptidoglycan synthesis (Stone and Strominger, 1971).

There have been several reports on optimisation of bacitracin production namely, by optimisation of the medium and fermentation conditions (optimum temperature, oxygen levels and optimum pH). Also, the levels of bacitracin production have been shown to increase through elicitation process (Murphy et al., 2007). This antibacterial product was chosen for this study, since its production procedure has been well developed, the methods of product detection have been reported and optimised and the producing bacterium, *B. licheniformis*, has been well characterised in the literature.

1.2.3.4. Factors affecting the production of bacitracin

Different parameters affecting microbial production of bacitracin include microbial related factors (e.g. selection and genetic manipulation of microbes as higher producers), growth conditions (e.g. different substrates and medium compositions) and bioreactor/bioprocess design (e.g. fermentation process conditions, recovery and purification techniques).

Optimisation of microbial growth conditions for bacitracin production includes the choice of growth medium, initial pH and growth temperature (Haddar et al., 2007). Like other secondary metabolites, bacitracin is normally produced at the stationary phase due to the suppression of synthase genes during the exponential growth phase. However, Haavik (1974) has shown that in appropriate medium, bacitracin can be produced during the exponential growth phase. They have reported that the production of bacitracin occurred in parallel to growth when *B. licheniformis* was grown on defined medium in

the absence of glucose. The antibiotic was formed in parallel to active division of cells and reached its peak at the same time as the culture entering its stationary growth phase (Haavik, 1974). Bacitracin activity reduces at alkaline pH values. This is due to the oxidation of bacitracin A, leading to its conversion to bacitracin F. Murphy found that the amount of bacitracin A achieved from pH-controlled bioreactors was 54% higher than set-ups without pH control. The optimum level of pH for bacitracin production was reported as 7 (Aftab et al., 2012; Murphy, 2008).

1.3. Magnetic field

Magnetic field (MF) is the field produced around permanent magnets or moving charged particles (usually referred to as magnetic field since both fields exist around a moving charged particle). Strength of MF at any given point is dependent upon distance from the source (magnet or moving charges) and is measured in Tesla in the SI. The Earth produces MF, which is the reason why magnetic dipole on the needle of a compass works (Jiles, 2015). The Earth's magnetic field is within the range of 25-65 μT .

MF produced by permanent magnets is usually described in physics through arrows going from the North pole of the magnet to its south pole. A simple illustration used in physics for description of magnetic field is exposure of iron filings to a bar magnet, resulting in specific arrangement of filings based on field direction (Fig. 5).



Figure 5. Classical demonstration of iron fillings around a bar magnet (Giordano, 2012)

Magnetic field can also be produced via moving charged particles. Therefore, electric wires carrying electric current produce magnetic field. There are

different types of magnetic field depending on the strength of electric field, as well as the direction of movement of charges.

Magnetic field produced by a direct constant current is termed as static magnetic field. The direction and intensity of MF remain the same and do not change by time. When an alternating current (AC) passes through a wire, the resulting magnetic field changes direction at certain frequencies.

This was first discovered by Faraday, who suggested that a changing magnetic field can induce movement in charged particles. Faraday's law described electromotive force as the electric force produced in a wire resulting in electric current (Faraday, 1833). Maxwell later introduced the four Maxwell equations describing how time-varying electric field can induce a time-varying magnetic field (Chabay and Sherwood, 2015; Maxwell, 1865).

Magnetic field produced by AC has three properties: intensity, frequency of changing direction and direction of the field at each given time. Magnetic field produced from AC is described by Maxwell's law and is in the form of waves. This wave is characterised by surrounding medium composition, source and boundaries. Hence, these waves can be spread indefinitely in free space or bounded to limited space such as a coaxial line (Guru and Hiziroglu, 2004).

At any given point inside a magnetic field, a magnetic force is present on any moving charged particle (q) with a direction perpendicular to that of the movement. This is described by Lorentz force law:

$$\vec{F} = q\vec{v} \times \vec{B}$$

Where F is the magnetic force (Newton), q is charge, v is velocity of the charged particle ($m \cdot s^{-1}$) and B is intensity of the magnetic field (T). Direction of magnetic force is determined by right hand rule. This force has the opposite direction on a negatively charged particle.

One type of magnets using electric current (electromagnets) is a solenoid. It is a metal cylinder coiled by electric wire. The electric charges running through the wire produce a homogeneous magnetic field inside the cylinder with a

specific intensity. The direction of this magnetic field is determined through the right hand grip rule. If the right hand is wrapped around the coiled wire with direction of the thumb being the same as that of the electric current, direction of bent fingers show the direction of magnetic field.

Magnetic field has varied effects on microorganisms. This has been summarised in section 1.3.2.

1.3.1. Use of Magnetic field in biotechnology and biomedical sciences

Magnetic field has been used in different areas of life sciences and healthcare industry including medical devices, drug delivery systems, biotechnology and bioprocess optimisations.

Due to its mechanical and thermodynamic characteristics, magnetic field is used in medical devices, which can be divided into permanent magnetically driven devices and magnetically driven devices (Sliker et al., 2015). As the name suggests, permanent magnetically driven medical devices use permanent magnets as their driving force in diagnosis, therapy, treatment or curing diseases. Fig. 6 shows some examples of these devices (Sliker et al., 2015).

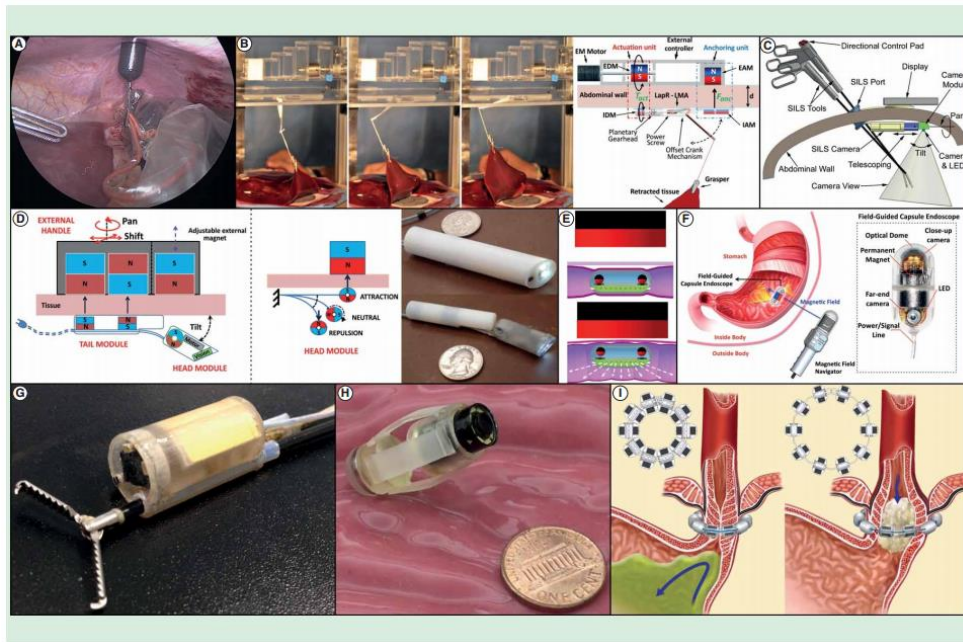


Figure 6. Examples of medical devices that utilize permanent magnets for operation include: (A) a magnetic retraction and triangulation device for single-port laparoscopic surgery, (B) a laparoscopic tissue retractor, (C) a magnetic camera system for single-port laparoscopic surgery, (D) magnetic tilt control for a laparoscopic camera, (E) a remotely triggered capsule for controlled colonic insufflation, (F) a magnetic field-guided capsule endoscope control system for navigation in the gastrointestinal tract, (G) a magnetic air capsule robotic system for colonoscopy, (H) a magnetically controlled compliant capsule endoscope with a magnetically actuated drug delivery mechanism and (I) a magnetic sphincter for treatment of gastroesophageal reflux disease. Reprinted from (Sliker et al., 2015)

Magnetically driven devices, use magnetic field as the driving force for operation. These are generally larger and more complex devices than permanent magnetically driven devices (Sliker et al., 2015). These include Magnetic Resonance Imaging (MRI) systems in radiology or magnetic therapy, where magnetic energy is used for treatment or diagnosis of a disease (Malmivuo and Plonsey, 1995). Magnetic field has also been under investigation for its potential for cancer treatment (Williams et al., 2001). In recent years, application of magnetic field has attracted much interest in tissue engineering and drug delivery systems. Magnetic field has been used in drug delivery systems as a means to achieve high throughput and better product separation with minimum shear application to cells and their products (Ignatyeva et al., 2014; Setchell, 1985). MF is used in separation systems as a purification method, which can be easily automated. It is used in separation

of different materials including viruses, proteins, DNA and cells (Borlido et al., 2013). Drug delivery nanocarriers can be engineered to release the drug on demand by exposure to oscillating MF (Saint-Cricq et al., 2015).

The use of magnetic field on microbial cultures has also been under investigation as more efforts have been made by researchers to improve bioprocesses and productivity. One such example includes the application of magnetic field as a biostimulator to increase efficiency of biofuel production by algae (Hunt et al., 2009).

Magnetic fields of various types, amplitudes, frequencies and waveforms have been recently used in microbial biotechnology, including their application in sterilisation (Rogers, 2014), cell growth and metabolite production (Hönes et al., 1998; Ružič et al., 1997), electrophoresis and dielectrophoresis, (DeFlaun and Condee, 1997; Jaspers and Overmann, 1997), as a means of cell separation and in monitoring systems in biotechnology such as Nuclear magnetic resonance (NMR) spectroscopy, Dielectric Spectroscopy and biosensors. In general, specific and high efficiency bioprocesses can be developed by linking electrochemical processes and cell metabolism (Velizarov, 1999).

1.3.2. Effect of magnetic field on microorganisms

Effect of MF on microorganisms has attracted much interest due to the developments in biotechnology. Studies on the application of magnetic field on microbial cultures have shown improvements in production of some microbial products.

Alvarez et al. (2006) applied 5, 12.5 and 20 mT MF on *Lactococcus lactis* and reported nisin production yield of 5 times higher than the control when cultures were exposed to 5 mT MF (Alvarez et al., 2006). They used 5 L bioreactors coupled with a magnetic field generator. This device was made up of a metal box holding three couples of parallel magnets facing opposite poles. The magnets were set in series and the culture medium was circulated through the device using a pump as presented in Fig. 7.

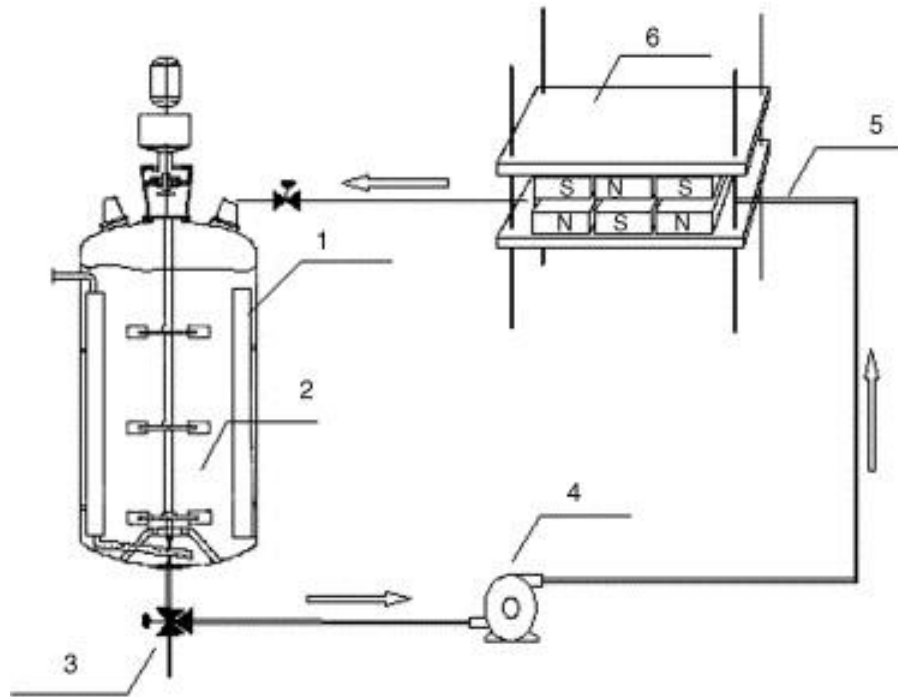


Figure 7. Schematic presentation of MFG setup used by Alvarez et. al (2006). (1) STR, (2) *Lactococcus lactis* cell suspension, (3) three-way valve, (4) peristaltic pump, (5) Stainless steel tube, (6) MFG. Reprinted from (Alvarez et al., 2006)

Same group of researchers applied two different intensities of MF (5 and 20 mT) to *Saccharomyces cerevisiae* batch bioreactor cultures and reported 17% increase in ethanol productivity of the culture exposed to 20 mT MF. They also found that MF exposed cultures reached their final stage of fermentation earlier than controls. They used 5 L bioreactors coupled with two magnetic field generators (shown in Fig. 8). The first magnetic field generator was similar to the previous report; a metal box holding series of three couples of magnets, each couple parallel to each other facing opposite poles. MF was adjusted in this generator to the intensity of 5 and 20 mT. This was then followed by another magnetic field generator consisting of a solenoid producing approximately 8 mT MF. *S. cerevisiae* culture medium circulated through the first device in two experiments (with 5 and 20 mT intensities) and through both in the third. 20 mT MF with circulation through both devices resulted in higher ethanol productivity (Perez et al., 2007).

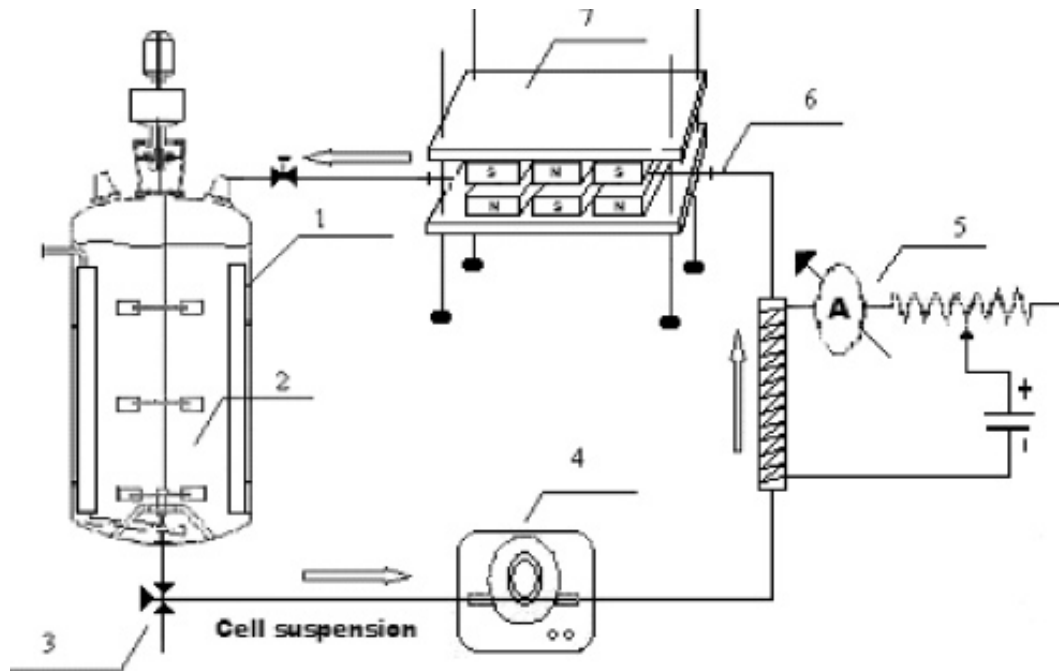


Figure 8. Schematic presentation of MFG setup used by Perez et. al (2007). (1) STR, (2) *S. cerevisiae* cell suspension, (3) three-way valve, (4) peristaltic pump, (5) solenoid coupled with current source of 2 A, (6) stainless steel tube, (7) main MFG. Reprinted from (Perez et al., 2007)

Another report on the effect of MF on production of microbial products stated that citric acid and cellulase production by *Aspergillus niger* sp. was enhanced by exposing the cellular cultures to MF of 0.2-1 mT, 50Hz. Production yield was shown to be dependent upon time of exposure and strength of magnetic field, which increased by increasing these parameters (Gao et al., 2011). In their experiments, Gao et. al (2011) used 250 mL shaken flask cultures of *A. niger* for two days, after which 1 mL of each was transferred to glass bottles, which were then exposed to MF for periods of 4,6 and 8 h. The MF apparatus was made up of six cylindrical coils attached to a transformer. Each set of coils had different number of threads leading to different intensity in each coil. The glass bottles were placed at the centre of each coil, on a shaker at 200 rpm

speed. The set-up used in their experiment is shown in Fig. 9 below.

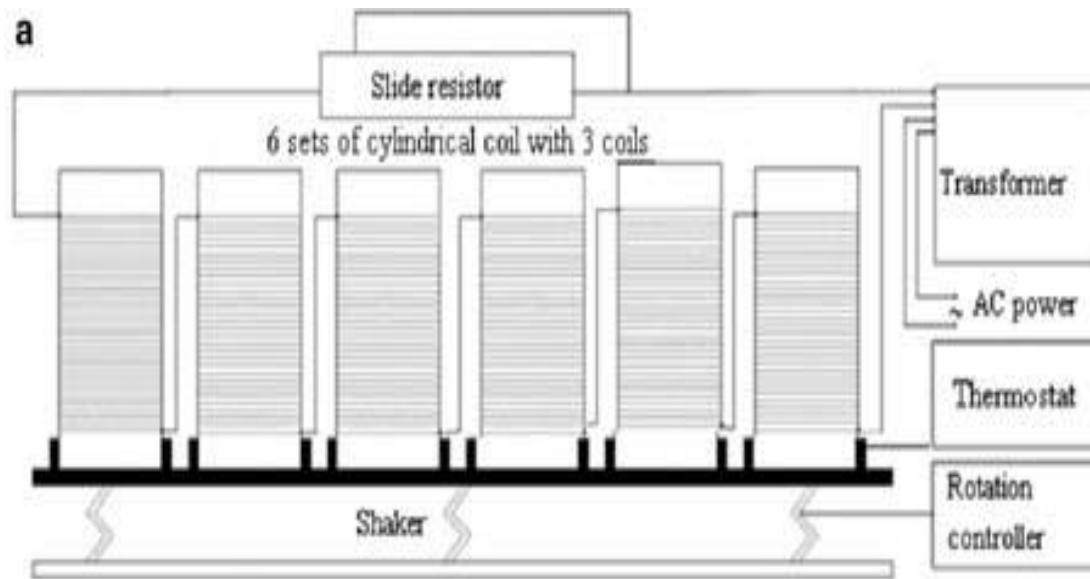


Figure 9. Schematic of the magnetic device system used in the study of effect of MF on *A. niger* for production of citric acid and cellulase (reprinted from Gao et al., 2011)

There is also evidence of increased insulinase production by *Geotrichum candidum* sp. after application of low MF, which suggests enhanced enzyme activity for the cultures grown under 7 mT magnetic field. This study was carried out through solid state fermentation of *G. candidum* in 250 mL shaken flasks placed inside cylindrical coils wrapped in copper wire (Canli and Kurbanoglu, 2012).

Also, in the only study carried out so far on production of PHAs in activated sludge exposed to low intensity (7 mT) static magnetic field, an increase of 32% was reported. 1 L sequence batch reactors for growth of activated sludge were used for this purpose. Reactors were placed at the centre of two parallel permanent magnets producing 7 mT MF (Xu et al., 2010).

Effects of magnetic field on morphology, viability and growth of microbial species have also been investigated. These include increased growth of nitrite oxidising bacteria and *E. coli* sp. and increased viability of *E. coli* sp. and *P. aeruginosa* sp. under MF exposure (Martirosyan et al., 2013; Rodriguez Justo et al., 2006; Segatore et al., 2012; Wang et al., 2012). Other studies on several

types of bacteria suggest that bacterial growth can be inhibited or stimulated depending on the strength and frequency of the applied magnetic field (Bajpai et al., 2012; Inhan-Garip et al., 2011; Moore, 1979; Nagy and Fischl, 2004). Al-Khaza'leh and Al-fawwaz (2015) applied 30, 50 and 80 mT MF on three microorganisms, *E. coli*, *Staphylococcus aureus* and *B. subtilis*. They reported a decrease in growth rates of *E. coli* and *S. aureus* and an increase in growth rate of *B. subtilis*. Growth rate of the latter microorganism increased with increasing the intensity of magnetic field (Al-Khaza'leh and Al-fawwaz, 2015).

Table 2 below is a summary of existing literature on effect of MF (static and time-varying) on microorganisms.

Table 2. Summary of available literature on the effect of magnetic field on microorganisms

Reference	Microorganism	Magnetic Field		
		Frequency	Intensity	Effect
Moore 1979	5 bacterial spp.	0-0.3 Hz	50-900 G	Increased/decreased growth Upon frequency and strength
	1 yeast, fungus sp.			Unaffected germination
Ramon et al. 1987	<i>B. subtilis</i> mutant	800 Hz	0.8 mT	Little to no cell cohesion
		1000 Hz	2.5 mT	
Wittekindt et al. 1990	<i>Mycotypha Africana</i> spp.	Static	12.5-380 pT	Increased germination rate by 2-3 times at low intensities Decreased germination by up to a factor of 4 at higher intensity
Strasak et al. 1998	<i>E. coli</i> spp.	50 Hz	5-21.5 mT	Unaffected morphology Increased viability in liquid medium Decreased viability in solid medium
Kohno et al. 2000	<i>Streptococcus mutans</i> spp.	Static	30, 60, 80, 100 mT	Decreased growth rate- unaffected cell viability
	<i>Staphylococcus aureus</i> spp.			Decreased growth rate- unaffected cell viability
	<i>E. coli</i> spp.			Unaffected growth
Piatti et al. 2002	<i>Serratia marcescens</i> spp.	Static	8±2	Decreased viability- decreased growth
	<i>Hordeum vulgare</i> spp.		mT	Unaffected viability
	<i>Rubus fruticosus</i>			Unaffected viability

Reference	Microorganism	Magnetic Field		
		Frequency	Intensity	Effect
Strašák et al. 2002	<i>E. coli</i> spp.	50 Hz	2.7–10 mT	Decreased growth Decreased viability with increasing MF intensity and duration
Del Re et al. 2003	Recombinant <i>E. coli</i>	50 Hz	0.1-1 mT	Unaffected morphology Unaffected viability
Re et al. 2004	<i>E. coli</i> spp.	Pulsed square	0.1-1 mT	Decreased viability
		Sinusoidal	0.1-1 mT	Increased viability
Fojt et al. 2004	<i>E. coli</i> spp.	50 Hz	10 mT	Decreased growth Decreased viability
	<i>Leclercia adecarboxylata</i> sp.			Decreased growth Decreased viability
	<i>Staphylococcus aureus</i> sp.			Decreased growth Decreased viability
Lipiec et al. 2004	<i>Ervinia carotovora</i> spp.	Oscillating	5,10, 15, 20 T	Decreased viability
	<i>Streptomyces scabies</i> spp.			Decreased viability
	<i>Alternaria solani</i> spp			Decreased viability
Nagy and Fischl, 2004	<i>Alternaria alternate</i> spp	Static	0.1 mT	Increased growth by 68-133%
	<i>Curvularia inaequalis</i>			Decreased viability by 10%
	<i>Fusarium oxysporum</i> conidia			Decreased viability by 79-83%
Gao et al. 2005	<i>Shewanella oneidensis</i> MR-1	Static	14.1 T	Unaffected growth

Reference	Microorganism	Magnetic Field		
		Frequency	Intensity	Effect
Chua and Yeo 2005	<i>B. licheniformis</i>	Perpendicularly polarised magnetic media		Change in cell adhesion and biofilm formation Significant morphological change Increased growth
Nagy 2005	<i>Alternaria alternata</i> and <i>Curvularia inaequalis</i> spp.	Static	0.1 mT	Increased growth by 68-133 %
	<i>Fusarium oxysporum</i> conidia		0.5 mT 1 mT	Decreased growth by 79-83%
Alvarez et al. 2006	<i>Lactococcus lactis</i> subsp	Static	5-20 mT	Increased nisin production
Manoliu et al. 2006	Cellulolytic fungi	Continuous wave and pulsatory		Increased hydrogen peroxide
Justo et al. 2006	<i>E. coli</i> spp.	Oscillating	0.01-0.1 T	Increased growth by 100 times
Perez et al. 2007	<i>Saccharomyces cerevisiae</i>	Static	5-20 mT	Increased productivity by 17%
Fojt et al. 2007	<i>Paracoccus denitrificans</i> sp.	50 Hz	10 mT	Decreased viability by 21% Decreased denitrification activity
Novák et al. 2007	<i>Saccharomyces cerevisiae</i>	50 Hz	<10 mT	Decreased growth rate Decreased cell viability

Reference	Microorganism	Magnetic Field		
		Frequency	Intensity	Effect
Cellini et al. 2008	<i>E. coli</i> spp.	50 Hz	0.1, 0.5, 1 mT	Changed morphology Unaffected cell viability
Fojt et al. 2009	Rod-like bacteria (<i>E. coli</i> spp.)	50 Hz	10 mT	Unaffected morphology Decreased growth
	Spherical bacteria			Unaffected morphology
Harris et al. 2009	<i>Arabidopsis thaliana</i> spp.	Static	500 μ T	No significant MF responses
Obermeier et al. 2009	<i>Staphylococcus aureus</i> spp.	Direct current sinusoidal and static electric field		Decreased viability by 36-37%
	<i>Staphylococcus aureus</i> spp.			Unaffected morphology Unaffected viability
Pérez Medina et al. 2010	<i>S. aureus</i> spp.	Static	450 mT	Decreased growth rate
		$0.0 \leq f \leq 1.0$ kHz	Oscillating	Increased growth rate
Di Campli et al. 2010	<i>H. pylori</i> ATCC 43629	50 Hz	1 mT	Decreased cell mass Decreased viability
Xu et al. 2010	Activated sludge	Static	7 mT	Increased PHB production by 32%
Cohen et al. 2010	<i>E. coli</i> spp.	99 GHz radiation		Unaffected viability Unaffected metabolic activity

Reference	Microorganism	Magnetic Field		
		Frequency	Intensity	Effect
Gao et al. 2011	<i>Aspergillus Niger</i> spp.	50 Hz	1 mT	Increased citric acid production Increased cellulose activity
Inhan-Garip et al. 2011	Three Gram-positive bacteria	50 Hz	0.5 mT	Significant ultrastructural changes Decreased growth rate
	Three Gram-negative bacteria			Significant ultrastructural changes Decreased growth rate
Al-Khaza'leh and Al-fawwaz 2015	<i>E. coli</i> spp.	Static	30,50,80 mT	Decreased growth rate
	<i>Staphylococcus aureus</i> spp.			Decreased growth rate
	<i>B. subtilis</i> spp.			Increased growth rate
Fijałkowski et al. 2015	<i>Glucanacetobacter xylinus</i>	50 Hz Rotating (RMF)	34 mT	Increased wet cellulose production Decreased dry cellulose production
Oncul et al. 2016	<i>Staphylococcus aureus</i> spp.	50 Hz	1 mT	Hyperpolarization-slight decrease in growth
	<i>E. coli</i>			Hyperpolarization-slight decrease in growth
Pillet et al. 2016	<i>B. pumilus</i>	Different intensities and pulses		Morphology change: surface damage Decreased hydrophobicity
Mhamdi et al. 2016	<i>E. coli</i>	Static	0.5 T	Decreased cell adhesion Orientation of bacteria cells was affected

As seen in the summary above, inconsistent results drawn from existing literature on the effect of MF on microorganisms have made it difficult to determine whether MF can be used in the biotechnology industry. The systems

used in each paper are different from the rest. An extensive systematic approach would enable researchers to further investigate this subject in a more comprehensive manner. Establishing a reproducible defined system would be the key to potential use of MF effect in biotechnology.

In this research, focus was put on establishing a system that could be used for growth of both Gram positive and Gram negative bacterial species with the aim of production of industrially viable microbial products.

1.4. Hypothesis

The present study was based on the hypothesis that static magnetic field influences the physiology and morphology of bacterial species, potentially leading to enhanced production of industrially viable microbial products.

1.5. Aim

The overall aim of this research was to investigate the effect of static magnetic field on production of industrially viable microbial products.

1.6. Objectives

To address the aim of this research, a bioreactor system was coupled with an MF generator to investigate the effect of MF on model bacteria of Gram-positive and Gram-negative groups, *B. licheniformis*, *Pseudomonas putida* and *Bacillus subtilis* were used with the newly designed system. The following objectives were then investigated separately:

- Effect of different intensities of MF on growth profile of bacterial culture;
- Effect of different intensities of MF on product concentrations (Bacitracin and P(3HB) were used as model industrial products of the chosen strains);
- Effect of different intensities of MF on cell morphology;
- Effect of different intensities of MF on carbohydrate production and nutrient carbon consumption by *B. subtilis*;
- Effect of different intensities of MF on nutrient carbon consumption by *P. putida*;

- Effect of different intensities of MF on P(3HB) structure.

Chapter 2

Materials and Methods

2. Materials and Methods

This chapter covers all materials used in the study and the method adopted to carry out the experiments. Materials include chemicals, microorganisms, and equipment. Methods are then explained in detail.

Table 3 shows a summary of this chapter.

Table 3. Summary of materials and methods chapter

Chapter 2	Categories		
Materials	Chemicals	Media for maintenance, growth and production	Nutrient Agar Nutrient Broth M20 MGM E2
		Assay chemicals	HPLC buffers Total carbohydrate assay Glutamic acid Crotonic acid
	Microorganisms	Strains	<i>Bacillus licheniformis</i> NCIMB8874 <i>Bacillus subtilis</i> NCTC3610 <i>Pseudomonas putida</i> KT2440
	Equipment		Stirred Tank Bioreactors (STRs) Magnetic Field Generator (MFG) Shaken Flasks (SF) Shaker/incubator High Performance Liquid Chromatography (HPLC) Microscope (visible light, confocal) Fourier Transform Infra-Red (FTIR) Spectroscopy Freeze drier pH meter Spectrophotometer Balances Scanning Electron Microscopy (SEM)

Chapter 2	Categories	
Methods	Preparations	Culture maintenance Media preparation Inoculum preparation
	Processes	SF fermentation process Bioreactor fermentation
	Procedures	Optical Density Colony count Cell Dry Weight High Performance Liquid Chromatography Total carbohydrate assay Glucose assay L-Glutamic acid assay P(3HB extraction) Crotonic acid assay (for determination of P(3HB) concentration) Sudan Black test Microscopic observations Nile red staining Scanning Electron Microscopy Fourier Transform Infra-Red Spectroscopy
	Calculations	Specific growth rate Nutrient uptake rate Product yield Carbohydrate formation rate Residence time through MFG Number of passes through MFG

2.1. Materials

Materials used in the experiments fall into chemicals, strains and equipment, and are explained in the following sections.

2.1.1. Chemicals

All chemicals used in this study were obtained from Sigma-Aldrich Company Ltd. (Dorset, UK) and Thermo Fisher Scientific (Paisley, UK) unless otherwise stated. All qualitative and quantitative assays were carried out using analytical grade reagents.

2.1.1.1. Media

Nutrient broth and nutrient agar were purchased from Sigma Aldrich and dissolved in distilled water as instructed by the company. The compositions are described in Table 4 and Table 5.

Table 4. Nutrient agar composition and concentration

Ingredient	Concentration (g. L⁻¹)
Agar	15
Meat extract	5
Peptone	5
Sodium chloride	5
Yeast extract	2

Table 5. Nutrient broth composition and concentration

Ingredient	Concentration (g. L⁻¹)
D(+)-glucose	1
Peptone	15
Sodium chloride	6
Yeast extract	3

Minimal medium (M20) was used for growth of *B. licheniformis* and bacitracin production. The medium constituents are shown in Table 6 below.

Table 6. M20 composition and concentration

Ingredient	Concentration (g. L⁻¹)
L-Glutamic acid	20
Citric acid	1
NaH ₂ PO ₄ .2H ₂ O	20
KCl	0.5
Na ₂ SO ₄	0.5
MgCl ₂ .6H ₂ O	0.2
CaCl ₂ .2H ₂ O	0.01
MnSO ₄ .H ₂ O	0.01
FeSO ₄ .7H ₂ O	0.01

Modified G medium (MGM) with sucrose as main carbon source as described by Akaraonye *et al.* , was used for production of P(3HB) from *B. subtilis* NCTC 3610 (Akaraonye et al., 2010). Medium constituents are shown in Table 6 below.

Table 7. MGM composition and concentration

Ingredient	Concentration (g. L⁻¹)
(NH ₄) ₂ SO ₄	2
MgSO ₄ .7H ₂ O	0.41
K ₂ HPO ₄	0.5
CaCl ₂ .2H ₂ O	0.1
Yeast extract	2.5
Sucrose	20
Trace elements	1 (mL. L ⁻¹)
Trace element stock	Concentration (g. L⁻¹)
FeSO ₄	5
MnSO ₄ .H ₂ O	3
CuSO ₄ .5H ₂ O	0.5
ZnSO ₄ .7H ₂ O	0.5
CoCl ₂	5

E2 mineral medium supplemented with glucose was used for production of P(3HB) through growth of *Pseudomonas putida* KT2440 as described by Le Meur et al. (2012). Medium constituents are shown in Table 8 below.

Table 8. Modified E2 medium composition and concentrations

Ingredient	Concentration (g. L⁻¹)
NaNH ₄ HPO ₄ .4H ₂ O	3.5
KH ₂ PO ₄	3.7
K ₂ HPO ₄	7.5
Glucose	10
trace elements	1 (mL. L ⁻¹)
Trace element stock	Concentration in 1 M HCL (g. L⁻¹)
FeSO ₄	2.78
CaCl ₂ .2H ₂ O	1.47
MnCl ₂ .4H ₂ O	1.98
CoCl ₂ .6H ₂ O	2.38
CuCl ₂ .2H ₂ O	0.17
ZnSO ₄ .7H ₂ O	0.29

2.1.1.2. Assay chemicals

Chemical assays carried out in the experiments include HPLC for bacitracin detection, total carbohydrate assay, glutamic acid assay and crotonic acid assay for P(3HB) concentration.

a. HPLC buffers

Two buffers were used for HPLC analysis of bacitracin. These consisted of the following:

Buffer A: Methanol – acetonitrile (1:1 v/ v) – KH_2PO_4 (0.05 M, pH=6.0): (44:56 v/v).

Buffer B: Methanol – acetonitrile (1:1 v/ v) – KH_2PO_4 (0.05 M, pH=6.0): (55:45 v/v).

All chemicals used for this analysis were of HPLC grade purity. pH was adjusted using HPLC grade H_3PO_4 (20%) and KOH (10%) solutions.

b. Total carbohydrate assay chemicals

Chemicals used in this assay include 5% solution of phenol in water and concentrated sulphuric acid purchased from Sigma Aldrich UK.

c. Glutamic acid assay chemicals

Glutamic acid assay involved the use of ninhydrin reagent. Constituents of this solution and relative concentrations are shown in table below.

Table 9. Composition and concentration of ninhydrin solution used for glutamic acid assay

<i>Ingredient</i>	<i>Quantity</i>
Stannous chloride ($\text{SnCl}_2 \cdot 2\text{H}_2\text{O}$)	0.16 (g. L^{-1})
Ninhydrin	40 (g. L^{-1})
Citrate buffer (0.2 M, pH 5.0)	500 mL. L^{-1}
2-methoxyethanol	500 (mL. L^{-1})

d. Crotonic acid assay chemicals

Chemicals used in this assay include: sulphuric acid, Chloroform and 15% sodium hypochlorite solution, all of which were purchased from Sigma Aldrich, UK.

2.1.2. Microorganisms

Bacillus licheniformis NCIMB 8874 was purchased from National Collection of Industrial and Marine bacteria, UK.

Bacillus subtilis NCTC 3610 was obtained from the bacterial culture collection of the University of Westminster, London, United Kingdom (UK).

Pseudomonas Putida KT2440 was a kind gift from Professor Manfred Zinn, Head of Research Group Biotechnology and Sustainable Chemistry, University of Applied Science and Arts Western Switzerland (HES-SO// Valais-Wallis).

2.1.3. Equipment

A range of equipment was used in this study as listed below:

STRs and their controls including probes (pH, dissolved oxygen, anti-foam, temperature, etc.) for carrying out STR fermentations of bacterial cultures. The set up used in the experiments are explained in processes section of the methods.

The MFG device was used to produce MF of different intensities.

SFs of 20, 100 and 500 mL were used for spore inoculum preparations and SF fermentation processes.

shaker/incubator, HPLC system, microscopes including visible light, confocal and scanning electron microscopes, FTIR system, freeze drier, spectrophotometer, centrifuges, plate reader, freeze drier and balances were other pieces of equipment used in this research.

2.1.3.1. STRs

STRs from Electrolab (model: Fermac 310/60) with 2 L total volume were used for the fermentation process. Controller units were housed in the station to which the STR vessel was attached. All controllers were attached to a computer and online data was recorded and managed throughout the processes by Fermentation Management software.

Experiment were carried out using two STRs. Stirrers and impellers, thermometers, dissolved oxygen (DO) probes, antifoam probes, pH probes and heating jackets purchased from Electrolab (UK) along with filters purchased from VWR and PALL corporations (UK) were attached to each STR

system. Other sensors could be installed as well, but the ones mentioned are commonly used.

Sterile tubing was fitted to multichannel peristaltic pumps purchased from Watson Marlow (UK) and used as means of culture circulation and connection to the sampling port.

2.1.3.2. MFG

To apply MF to bacterial cultures, magnetic field generator (MFG) was designed and constructed by research group of Professor Izzet Kale at the Department of Electrical Engineering, Faculty of Science and Technology of the University of Westminster. MFG was attached to an SF and/or an STR, while the microbial culture (*B. licheniformis*, *B. subtilis* or *P. putida*) was circulated through the device by a peristaltic pump.

The MFG consisted of a solenoid of copper wires twisted around a metal cylinder. MF was induced inside the solenoid when electric current passed through the wire. Direction of the induced MF was the same as the movement of culture medium, with different intensities. The intensity of MF was changed via changing the voltage of the current and was measured by a Gauss meter inserted into the inlet placed in the middle of the cylinder for this purpose. The solenoid was housed inside a metal box, making it possible to be autoclaved as part of the system without being damaged.

The MFG was attached to an AC/DC converter apparatus, which converted alternating to direct current, resulting in production of a static electromagnetic field inside the solenoid.

Culture circulated outside of the STR through tubing leading to a glass tube of the same diameter. The glass tube was placed inside the solenoid. At each given point of time, 8 mL of culture was exposed to the MFG. This is based on the volume of glass tube inside the solenoid. Since the circulation rate of culture was constant in all experiments carried out in this research, residence time was 0.8 min.

Schematic design of the MFG and the set-up of fermentation process is presented Fig. 10 and Fig. 11.

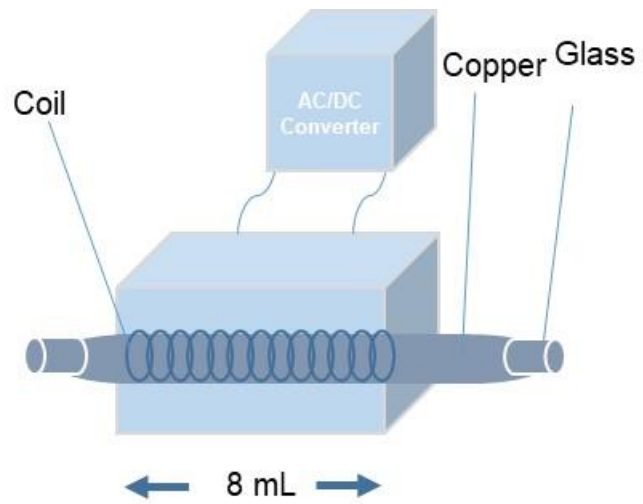


Figure 10. Schematic design of MFG

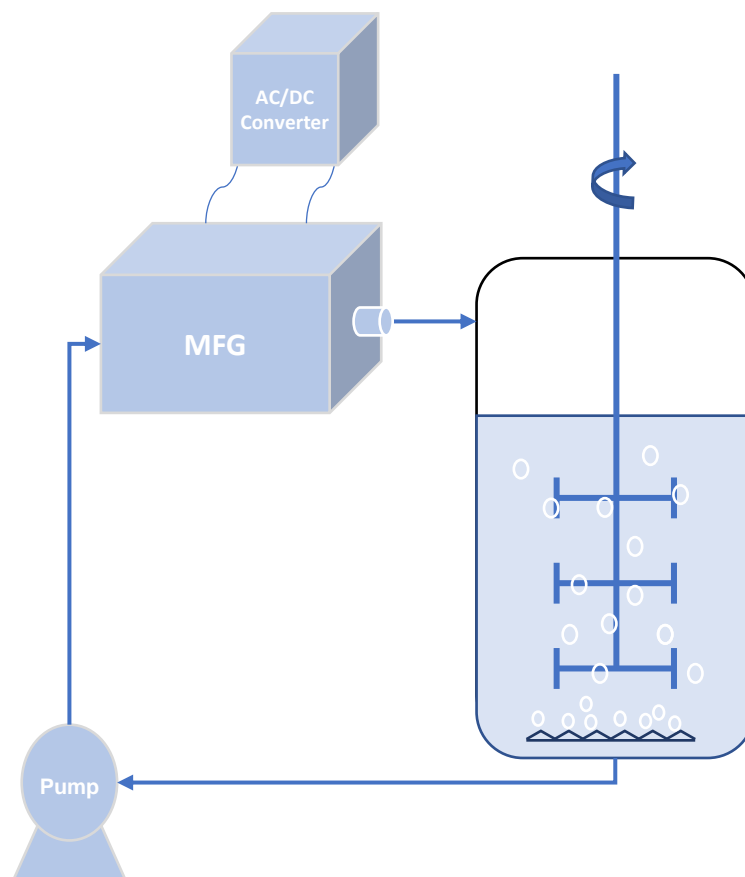


Figure 11. Schematic design of MFG coupled with bioreactor process system

2.1.3.3. Shaker/incubator

Cultures were incubated in New Brunswick Innova 4430 orbital shaker incubator from Thermo Fisher Scientific.

2.1.3.4. HPLC

High pressure liquid chromatography (HPLC) assay for detection of bacitracin in samples obtained from *B. licheniformis* cultures was carried out using Thermo Scientific UltiMate 3000 RSLCnano model HPLC apparatus. Data was detected and analysed through Chromeleon™ Software by Thermo Scientific.

2.1.3.5. FTIR spectroscopy

PerkinElmer FT-IR spectrometer, Spectrum two (UATR 2) model was used for FTIR analysis. Spectrum software, application version 10.4.3.339 by PerkinElmer, Inc. was used for obtaining data from the spectrometer.

2.1.3.6. Freeze drier

Freeze drier was Thermo Savant ModulyoD.

2.1.3.7. pH meter

Metler-Toledo S230 pH/conductivity meter was used for pH measurements. The probes were soaked in KOH (3 M) buffer.

2.1.3.8. spectrophotometer

Jenway 6503 UV-vis spectrophotometer was used for spectrophotometric measurements.

2.1.3.9. Balances

Sartorius analytical balance, model number AZ124/ 29212222 and Pioneer balance, Ohaius model were used.

2.1.3.10. SEM

Scanning Electron microscope was used for bacterial images. This equipment was Quanta scanning electron microscope, model: FEI Quanta 200F. This was carried out at the school of Pharmacy of the University College London.

2.2. Methods

Methodology of using materials described above are explained in this section. These methods include preparation and maintenance techniques, processes used (including PHB production and extraction) and chemical and biochemical assays carried out.

2.2.1. Maintenance and preparations

Culture maintenance, inoculum and media preparation techniques are described below.

2.2.1.1. Culture maintenance

Stock cultures were maintained in sterile nutrient broth (31 g.L^{-1}) containing 20% glycerol in cryovials and were kept at $-18 \text{ }^{\circ}\text{C}$.

Working cultures of each bacterial strain were obtained by incubating a single colony on sterile nutrient agar slants (containing approx. 15 mL of nutrient agar) at $37 \text{ }^{\circ}\text{C}$ for 48 h in an incubator. These slants were then maintained at $4 \text{ }^{\circ}\text{C}$ and reused for making fresh petri dish cultures with single colonies for inoculum preparations.

Culture of each bacterial strain was then transferred from slants onto petri-dishes containing nutrient agar (NA) via streaking method. This was performed under aseptic conditions (use of Bunsen burner flame). The petri dishes were then incubated for 24 h at $37 \text{ }^{\circ}\text{C}$ in an incubator.

2.2.1.2. Media

Minimal medium (M20) was used for growth of *B. licheniformis* and bacitracin production. M20 chemicals were added to de-ionized water and autoclaved at 121 °C for 15 min. L-Glutamic acid and FeSO₄·7H₂O were filter-sterilised separately (using a 0.2 µm syringe filter) into the sterile solution. pH of the medium was adjusted to 6 by addition of 4 M NaOH solution.

A modified G medium (MGM) with sucrose as main carbon source as described by Akaraonye et. al, was used as P(3HB) production medium for growth of *B. subtilis* NCTC 3610 (Akaraonye et al., 2010). The medium constituents were as follows:

The minimal salts medium was sterilised at 121 °C for 15 min in an autoclave. Sucrose was prepared and sterilised in the autoclave separately at 110 °C for 10 min and mixed aseptically with the salts after sterilisation. Trace elements (FeSO₄, MnSO₄·H₂O, CoCl₂, ZnSO₄·7H₂O and CuSO₄·5H₂O) were added to the sterile mixture by filter sterilisation using syringe driven filters of 0.2 µm pore size.

E2 medium supplemented with glucose was used as P(3HB) production medium for growth of *P. putida* KT2440 (Le Meur et al., 2012).

Trace elements were prepared as a stock by dissolution in 1 M hydrochloric acid.

The trace elements consist of FeSO₄ (2.78 g. L⁻¹), CaCl₂·2H₂O (1.47 g. L⁻¹), MnCl₂·4H₂O (1.98 g. L⁻¹), CoCl₂·6H₂O (2.38 g. L⁻¹), CuCl₂·2H₂O (0.17 g.L⁻¹) and ZnSO₄·7H₂O (0.29 g.L⁻¹).

Minimal medium salts: NaNH₄HPO₄·4H₂O 3.5 g. L⁻¹, KH₂PO₄ 3.7 (g. L⁻¹), K₂HPO₄ (7.5 g. L⁻¹) dissolved in water and 1 mL. L⁻¹ of MgSO₄·7H₂O (246.5 g. L⁻¹) were autoclaved at 121 °C for 15 min. Glucose was autoclaved separately at 110 °C for 10 min and added afterwards. The trace elements (1 mL. L⁻¹) and MgSO₄·7H₂O (1 mL. L⁻¹) were filter sterilised and added to the above.

2.2.1.3. Inoculum preparation

Inocula were prepared by growing pre-inocula of the specified bacterial strains. This was performed by inoculating required number of 100 mL shaken flasks (SF) containing 20 mL of the relevant production/growth medium for each strain. Each shaken flask was then inoculated under aseptic conditions (close to a Bunsen burner) with a loopful of single colonies of the relevant strain grown on petri dishes prior to each run. These were then incubated in a rotary shaker at culture conditions specific for each (37°C, 200 rpm for *B. licheniformis*; 30 °C, 200 rpm for *B. subtilis* and 37 °C and 180 rpm for *P. putida*). The cultures were incubated for approx. 12 h and were used (10 mL) to inoculate 500 mL shaken flasks containing 90 mL of the relevant medium (M20, MGM or E2). The shaken flasks were then incubated under the relevant condition (same as for 50 mL flasks) for approx. 16 h, after which time, they were used as inoculum for 2 L benchtop bioreactors (10% v/v).

For SF runs, the inocula was prepared by transferring a loop full of *B. licheniformis* into sterile 20 mL nutrient broth in 100 mL shaken flasks. This was then incubated for 16 h at 37°C and 200 rpm. 2 mL of the 16 h old inoculum was then used to inoculate 18 mL of M20 medium in 100 mL SFs for the SF process.

2.2.2. Processes

Two processes were used in the presented experiments; shake flask and bioreactor fermentation. Full specification and methodology used in these processes is described below.

2.2.2.1. Shaken flask (SF) fermentation process

Shaken flask study of the growth curve of *B. licheniformis* was performed in triplicates of 500 mL shaken flasks with 100 mL working volume and 10% inoculum. Shaken flasks were placed in a rotary shaker at 200 rpm with controlled temperature at 37°C.

For shaken flask runs with the MFG, 100 mL shaken flasks with 20 mL working volume were inoculated with 2 mL aerobic 16-hour-old inoculum. The shaken flasks were placed in a water bath, where temperature and shaking was controlled at 37 °C and 200 rpm, respectively.

Each shaken flask had an outside circulation. This was through a multichannel peristaltic pump. One of the shaken flasks was attached to the MFG, which has been denoted as “the test SF”. The setup without the MFG system, is denoted as “the control SF” in this thesis. Fig. 12 shows the experimental set up of the test and the control SFs used in these experiments. The setup with the MFG is designated as “Test”.

Conditions for bacitracin production from *B. licheniformis* were: 10% of working volume inoculum, temperature 37 °C and 200 rpm shaker speed.

Conditions for P(3HB) production from *B. subtilis* were: 10% of working volume inoculum, temperature 30°C and 200 rpm shaker speed.

Conditions for P(3HB) production from *P. putida* were: 10% working volume inoculum, temperature 30 °C and 180 rpm shaker speed.

As shown in Fig. 12 the water bath was used to keep the desired temperature and rotation.

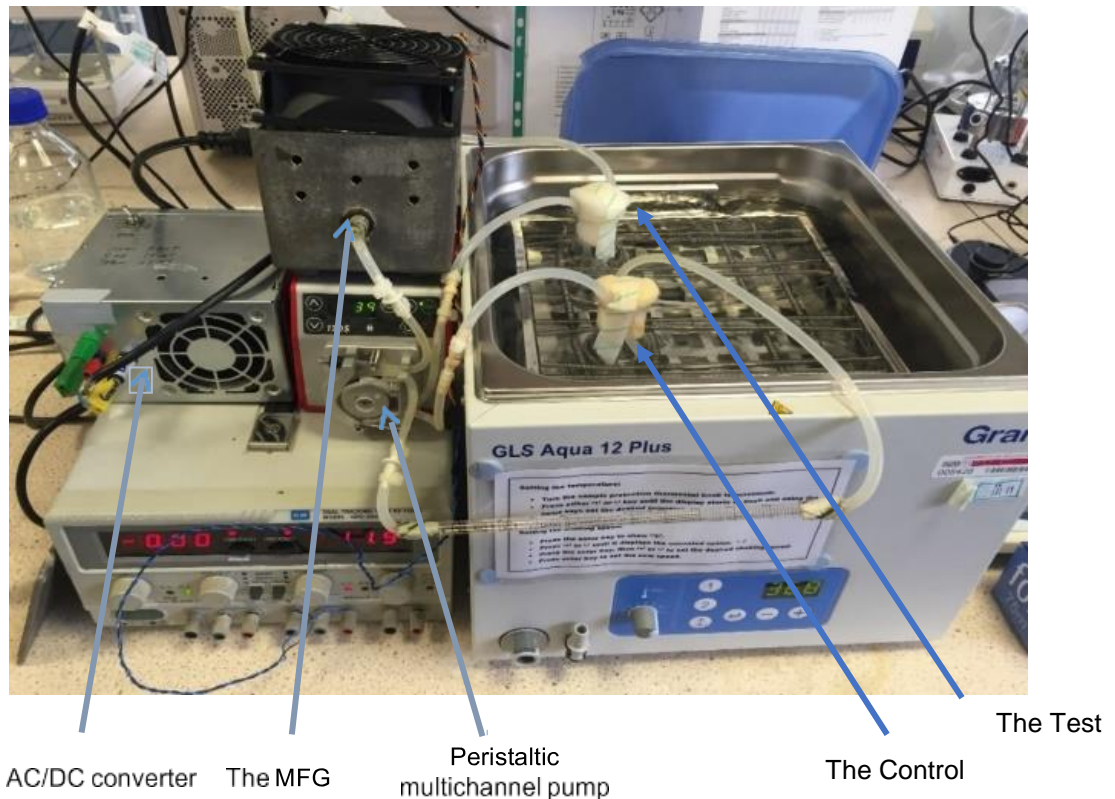


Figure 12. Complete process set-ups. The test shaken flask (back) is attached to the MFG, with circulation of microbial culture via the pump. The control shaken flask (front) is attached to a peristaltic pump to mimic the effects of outside circulation.

2.2.2.2 Bioreactor fermentation

Two 2-L STRs (1.5 L working volume) were used in this study. These were Electrolab FerMac310/60 attached to their individual control stations. Each had three turbine type impellers.

Novel bioprocess modifications were made to one STR (coupled with the MFG), where a controlled circulation system was added to the bioreactor allowing for batch mode fermentation. This modification was made after consideration of process design factors. All experiments were carried out in batch mode.

Each STR was inoculated with 150 mL of aerobic 16-hour-old bacterial inoculum (as mentioned earlier). In STR runs, each bioreactor had an outside circulation using a peristaltic pump. One of the STRs was attached to the MFG, which has been denoted as “the test STR”. The setup without the MFG system, is denoted as “the control STR” in this thesis. Fig. 13 shows the complete process set-up. The setup with the MFG system, is designated as “the Test STR”.

Fermentation conditions for bacitracin production were: 10% working volume inoculum, temperature 37°C, air flow-rate 1 vvm, Dissolved Oxygen kept above 30% air saturation level by changing the agitation rate between 200-600 rpm.

Foaming was controlled by an automated sterile anti-foam addition system. The antifoam used for this purpose was of organic nature (Antifoam 204, Sigma).

Fermentation conditions for P(3HB) production by *B. subtilis* and *P. putida* were: 10% working volume inoculum, temperature 30°C, air flow-rate 1 vvm, Dissolved Oxygen kept above 40% saturation level by changing the agitation rate between 200-600 rpm.

Samples were taken from the STRs at different time points. Optical density (OD) was measured for each sample at wavelengths related to each strain (650 nm for *B. licheniformis* and 600 nm for *B. subtilis* and *P. putida*). Each sample was observed under light microscope, plated out using streak plate method for colony counts and then centrifuged at 11,000 rpm for 10 min, pellets and supernatants were separated and used in further analysis and assays including HPLC, total carbohydrate assay, glutamic acid assay, crotonic acid assay and glucose assay.

The exit gas (%CO₂) after passing through the condensers was detected and analysed by FerMac 368 Gas Analyser. The gas analyser was calibrated using

a standard gas mixture containing 5.09 % CO₂, 18.28 % oxygen, and 76.63 % nitrogen.

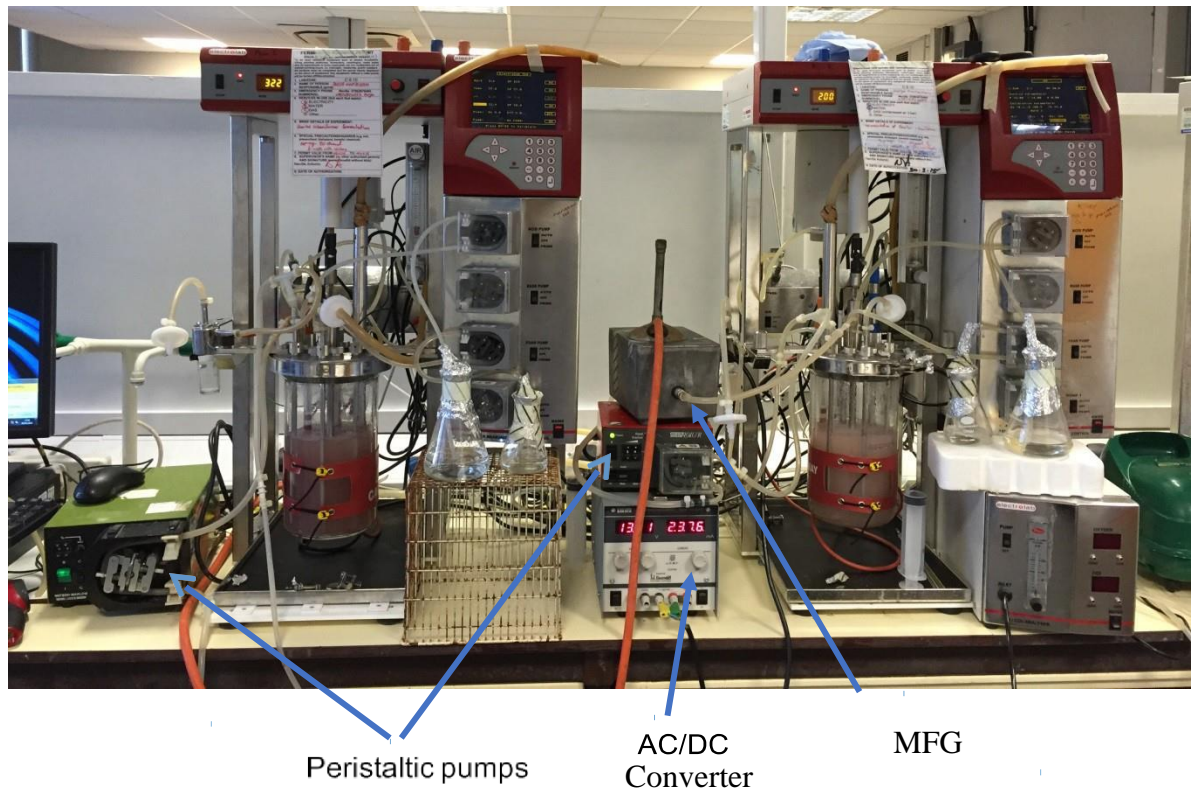


Figure 13. Complete process set-ups. The test bioreactor (right) is attached to the MFG, with circulation of microbial culture via the pump. The control bioreactor (on the left) is attached to a peristaltic pump to mimic the effects of outside circulation.

2.2.3. Procedures

Samples taken from the runs described above along with those from the control were assayed and compared. To this end, a range of microbiological and biochemical assays were carried out. The analytical techniques included spectrophotometry and High-Performance Liquid Chromatography (HPLC), and the biochemical assays include total carbohydrate assay, Glutamic acid assay, crotonic acid assay and Sudan Black test.

2.2.3.1 Optical Density (OD) measurements

The biomass concentration of *B. licheniformis* was calculated based on optical density measurements of the samples at 650 nm (OD₆₅₀), with sterile M20 medium as blank.

The biomass concentrations of *B. subtilis* and *P. putida* were calculated based on optical density measurements of the samples at 600 nm (OD₆₀₀), with sterile MGM and E2 medium as blank, respectively.

2.2.3.2 Colony Forming Unit (CFU) counts

Samples of each run were diluted in series up to 10⁸-fold with phosphate buffer. Diluted samples (100 µL) were spread on nutrient agar petri dishes using spread plate technique. This was performed under aseptic conditions.

The cultures were then incubated at 37 °C for 24 h. Number of colonies formed on each plate were then counted by naked eye and reported as CFU per mL of culture medium.

Each spread plate was performed in triplicates.

2.2.3.3 Cell dry weight (CDW)

Samples taken from each STR (10 mL) at different time points, were centrifuged at 8,000 rpm for 10 min in pre-weighed falcon tubes. The cell pellet was then freeze-dried and weighed. The weight difference between the empty tubes and freeze-dried samples per mL of total liquid sample, was denoted as cell dry weight at the given time point.

2.2.3.4 High Performance Liquid Chromatography (HPLC)

Bacitracin was detected using an optimised reversed phase chromatography method. This method was published previously (Pavli and Kmetec, 2001). However, the column used was a new version of the one described in their paper hence the method was optimised and modified.

This method used a gradient elution system, with a C8 Kinetex column from Phenomenex, and the following buffers:

Buffer A: Methanol – acetonitrile (1:1 v/ v) – KH_2PO_4 (0.05 M, pH=6.0): (44:56 v/v).

Buffer B: Methanol – acetonitrile (1:1 v/ v) – KH_2PO_4 (0.05 M, pH=6.0): (55:45 v/v).

The program was 20 minutes for each sample, at the optimum temperature of 40°C , flow-rate of $1.4 \text{ mL}\cdot\text{min}^{-1}$, UV detection at 254 nm and $20 \mu\text{L}$ injection.

A standard curve was obtained by running standard samples from zinc bacitracin standard solutions of 1000, 800, 600, 400, 200, 100, 0 $\text{mg}\cdot\text{L}^{-1}$

All samples were assayed in duplicates and standards were assayed in triplicates.

2.2.3.5 Total carbohydrate assay

This assay was performed based on a previously optimised method. Phenol (5% solution, $200 \mu\text{L}$) was added to $200 \mu\text{L}$ of sample in an Eppendorf tube, to which 1 mL sulfuric acid was added slowly.

The mixture was left undisturbed for 10 minutes and was mixed on a vortex afterwards. Thirty minutes was allowed for the reaction to take place.

Each sample was then transferred into a 96-well-plate ($180 \mu\text{L}$) and absorbance read at 490 nm in a microplate reader.

A standard curve was produced using known concentrations of glucose solution (0-100 $\text{g}\cdot\text{L}^{-1}$).

All samples and standards were analysed in triplicates.

2.2.3.6 Glucose assay

Glucose concentration of each sample was determined by using glucose assay based on enzymatic quantification method (Sigma Aldrich- Glucose (HK) Assay Kit Product Code GAHK-20).

Each sample was centrifuged at 11,000 rpm for 10 min and the supernatant was separated. Amount of glucose content in supernatant was measured according to manufacturer's instructions.

A standard curve was produced using glucose standard solution provided in the assay kit.

Assay was performed on triplicate samples/standards.

2.2.3.7 L-Glutamic acid assay

L-Glutamic acid was quantified using a previously optimised colorimetric method (Sukan, 2015). Ninhydrin reagent was prepared by addition of equal volumes of the following solutions:

Solution A: Stannous chloride (1.6 g.L^{-1}) was added to Citrate buffer (0.2 M) at pH=5

Solution B: Ninhydrin was dissolved in 2-methoxyethanol to reach a concentration of (40 g.L^{-2}).

Solution A was then added to solution B. The reagent was stored at -20°C away from light.

Each diluted fermentation sample/standard was added to an Eppendorf tube (50 μl), 450 μl de-ionized water and 500 μl of ninhydrin solution were added. The solution was then mixed well on vortex and placed in boiling water for 20 minutes after which time, 150 μl of each was added to the wells of a 96-well-plate and 50 μl of diluent solution consisting of 1:1 v/v of n- propanol and water was added to each well. Incubation took place for 15 minutes in the dark after which time; the absorbance was measured in a microplate reader at 570 nm.

This method detects up to $100 \mu\text{g.L}^{-1}$ of Glutamic acid.

Standards and samples were analysed in triplicates.

2.2.3.8 P(3HB) extraction

Cells were harvested by centrifugation at 6000 rpm for 15 min. Pellets were then freeze dried for 48 h. For every gram of the freeze-dried cells, 50 mL of chloroform and 50 mL of 15% sodium hypochlorite solution was added.

This mixture was incubated in a rotary shaker at 100 rpm and 37 °C for 1 h. This was then centrifuged at 4000 rpm for 10 min, after which time three different phases were obtained. The bottom phase (chloroform) was then pipetted out of the mixture, to which 10 volumes of ice-cold methanol was added and left over night for precipitation of P(3HB) (Law and Slepecky, 1961).

2.2.3.9 Crotonic acid assay

An optimised method of crotonic acid assay defined by Law and Slepecky (1961) was used to quantify the PHB content of the cultures of *P. putida* and *B. subtilis*.

The extracted P(3HB) from the chloroform phase, was re-dissolved in chloroform and 100 µl was transferred into a clean tube, air dried and mixed with 5 mL concentrated sulfuric acid. The tube was incubated in an 80 °C water bath for 1 h and was mixed vigorously, but intermittently before incubation, half-way through and after incubation. The addition of sulfuric acid converts the polymer to crotonic acid, which is detectable at 235 nm and the concentration was calculated using a calibration curve.

Calibration curve was produced by running crotonic acid assay as described above on known standard solutions prepared from standard PHB (Sigma Aldrich, UK) with concentration range of 0-1 mg/mL.

2.2.3.10 Sudan Black test

P. putida and *B. subtilis* samples from the bioreactors were grown on nutrient agar petri dishes for 48 h. Approx. 8 mL Sudan black solution (0.02% Sudan black B in 96% ethanol) was poured and spread on the petri dishes, which

were incubated for 30 min. The solution was then decanted and stained cultures were rinsed with 10 mL of 96% ethanol to wash excess dye. The dark blue coloured colonies were regarded as positive for P(3HB) (Agrawal et al., 2015).

2.2.3.11 Microscopic observations

Samples taken from each fermentation experiment, were observed straight after sampling without pre-treatment/staining. Bacterial fermentation samples (10 μ L) were placed on a microscope slide, covered with a cover slip and observed using X400 magnification of a Nikon microscope with phase contrast settings.

Phase contrast microscopy can indicate the P(3HB) inclusion bodies formed within the cells and helps with identification of P(3HB) production.

2.2.3.12 Nile red staining and Confocal microscopy

PHB granules inside bacterial cells were visualised using Nile red staining and confocal microscopy method (Jendrossek et al., 2007). The bacterial cells of each sample were collected as the pellet obtained from centrifugation of bioreactor samples at 11,000 rpm for 10 min. Nile red solution 0.02 to 0.1 volumes ($0.5 \mu\text{g. mL}^{-1}$ in ethanol) was then added to the cell pellet. Bacteria were then immobilised by placing $10 \mu\text{g. mL}^{-1}$ of the cell suspension on a microscope slide covered with a cover slide and was fixed with heat. The cells were then imaged on a Leica confocal laser scanning microscope. Nile red was excited with 543 nm light (green helium-neon laser).

2.2.3.13 Scanning Electron Microscope (SEM)

The morphological effect of magnetic field on bacterial strains used in this study was investigated using a Scanning Electron Microscope. The imaging of the bacterial cells was carried out at the University College London School of Pharmacy, London, UK.

The cells were centrifuged at 11,000 rpm for 10 min, cell pellets of approx. 100 μL were fixed using 1.5 mL of 3% glutaraldehyde buffer. These samples were then centrifuged again and pellets were freeze dried. Images were taken from these freeze-dried pellets.

2.2.3.14 Fourier Transform Infrared Spectroscopy (FTIR)

Fourier Transform Infrared Spectroscopy (FTIR) was used as a method for identification of the type of PHA and confirmation of P(3HB) chemical structure. The FTIR system used in this study was a Perkin Elmer System 2000 FTIR spectrophotometer.

Standard sample of P(3HB) purchased from Sigma Aldrich were analysed directly on the diamond crystal of the system. Infrared absorption spectra was then recorded over the wavelength region of 4000-500 cm^{-1} . Spectra were collated and compared based on 64 scans with 2 cm^{-1} resolution.

2.2.3.15 Statistical analysis

Data obtained from each set of experiments, was taken in duplicates/triplicates for statistical reproducibility and each set of experiments was carried out twice/three times, for biological reproducibility studies.

These data were analysed using one-way analysis of variance (ANOVA). This was then followed by Tukey-Kramer test. P values of less than 0.05 were considered significant. Data analysis was carried out in Microsoft Office Excel software version 2016.

2.2.4. Calculations

Results of each experiment have been reported in this thesis. Calculations of specific growth rates, nutrient uptake rates, product yield, product formation rate, carbohydrate formation rate, residence time of the culture in the MFG and number of circulations are described in this section.

2.2.4.1. Specific growth rate

Specific growth rate was calculated as the gradient of the growth profile in logarithmic scale using the equation below:

$$\mu = \frac{1}{X} \times \frac{dX}{dt} \quad 1. \text{ Calculation of specific growth rate}$$

μ : Specific growth rate (h^{-1})

X: Cell Dry Weight (g. L^{-1})

t: Time (h)

2.2.3.2. Nutrient uptake/consumption rate

Nutrient uptake rate was calculated using the nutrient concentration at certain time points using the equation below.

$$S = \frac{|\Delta C|}{\Delta t} \quad 2. \text{ Calculation of substrate consumption rate}$$

S: substrate uptake/consumption rate ($\text{g. L}^{-1} \text{ h}^{-1}$)

ΔC : Substrate concentration change at period of Δt (g. L^{-1})

Δt : Time period for rate calculation (h)

2.2.3.3. Product yield

Calculation of cell product yield was carried out using the product concentration against cell dry weight over a given period of time.

$$Y_{p/x} = \frac{\Delta P}{\Delta X} \quad 3. \text{ Calculation of product yield}$$

$Y_{p/x}$: cell production yield ($\text{g. L}^{-1} \text{ product/g. L}^{-1} \text{ CDW}$)

Δp : Product concentration change at period of Δt (g. L^{-1})

Δx : Cell dry weight change at period of Δt (g. L^{-1})

2.2.4.2. Product formation rate

Production rate of bacitracin and P(3HB) was calculated using the concentration of product over a period of time.

$$Q_p = \frac{\Delta p}{\Delta t}$$

4. Calculation of product formation rate

Q_p = Rate of product formation (mg. L⁻¹ h⁻¹)

Δp = Change of product concentration at period Δt (mg. L⁻¹)

Δt = Time period (h)

2.2.4.3. Residence time in MFG

Residence time of fermentation culture in the MFG device was calculated based on the dimensions of glass tube inside the solenoid, which determines volume of exposed culture. Residence time can be calculated using Eq. 5.

$$t_R = \frac{V}{F}$$

5. Calculation of Residence time in the MFG

t_R : Residence time (min)

F : Flow rate (mL. min⁻¹)

V : Culture volume (mL)

The glass tube used in these studies had a capacity of 5 mL. This part was completely installed inside the solenoid. The volumetric flow rate for circulation through the MFG was 10 mL. min⁻¹ in the experiments carried out in this study. Therefore, residence time was 0.5 min.

2.2.4.4. Number of circulations through the MFG

Number of circulation of the total culture at a given time can be calculated as below.

$$n = \frac{V_T}{F \times t}$$

n : number of circulations of the total culture through the MFG

V_T : Total culture volume (mL)

F: circulation rate (mL. min⁻¹)

t: Time (h)

Chapter 3

Results

3. Results

Results of this study are presented under three categories based on the microorganisms under investigation; *Bacillus licheniformis*, *Bacillus subtilis* and *pseudomonas putida*.

The first strain in this research is *B. licheniformis* as a gram-positive model bacterium producing antibiotic bacitracin. This strain is analysed in relation to four factors: biomass concentration, bacitracin concentration, total carbohydrate content and glutamic acid consumption.

Results of each factor are reported within four experimental set-ups depending on the intensity of the magnetic field and the scale of the process. These set-ups include:

- Small-scale study in 100 mL shaken flasks with magnetic field intensity of 28 mT.
- Laboratory-scale STRs with 2L total volume with magnetic field intensity of 28 mT.
- Laboratory-scale STRs with 2L total volume with magnetic field intensity of 10 mT without pH control.
- Laboratory-scale STRs with 2L total volume with magnetic field intensity of 10 mT with pH control.

The studies on *B. licheniformis* aim to prove the possibility of scale-up of the system. Therefore, the next experimental results are dedicated to the effects of magnetic field on two strains producing biopolymer P(3HB).

The second strain reported in this chapter is *B. subtilis* as a Gram-positive model bacterium to produce P(3HB). Factors considered in this analysis are biomass concentration, morphological changes to the cells, P(3HB) confirmation and its concentration.

Results of each factor are reported within two experimental batch set-ups of STRs with two intensities of magnetic field, as outlined below:

- Laboratory-scale STRs with 2L total volume with magnetic field intensity of 18 mT.
- Laboratory-scale STRs with 2L total volume with magnetic field intensity of 28 mT.

The third strain reported in this chapter is *P. putida* as a Gram-negative model bacterium for the production of P(3HB). Factors considered in this analysis are biomass concentration, morphological changes to the cells, confirmation of P(3HB) formation with FTIR, P(3HB) concentration and glucose consumption. Results of each factor are reported within two experimental batch set-ups of STRs with two intensities of magnetic field as outlined below:

- Laboratory-scale STRs with 2L total volume with magnetic field intensity of 18 mT.
- Laboratory-scale STRs with 2L total volume with magnetic field
- Intensity of 28 mT.

Table 10. An outline of the results presented in this thesis

Overview of results structure					
	Batch Number	<i>Bacillus licheniformis</i>	<i>Bacillus subtilis</i>	<i>Pseudomonas putida</i>	
Parameters	1	Biomass concentration	Biomass concentration	Biomass concentration	
	2	Bacitracin concentration	Morphological changes to the cells	Morphological changes to the cells	
	3	Total carbohydrate content	P(3HB) confirmation and concentration	Confirmation of polymer's chemical structure with FTIR	
	4	Glutamic acid consumption	-	P(3HB) concentration	
	5	N/A	N/A	Glucose consumption	
Fermenters; magnetic field intensity	1	Shaken flask	100 mL	2 L	2 L
		Magnetic field intensity	28 mT	18 mT	18 mT
	2	STR	2 L	2 L	2 L
		Magnetic field intensity	28 mT	28 mT	28 mT
	3	STR	2 L	-	-
		Magnetic field intensity	10 mT	-	-
	4	STR	2 L	-	-
		Magnetic field intensity	10 mT and pH control	-	-

3.1. Studies on the effect of magnetic field on *Bacillus licheniformis*

The MFG was used in SFs and STRs with two intensities of magnetic field (10 and 28 mT). This section covers experiments carried out to investigate the effect of magnetic field on growth profile, pH profile, product (bacitracin) concentration, substrate uptake and total carbohydrate profile of cultures of *B. licheniformis*.

The two MF intensities were chosen based on previous studies (summarised in the introduction chapter). Increased product and growth rates were observed between 5-30 mT. The initial 28 mT intensity was chosen as an upper intensity (Perez et al. 2007 reported highest ethanol productivity of *S. cerevisiae*) and 10 mT as lower intensity.

3.1.1. SF fermentation of *B. licheniformis* with 28 mT magnetic field

The SF fermentation studies were carried out three times in 100 mL shaken flasks with 20 mL working volume, where the medium was inoculated with 10% (2 mL) inoculum. Magnetic field (MF) intensity was set at 28 mT with the culture circulating through the MFG at a circulation rate of 10 mL.min⁻¹. This rate was chosen based on total volume of the liquid and tubing to provide maximum exposure. The circulation rate was kept the same in STR cultures to keep the same residence time. Results of a representative run are presented in this section.

3.1.1.1. Effect of 28 mT magnetic field on growth profile of *B. licheniformis* in SFs

Growth profile of *B. licheniformis* was obtained by OD₆₅₀ measurements at different time points of the fermentation period.

Fig. 14 shows the results obtained from these measurements in the control and MF exposed culture. Readings were taken in duplicates; error bars show standard deviation between these readings.

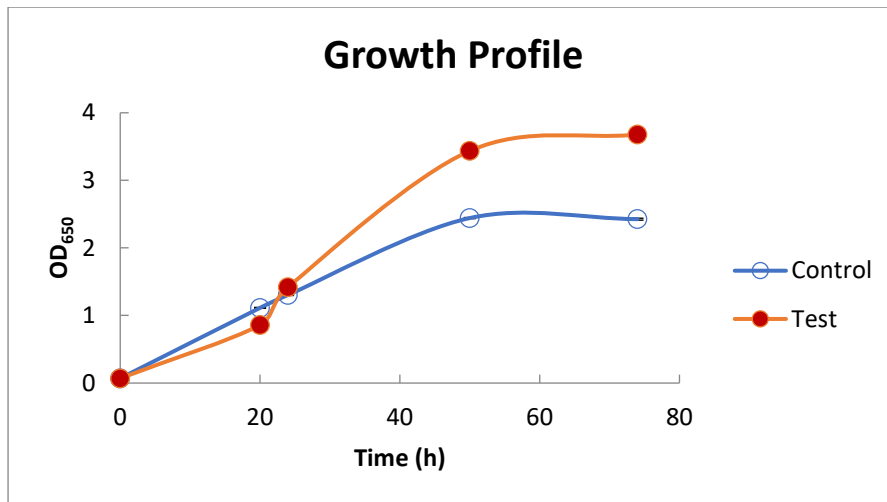


Figure 14. Growth profile of *B. licheniformis* in shaken flasks. The test was exposed to 28 mT MF.

Fig. 14 shows the growth profile of *B. licheniformis* in shaken flasks. Optical density in the control and the test cultures increased to around 1.4 after 24 h of incubation. The test culture had a further increase and reached its maximum of 3.4 after 50 h. The control culture also reached its maximum of 2.4 at the same time. The higher OD₆₅₀ in the test after 50 h, shows that higher biomass concentration was obtained after 1500 rounds of circulation of the culture through the MFG.

Growth profile of the two SFs on logarithmic scale is shown in Fig. 15.

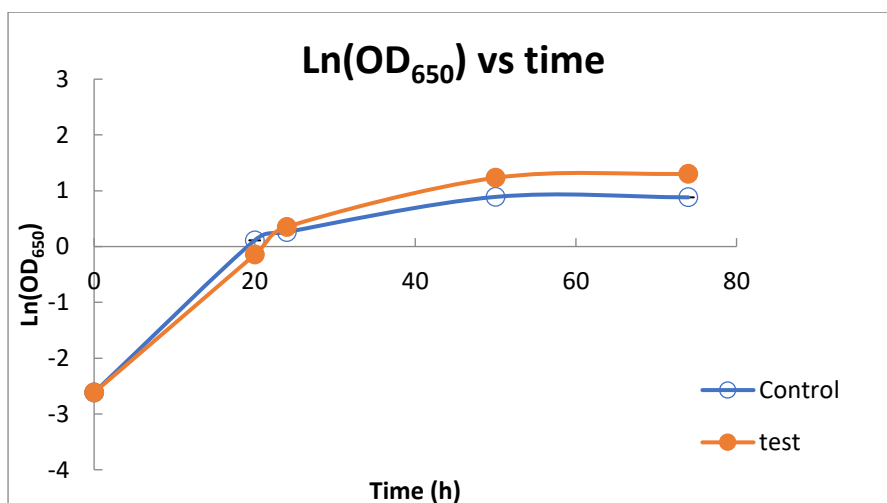


Figure 15. Logarithmic scale growth profile of *B. licheniformis* in shaken flasks. The test was exposed to 28 mT MF.

As shown in Fig. 15, both the control and the test followed the same growth trend, with doubling times of 10 and 9 h in the control and the test, respectively.

Table 11 below shows the results of percentage difference calculations of the growth rate and doubling time between the two SFs.

Table 11. Percentage differences of growth rate and doubling time between the test (exposed to 28 mT MF) and the control SFs

	<i>Growth rate (h⁻¹)</i>	<i>Doubling time (h)</i>
Control	0.067	10
Test	0.075	9
Percentage difference (%)	11.9	10

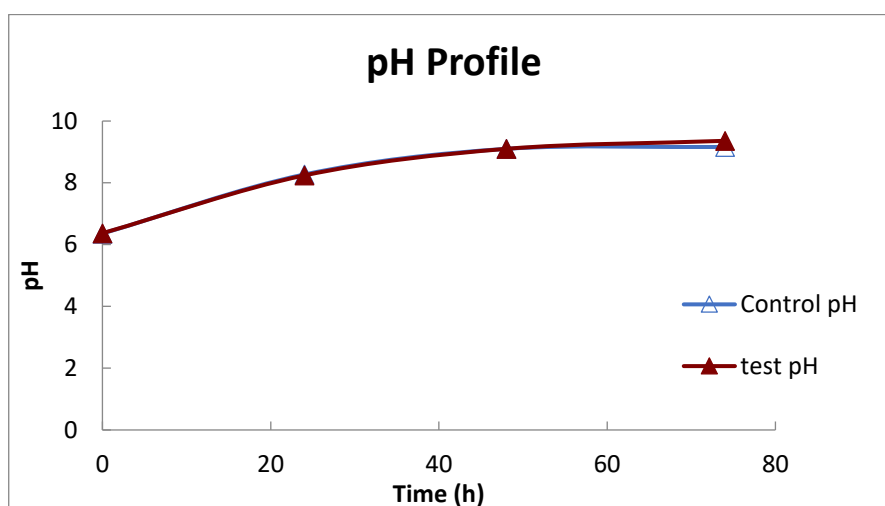


Figure 16. pH profile of *B. licheniformis* in 20 mL SFs. The test was exposed to 28 mT MF

Fig. 16 shows pH profiles of the Control and the Test cultures. It appears that the magnetic field had no effect on pH value of *B. licheniformis* culture.

3.1.1.2. Effect of 28 mT magnetic field on bacitracin concentration in SF cultures of *B. licheniformis*

The effect of magnetic field on bacitracin concentration was determined through HPLC analysis of the samples at different time points. Average of three bacitracin concentration measurements of each sample in both SFs are presented in Fig. 17.

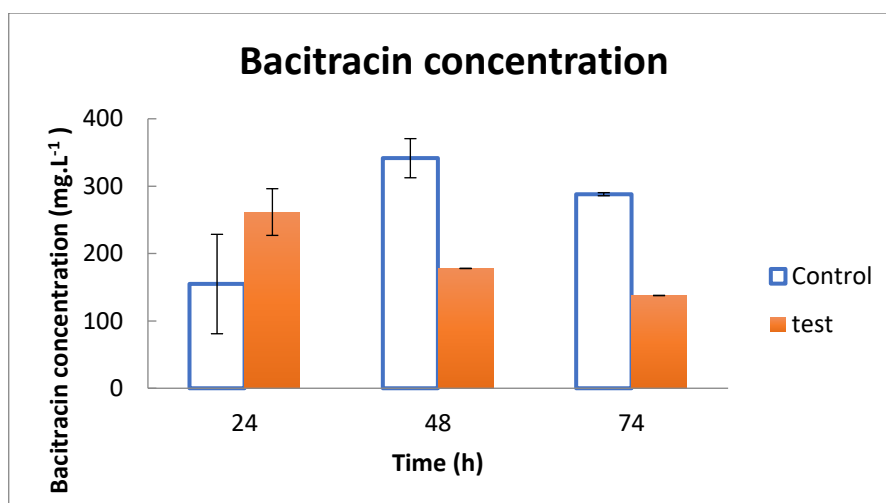


Figure 17. Bacitracin profile of *B.licheniformis* in 20 mL SFs based on average of three repeats. The test was exposed to 28 mT MF

As shown in Fig. 17, concentration of bacitracin followed different trends in the two SFs. The concentration in the control increased from 155 to 341 mg.L⁻¹ followed by a decrease to 288 mg.L⁻¹ after 74 h. However, bacitracin concentration in the test reached its maximum of 262 mg.L⁻¹ after 24 h and decreased to 138 mg.L⁻¹ eventually.

Table below summarises bacitracin production rates in the two SFs. Negative rate values indicate rate of decrease in concentration between the given time points. Positive values show increase in rates. Percentage differences are also reported between the test and the control cultures.

Table 12. Summary of bacitracin production rate of *B. licheniformis* in SFs at various stages of the runs. The test culture was exposed to 28 mT MF

<i>Time interval (h)</i>	<i>Control (mg. L⁻¹.h⁻¹)</i>	<i>Test (mg. L⁻¹.h⁻¹)</i>	<i>Percentage difference (%)</i>
0-24	6.4	10.9	69
24-48	7.8	-3.5	-145
48-74	-2.1	-1.5	-25

The test culture, which reached its maximum bacitracin content within the first 24 h, had 69% higher production rate (10.9 mg.L⁻¹.h⁻¹) than that of the control SF at 24h (6.4 mg.L⁻¹.h⁻¹). Culture medium had circulated 720 times through the MFG at this time point.

Bacitracin production rate of the control culture increased to 7.8 mg. L⁻¹.h⁻¹ between 24 to 48 h. In the test culture however, bacitracin production rate changed into a decreasing rate of 3.5 mg. L⁻¹.h⁻¹.

Bacitracin concentration then started decreasing between 48 to 74 h in the control culture at a rate of -2.1 mg. L⁻¹.h⁻¹. The test culture's bacitracin content decreased at a lower rate (-1.5 mg. L⁻¹.h⁻¹) than the control.

Although total bacitracin concentration was lower in the test culture after 24 h, production yield at this stage was 37 % compared to 24% in the control culture (Table 13).

Table 13 shows the yield of bacitracin per cell dry weight. Product yield in the control culture was 24-28% throughout the fermentation. Biomass of the test culture yielded 37% Bacitracin/CDW after 24 h, which decreased to 10% after the culture reached stationary phase.

Table 13. Bacitracin yield of *B. licheniformis* in 20 mL SFs. The test was exposed to 28 mT MF

(bacitracin concentration (g.L⁻¹) / Dry cell weight (g. L⁻¹) x100)

<i>Time (h)</i>	<i>Control bacitracin yield (%)</i>	<i>Test bacitracin yield (%)</i>
24	23.8	36.8
48	28.0	10.4
74	23.8	7.5

3.1.1.3. Effect of 28 mT magnetic field on Glutamic acid consumption of SF cultures of *B. licheniformis*

Glutamic acid was consumed in both SFs as the main carbon nutrient. The concentration of this compound was measured during the SF runs in samples of different time points. These data are presented in Fig. 18.

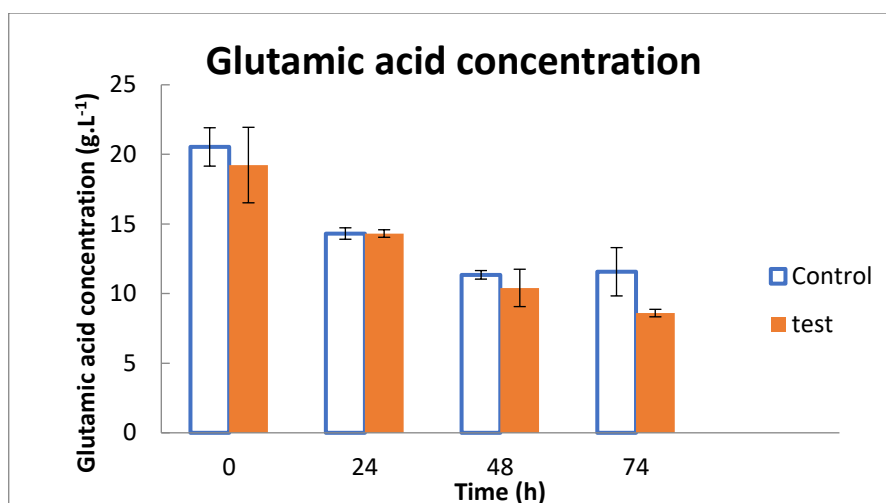


Figure 18. Glutamic acid consumption profile of *B. licheniformis* in 20 mL SFs. The test was exposed to 28 mT

The concentration of glutamic acid changed from the initial 20 g. L⁻¹ to around 11 g. L⁻¹ within the first 48 h in the control culture and remained the same afterwards. Glutamic acid concentration in the test culture followed a decreasing trend throughout the run and dropped to 8.6 g. L⁻¹ after 74 h of incubation.

Glutamic acid was consumed with the rate of 0.19 and 0.18 g. L⁻¹.h⁻¹ within the first 48 h in the control and the test SFs, respectively. The consumption was terminated after this time point in the control while it was still consumed in the test with a rate of 0.07 g. L⁻¹.h⁻¹.

3.1.1.4. Effect of 28 mT magnetic field on total carbohydrate content of SF cultures of *B. licheniformis*

The minimal growth medium used for growth of *B. licheniformis* in this study, did not contain any carbohydrates. The total carbohydrate content of the control and the test SFs was measured during the runs to investigate the release of polysaccharides throughout the run.

Fig. 19 shows the total carbohydrate content of the samples at different time points of the SFs throughout the run.

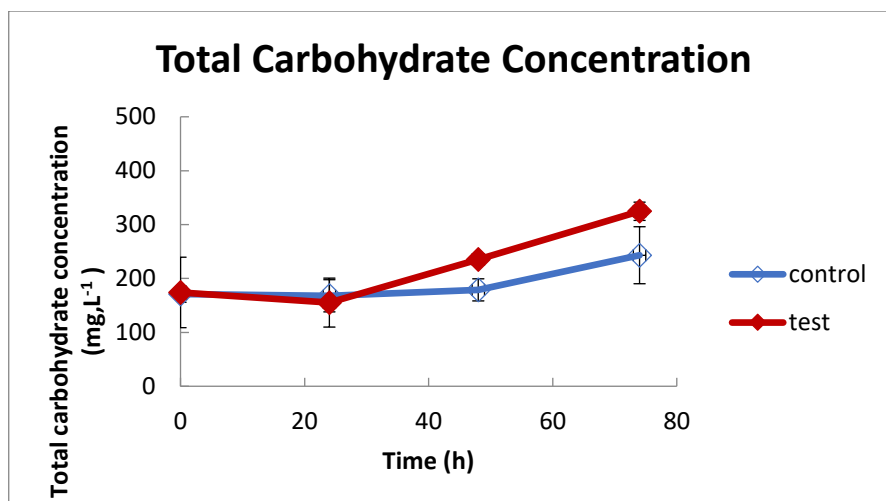


Figure 19. Total carbohydrate concentration of *B. licheniformis* in 20 mL SFs. The test was exposed to 28 mT

As shown in Fig. 19, total carbohydrate concentration increased in the medium of both cultures with percentage difference of 33% between the final concentrations in the test and the control. The initial carbohydrate concentration detected in both samples was due to carbohydrate content of the initial inoculum in nutrient broth.

These results indicate the release of carbohydrates into both the control and MF exposed cultures after 24 h. Table 14 below shows calculations of carbohydrate production rates in the two SFs.

Table 14. Summary of total carbohydrate production rates at two stages of growth of *B. licheniformis* in 20 mL SFs. The test was exposed to 28 mT

<i>Time interval (h)</i>	<i>Control (g. L⁻¹. h⁻¹)</i>	<i>Test (g. L⁻¹. h⁻¹)</i>
24-48	0.46	3.33
48-72	2.47	3.44

As shown in Table 14, the carbohydrate production rate in the control culture increased drastically after 48 h. The production rate of carbohydrates in the MF exposed culture remained almost the same between the two intervals of growth.

The release of carbohydrates started after 24 h in the test culture, while the culture was still at the logarithmic phase of growth and had circulated through the MFG for 720 rounds.

3.1.2. STR Batch fermentation of *B. licheniformis* with 28 mT magnetic field

Following the studies on the effect of magnetic field on *B. licheniformis* in shaken flasks, process scale was increased and the same design was applied to 2 L bench-top STRs.

The experimental set-up conditions were as follows: Two 2 L fermenters ran in parallel with working volume of 1.5 L, aeration rate of 1 vvm, agitation rate of 200 rpm, and DOT levels were kept at a minimum of 30%.

In order to eradicate potential effect of MF on cells at the beginning of growth and to keep MF exposure to end of logarithmic growth stage where bacitracin production started, MF exposure started after 16 h of incubation.

The magnetic field intensity was set at 28 mT with microbial culture circulating through the MFG at circulation rate of 10 mL.min⁻¹. The culture was circulated through the MFG for a total of 27 times at the end of these experiments.

The pH levels were monitored during the course of this fermentation but no pH control mechanism was applied.

The results of this section are shown through a representative run of duplicate runs.

3.1.2.1. Effect of 28 mT magnetic field on growth profile of *B. licheniformis* in STR

Growth profile of the control and MF exposed cultures was obtained through OD₆₅₀ measurement. These profiles are presented in Fig. 20. Values reported here are averages of duplicate readings from samples of a representative run. Error bars indicate standard deviation between the readings.

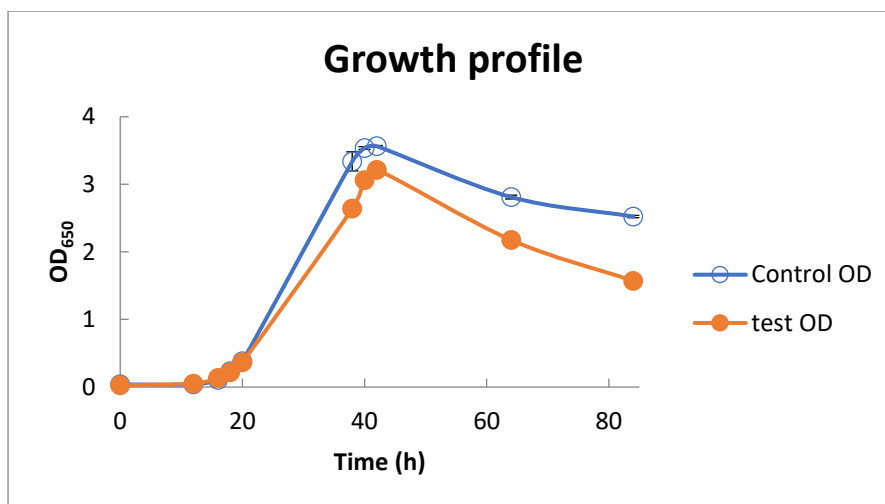


Figure 20. Growth profile of *B. licheniformis* in 2 L STRs. The test was exposed to 28 mT MF

As presented in Fig. 20, both cultures had a lag phase of 12 h, after which time the logarithmic growth phase started. The cells in the control culture reached a maximum of 3.6 after 42 h of incubation and the test culture reached its maximum of 3.2 at the same time.

Fig. 21 shows the growth profile of *B. licheniformis* in these experiments on logarithmic scale.

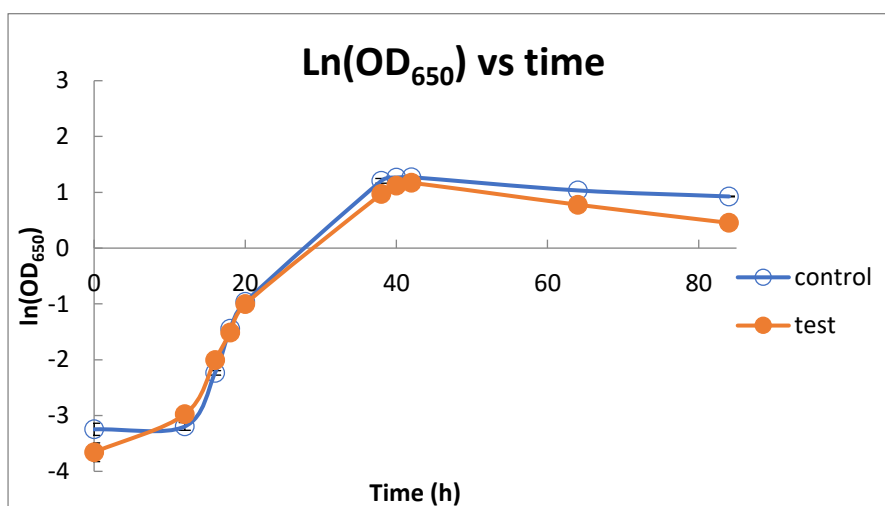


Figure 21. Growth profile of *B. licheniformis* in 2 L fermenters in logarithmic scale. The test was exposed to 28 mT MF

As shown in Fig. 21, the logarithmic growth phase started after 12 h and both cultures reached their stationary growth phase after 40h of incubation. Death phase started after 64 h of incubation.

The profile of growth in the test and the control cultures showed no significant difference between cell densities of the two STRs.

Doubling time of the STRs was calculated based on their maximum growth rates between 12-20 h (presented in Table 15).

Table 15. Growth rate and doubling time of *B. licheniformis* in 2 L STRs. The test was exposed to 28 mT MF

	<i>Growth rate (h⁻¹)</i>	<i>Doubling time (h)</i>
Control	0.27	2.55
Test	0.25	2.75
Percentage difference (%)	7.41	7.84

Table 16 shows the results of colony forming unit counts of averages of triplicate plates. The number of colony forming units is used as a measure of viable cells present in the samples of each STR at different time points.

Table 16. Colony forming unit counts in the samples taken from the two STRs of *B. licheniformis* in 2 L STRs. The test was exposed to 28 mT MF

<i>Time interval (h)</i>	<i>Control 10⁷ CFU. mL⁻¹</i>	<i>Test 10⁷ CFU. mL⁻¹</i>
16	22	17
38	172	161
42	204	200
64	266	250

These results are in line with the optical density measurements in the two STRs. This shows a decrease in the viability of cells under magnetic field exposure. After 8 rounds in the MFG at 38 h, number of cells in the test culture was 7% lower than that of the control culture.

pH profile of the two STRs is presented in Fig. 22 below.

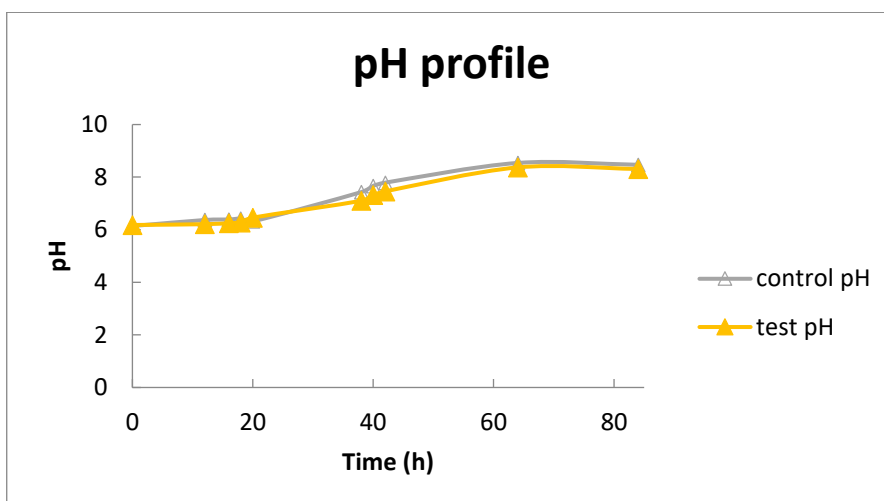


Figure 22. pH profile of the two STRs of *B. licheniformis* in 2 L STRs. The test was exposed to 28 mT MF

As shown in Fig. 22, the pH values of both control and test cultures increased from the initial value of 6 to 8.4 at 64 h.

pH value in both cultures remained at the optimum levels for bacitracin production until it reached around 7.3 at 40 h. It then increased further, making the culture medium undesirable for bacitracin stability.

3.1.2.2. Effect of 28 mT magnetic field on bacitracin concentration in STR cultures of *B. licheniformis*

Concentrations of bacitracin was determined throughout the fermentation period through HPLC analysis.

Bacitracin concentration profile of the cultures are presented in Fig. 23. The error bars show standard deviation between duplicate measurements.

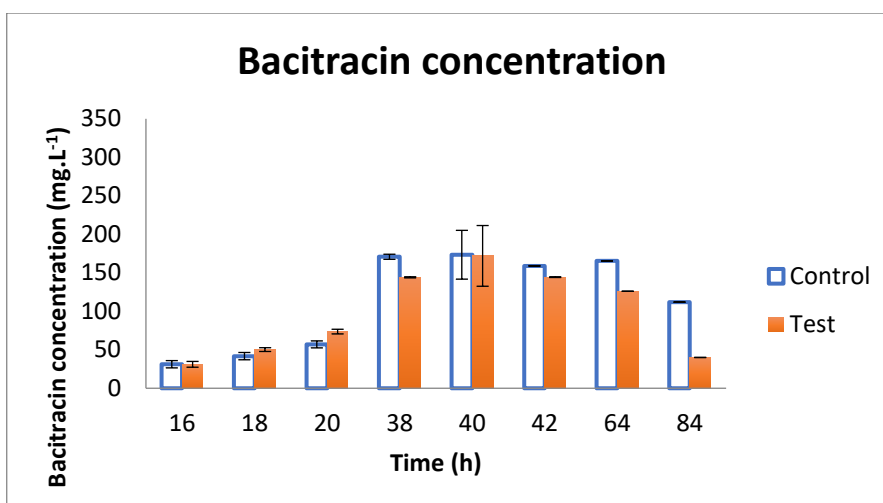


Figure 23. Bacitracin production profile of *B. licheniformis* in 2 L STRs. The test was exposed to 28 mT MF

As shown in Fig. 23, bacitracin concentration in both STRs followed the same increasing trend until 40 h of incubation, when both cultures reached their stationary growth phase and pH values increased.

Bacitracin production therefore continued until 40 h of incubation in both STRs. The production rates of bacitracin in the control and the test STRs in this period is presented in Table 17.

Table 17. Bacitracin production rates of *B. licheniformis* in 2 L STRs. The test was exposed to 28 mT MF

<i>Time (h)</i>	<i>Control (mg. L⁻¹.h⁻¹)</i>	<i>Test (mg. L⁻¹.h⁻¹)</i>
16-40	6.12	5.18

As shown in Table 17, the rate of bacitracin production was 15% lower in the MF exposed culture compared to that of the control culture.

3.1.2.3. Effect of 28 mT magnetic field on Glutamic acid consumption of STR cultures of *B. licheniformis*

Glutamic acid was consumed in both STRs as the main carbon source. The concentration of this compound was measured during the runs in samples of different time points.

Glutamic acid concentration results in the two STRs are presented in Fig. 24.

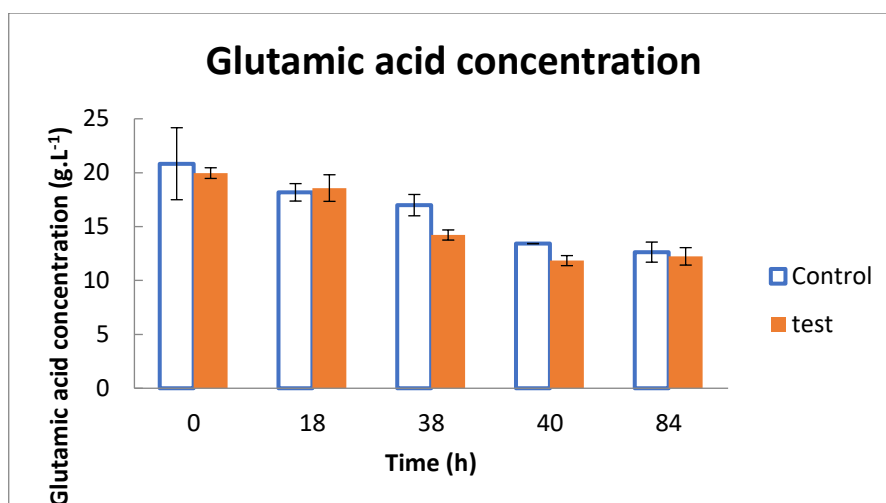


Figure 24. Glutamic acid concentration profile of *B. licheniformis* in 2 L STRs. The test was exposed to 28 mT MF

As shown in Fig. 24, the decrease in glutamic acid concentration (referred to as consumption of glutamic acid) continued until 40 h of incubation in both STRs. The average consumption rate of glutamic acid within the first 40 h of the fermentation period was 0.15 and 0.19 g. L⁻¹.h⁻¹ in the control and the test cultures, respectively.

3.1.2.4. Effect of 28 mT magnetic field on total carbohydrate content of STR cultures of *B. licheniformis*

Total carbohydrate content of the control and the test STRs was measured during the runs to investigate the release of polysaccharides throughout the fermentation period.

Fig. 25 shows the total carbohydrate content of the samples at different time points of the run. Results are presented as averages of triplicates. Error bars indicate the standard deviation between these readings.

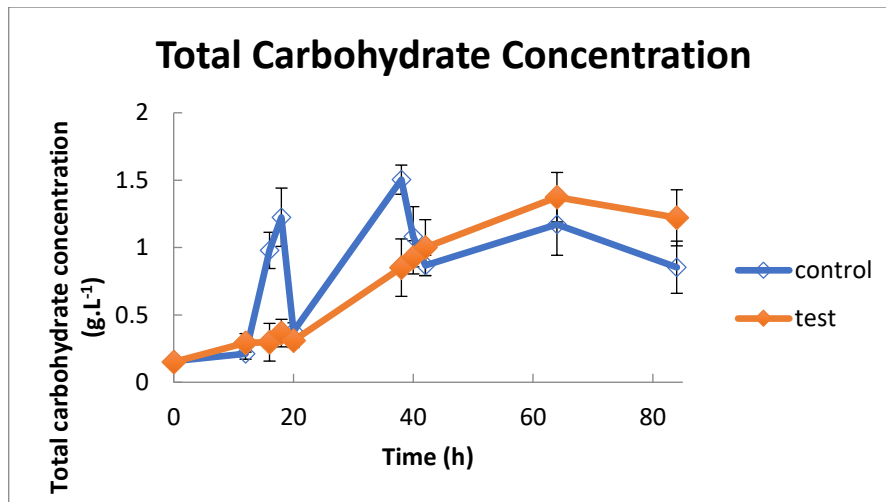


Figure 25. Carbohydrate production profile of *B. licheniformis* in 2 L STRs. The test was exposed to 28 mT MF

Total carbohydrate concentration fluctuated in the course of the control fermentation. However, there was a gradual increase in the test culture with a rate of 24 mg. L⁻¹.h⁻¹ in the period of 20-64 h.

3.1.2.5. Effect of 28 mT magnetic field on morphology of *B. licheniformis* in STR

Rod-shaped *B. licheniformis*, was observed under Scanning Electron Microscope (SEM). Changes in morphology were investigated by capturing images from samples of both control and the MF-exposed cultures (Fig. 26)

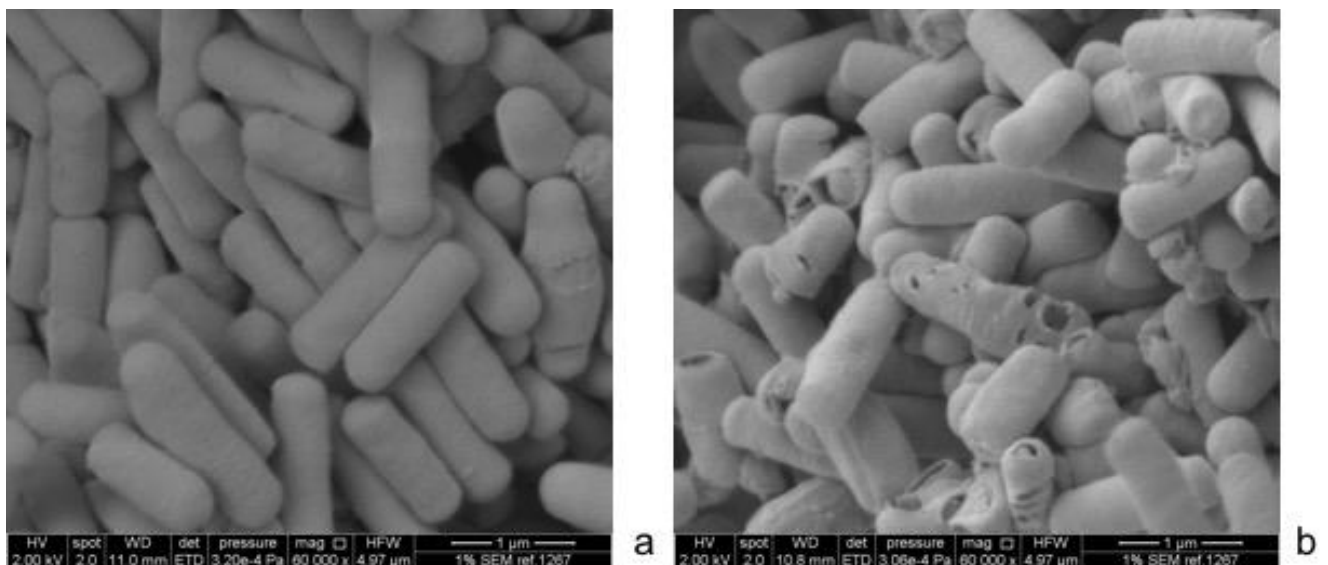


Figure 26. SEM images of a) the control and b) the test (exposed to 28 mT MF) samples of *B. licheniformis* in 2 L STRs with 60k magnification. The images were taken from samples after 64 h of incubation

Fig. 26 shows the cells of *B. licheniformis* in samples at the end of stationary phase of growth, visualised under SEM with 60,000 magnification. The right image, indicates the MF of 28 mT caused cell damage to bacterial walls.

3.1.3. STR Batch Fermentation of *B. licheniformis* with 10 mT magnetic field

Following the studies of the effect of magnetic field on *B. licheniformis* in bioreactors, the intensity of the induced magnetic field was changed to 10 mT through the MFG settings.

The experimental design was similar to the one reported in section 3.1.2 of this chapter.

Fermentation experiments were carried out in 2 L fermenters with 1.5 L working volume and 10% inoculum. Magnetic field intensity of 10 mT was applied to the test STR with a circulation rate of 10 mL. min⁻¹.

MF was applied after 16 h of incubation. The duration of these runs was 64 h, after which time the cultures had reached death phase of growth.

The runs were carried out in duplicates for biological repeatability. The results in this section are of a representative run of duplicate sets.

3.1.3.1. Effect of 10 mT magnetic field on growth profile of *B. licheniformis* in STR

Growth profile of the control and the MF exposed cultures was obtained through OD₆₅₀ measurement. These profiles are presented in Fig. 27. Values reported here are averages of duplicate readings and error bars represent standard deviations between the two readings.

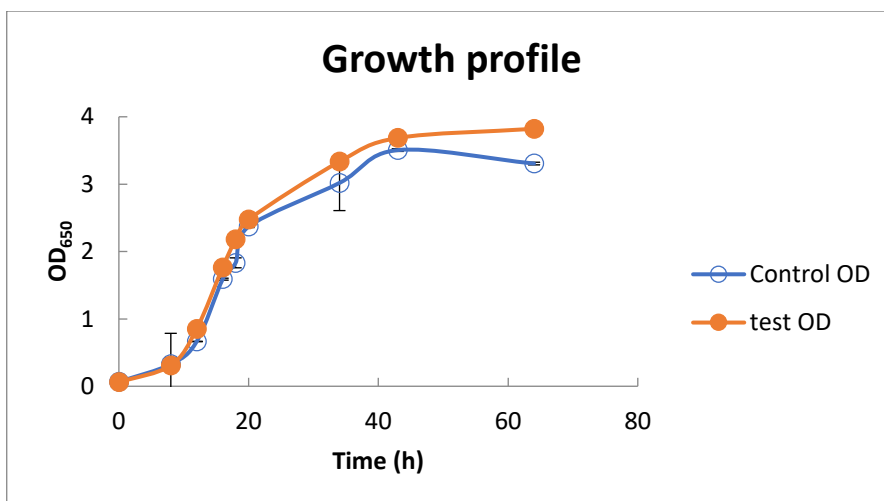


Figure 27. Growth profile of *B. licheniformis* in 2 L STRs. The test was exposed to 10 mT MF

Fig.27 shows the growth profile of *B. licheniformis* in the two STRs. The optical density in the control and the test cultures followed the same trend during the fermentation period. The logarithmic growth phase started after around 8 h in both cultures and increased to around 3.5 in the control and 3.7 in the test culture after 43 h of incubation.

Fig. 28 shows the results of optical density measurements in logarithmic scale.

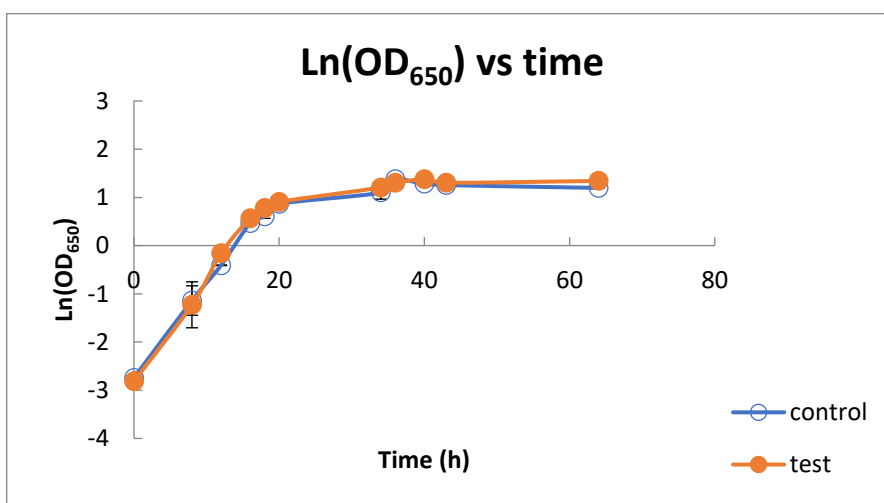


Figure 28. Logarithmic scale growth profile of *B. licheniformis* in 2 L STRs. The control and the test with outside circulation and 10 mT MF are shown.

As shown in Fig. 28, both the control and the test cultures followed the same growth trend, with doubling times of 1.5 and 1.3 h in the control and the test STRs, respectively.

pH profile of the cultures during the course of the runs is shown in Fig. 29.

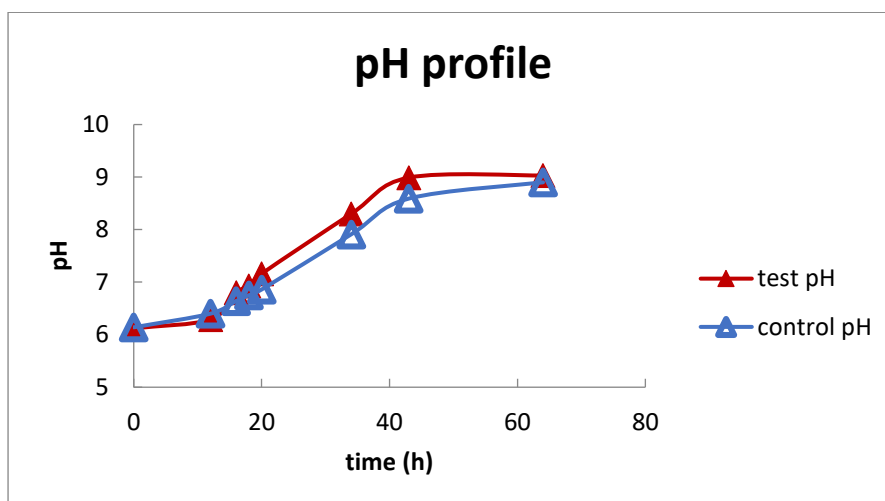


Figure 29. pH values of the cultures during the fermentation of *B. licheniformis* in 2 L STRs. The control and the test under 10 mT MF are shown.

pH of both cultures increased over time during the logarithmic growth phase (8-43 h). As shown in Fig. 29, both cultures followed the same increasing trend in the pH values and increased to around 9.

Bacitracin is stable at pH values of lower than 8 and oxidises rapidly under alkaline conditions with pH of higher than 8.

3.1.3.2. Effect of 10 mT magnetic field on bacitracin concentration in STR cultures of *B. licheniformis*

The concentrations of bacitracin was determined throughout the fermentation period by HPLC analysis.

Bacitracin concentration profile of the cultures are presented in Fig. 30. The results are averages of duplicate measurements with error bars representing standard deviations.

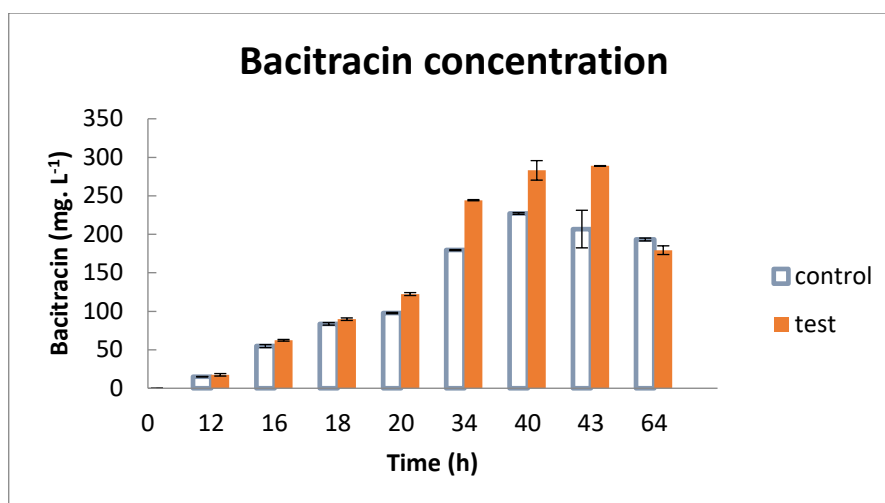


Figure 30. Bacitracin concentration of *B. licheniformis* culture in 2 L STRs. The control and the test under 10 mT MF are shown.

As shown in Fig. 30, bacitracin production started after 12 h of incubation in both STRs. The MF exposure started at 16 h, after which time the trend of bacitracin production in the two STRs changed.

Bacitracin content of the control culture, reached its maximum of 227 mg. L⁻¹ after 40 h of incubation and decreased afterwards.

The concentration of bacitracin in the test culture, reached its maximum of 289 mg. L⁻¹ at a later stage than that of the control. This was after 43 h of incubation, when the culture had circulated through the MFG for 10 rounds. The rate of increase in bacitracin content between the two STRs started to change after 18 h of incubation (as shown in Table 18).

Table 18. Summary of bacitracin production rate in Control and test (10 mT MF) 2 L STR cultures of *B. licheniformis*.

<i>Time interval (h)</i>	<i>Control (mg. L⁻¹. h⁻¹)</i>	<i>Test (mg. L⁻¹. h⁻¹)</i>	<i>Percentage difference (%)</i>
12-18	11.4	12	5.2
20-40	6.5	8	24.2

The MF exposed culture had 24% higher production rate (8 mg. L⁻¹.h⁻¹) than the control STR at 40 h (6.5 mg. L⁻¹.h⁻¹). At 40 h, when the culture medium had circulated 16 times through the MFG.

After 48 h, the rate of bacitracin production in both cultures decreased rapidly due to degradation of bacitracin in the culture.

3.1.3.3. Effect of 10 mT magnetic field on Glutamic acid consumption of STR cultures of *B. licheniformis*

Glutamic acid consumption was monitored during the runs. The concentrations of glutamic acid in the control and the test cultures are presented in Fig. 31 below.

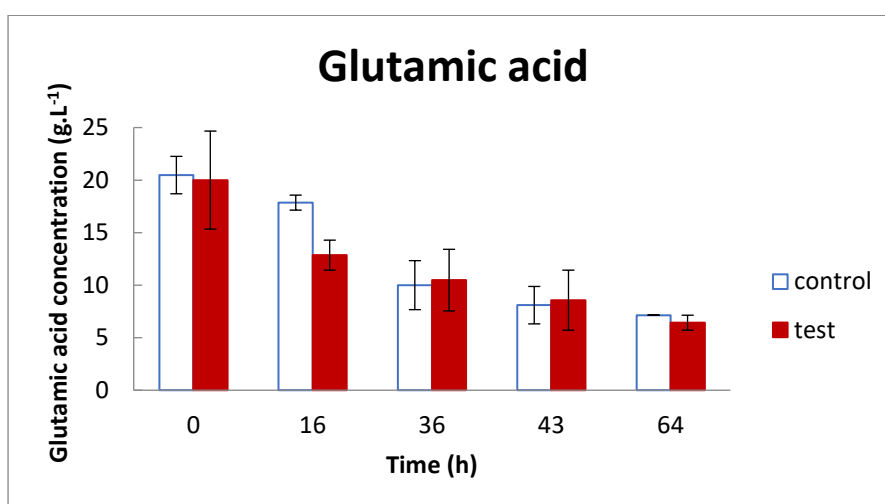


Figure 31. Glutamic acid concentration profile of *B. licheniformis* in 2 L STRs. The test was exposed to 10 mT MF

Concentration of glutamic acid changed from the initial 20 g. L⁻¹ to around 7 and 6.4 g. L⁻¹ in the control and the test STRs, respectively.

Consequently, consumption rate of glutamic acid within the first 36 h of incubation was calculated as 29 g. L⁻¹. h⁻¹ in the control and 26 g. L⁻¹. h⁻¹ in the test STR, respectively.

3.1.3.4. Effect of 10 mT magnetic field on total carbohydrate content of STR cultures of *B. licheniformis*

Total carbohydrate content of the control and the test STRs was measured during the runs to investigate the release of polysaccharides throughout the fermentation period.

Fig. 32 shows total carbohydrate concentrations in the culture medium during the course of the runs. Results are presented as averages of triplicates. Error bars indicate the standard deviation between these readings.

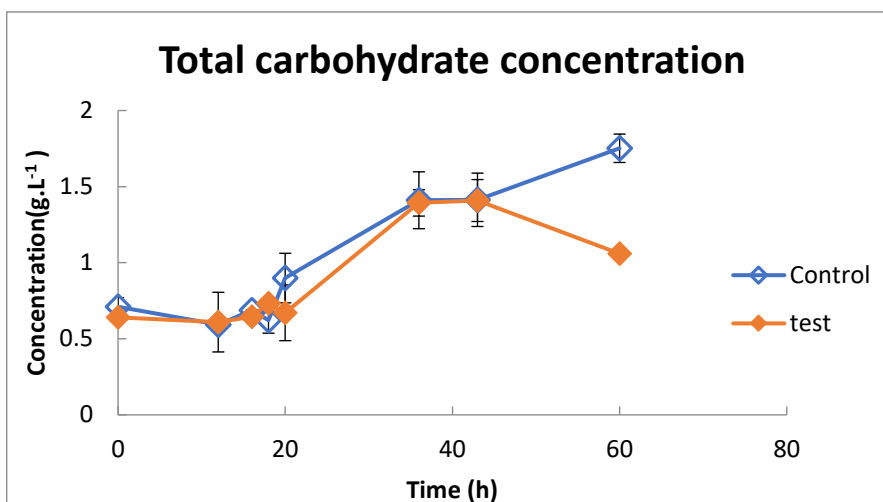


Figure 32. Total carbohydrate concentration profile in 2 L STRs including control and test STR exposed to 10 mT MF

As shown in Fig. 32, total carbohydrate content of the culture media remained almost the same until 18 h of incubation in both cultures. It then started to increase right after both cultures reached their stationary phase.

3.1.4. STR Batch Fermentation of *B. licheniformis* with 10 mT magnetic field and pH control

As seen in the previous section, during the fermentation of *B. licheniformis*, the culture medium becomes more alkaline until it reaches pH values of around 9 towards the end of fermentation. Since bacitracin A is reduced to bacitracin F under alkaline conditions, the concentration of bacitracin A in the culture medium decreases.

Another experiment was designed in order to compare the effect of magnetic field on bacitracin production when the pH of the medium is kept at its optimal value of 6-7.

This section summarises the results obtained from three sets of fermentation runs with pH control. These experiments were carried out in 2 L fermenters with magnetic field intensity of 10 mT, circulation rate of 10 mL. min⁻¹. The MFG was switched on after 16 h of incubation.

3.1.4.1. Effect of 10 mT magnetic field on growth profile of *B. licheniformis* in a pH-controlled STR system

Growth profile of the control and the MF exposed cultures was obtained through OD₆₅₀ measurement. These profiles are presented in Fig. 33. Values reported in this Fig., are averages of duplicate readings and error bars represent standard deviations between the two.

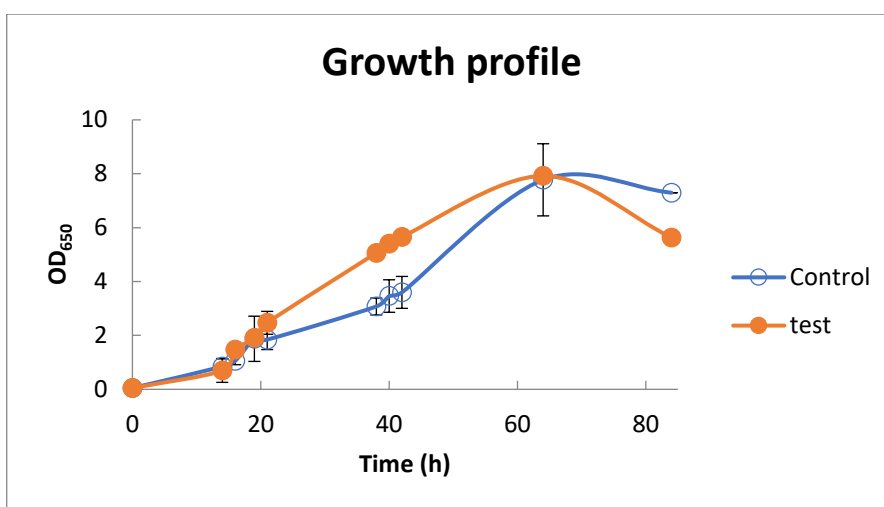


Figure 33. Growth profile of *B. licheniformis* in 2 L STRs with controlled pH. The test was exposed to 10 mT MF

Fig. 33 shows the results of optical density measurements between the two STRs. Optical densities of both cultures followed the same trend in the first 21 h of incubation. The OD₆₅₀ in the control culture increased to 3.6 after 42 h and reached 7.8 after 64 h of incubation. The OD₆₅₀ of the test culture increased to 5.6 after 42 h and reached its maximum of 7.9 after 64 h of incubation.

It appears that both cultures had a diauxic growth profile. Cells in both STRs had two logarithmic stages over 14-21 and 21-64 h intervals.

Fig. 34 shows the growth profile of this experiment on logarithmic scale.

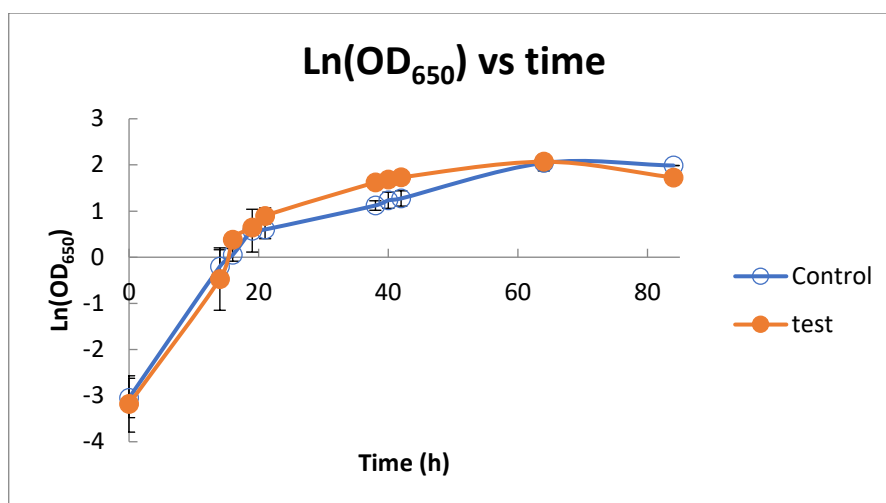


Figure 34. Logarithmic scale growth profile of *B. licheniformis* in 2 L STRs with controlled pH. The test was exposed to 10 mT MF

As shown in Fig. 34, the increase in the growth of the test culture between 21 and 42 h of incubation was faster in the test culture (0.04 h^{-1}) as compared to the control culture (0.02 h^{-1}). This leaves the possibility that the MF exposed *B. licheniformis* followed its initial growth by a diauxic profile after 21 h, which continued until 64 h.

According to their maximum growth rates of 0.16 h^{-1} (control) and 0.22 h^{-1} (test) between 14-19 h of incubation, doubling times of the two STRs was 4.4 and 3.1 h in the control and the test, respectively.

Table below shows results of percentage difference calculations of doubling time and maximum growth rate of the cultures after MF application at the logarithmic stage of growth.

Table 19. Percentage differences of doubling time and maximum growth rate between the control and the test cultures of *B. licheniformis* in 2 L STRs with controlled pH. The test was exposed to 10 mT MF

	<i>Control</i>	<i>Test</i>	<i>Percentage difference (%)</i>
Doubling time (h)	4.44	3.10	30.15
Maximum growth rate (h^{-1})	0.16	0.22	43.16

As shown in Table 19, maximum growth rate of the test culture was 43% higher than that of the control culture. This lead to a doubling time of 30% faster in the test culture compared to the doubling time of the control culture.

Cell viability during the course of fermentation was determined by counting the number of colonies formed on plates of samples taken from each STR at different time points. Table 20 shows the average CFU counts of triplicate plates for each sample.

Table 20. Colony forming unit counts in the samples taken from the two 2 L STRs of *B. licheniformis* with controlled pH. The test was exposed to 10 mT MF

<i>Time (h)</i>	<i>Control (10⁷ CFU. mL⁻¹)</i>	<i>Standard deviation between control samples (10⁷)</i>	<i>Test (10⁷ CFU. mL⁻¹)</i>	<i>Standard deviation between test samples (10⁷)</i>
21	101	11	108	19
40	300	200	400	100
64	400	141	433	115

The results from colony counts of the two cultures were in line with the OD₆₅₀ measurements. Number of viable cells in the test culture was 33% higher than that of the control at 40 h. Viable cells at 64 h were 8% higher in the test culture as compared to the control.

As the fermentation continued, the pH value in STRs increased from initial value of 6. Since the optimum pH for bacitracin stability in the culture medium is 6-7, pH-control mechanism was set to keep the pH levels below 7. Fig. 35 shows the changes in pH value of the STRs.

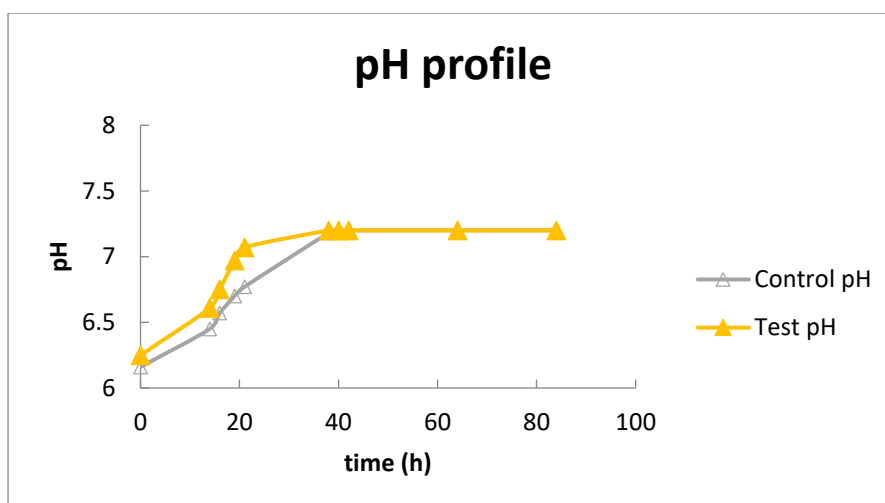


Figure 35. pH profile of *B. licheniformis* culture in 2 L STRs with controlled pH. The test was exposed to 10 mT MF

Fig. 35 shows the changes of pH in the two STRs. The initial pH value of both STRs was 6 and increased to 7 after 38 and 21 h in the control and the test cultures, respectively. It was then kept at 7 by mild acid addition to the culture. Mild acid addition started at 21 h and continued throughout the fermentation.

3.1.4.2. Effect of 10 mT magnetic field on bacitracin content of *B. licheniformis* in a pH-controlled STR system

As pH values above 7 negatively affect bacitracin A production, the pH of this system was maintained at 6-7. Bacitracin concentration was then determined throughout the fermentation period by HPLC analysis.

Bacitracin concentration profiles of both cultures are presented in Fig. 36. These results are averages of duplicate measurements with error bars indicating standard deviations.

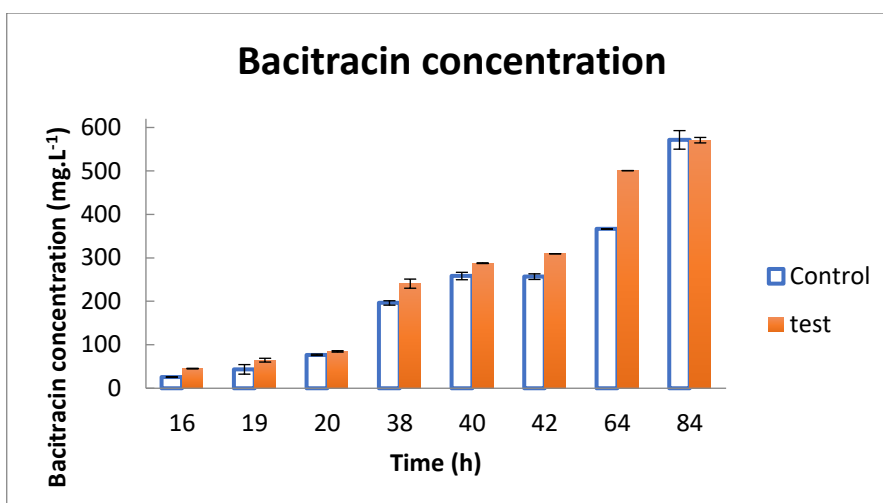


Figure 36. Bacitracin production profile of *B. licheniformis* in pH-controlled STRs. The test STR was exposed to 10 mT MF.

As shown in Fig. 36, bacitracin production started after 16 h of incubation in both STRs. It increased until the end of the fermentation period and reached a maximum of 571 mg. L⁻¹ after 84 h in both cultures.

Although bacitracin concentration in both STRs reached the same maximum value, the bacitracin obtained from samples of the test after 64 h of incubation (501 mg. L⁻¹) was 36% higher in concentration than that of the control culture (367 mg. L⁻¹).

The rate of increase in bacitracin content between the two STRs started to change after 20 h of incubation.

Bacitracin production rate of the control and the test cultures are presented in Table 21.

Table 21. Bacitracin production rate in the two pH-controlled 2 L STRs after the application of 10 mT MF (16-84 h).

<i>Time (h)</i>	<i>Control (mg. L⁻¹. h⁻¹)</i>	<i>test (mg. L⁻¹. h⁻¹)</i>	<i>percentage difference (%)</i>
16-84	7.7	8.2	6.6

As shown in Table 21 and Fig. 36, bacitracin concentration increased throughout the period of fermentation and the production rate of bacitracin between 16-84 h, was 6.6% higher in the test culture.

3.1.4.3. Effect of 10 mT magnetic field on Glutamic acid consumption in cultures of *B. licheniformis* in a pH-controlled STR system

Glutamic acid consumption was monitored during the runs through glutamic acid assay of samples from STRs at different time points. The concentrations of glutamic acid in the control and the test cultures are presented in Fig. 37 below.

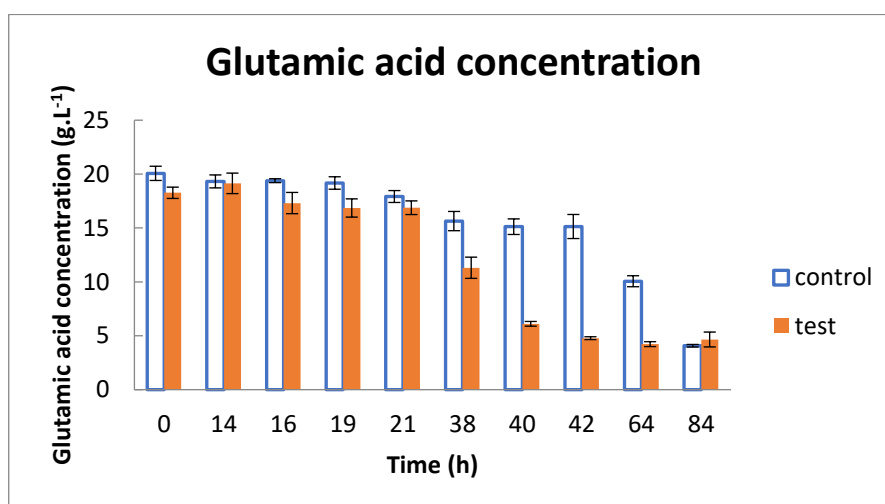


Figure 37. Glutamic acid concentration in the culture medium of *B. licheniformis* in 2 L STRs with controlled pH. The test was exposed to 10 mT MF

As shown in Fig. 37, glutamic acid was consumed at a very low rate during the first 21 h of fermentation in both STRs. It was then consumed more rapidly during the diauxic growth stage. This consumption was continued in the control culture after it reached the stationary growth phase.

Consumption rates at the three growth stages are calculated in Table 22 below.

Table 22. Glutamic acid consumption rate in the pH-controlled 2 L STRs of *B. licheniformis* with 10 mT MF exposure of the test STR.

<i>Time interval (h)</i>	<i>Control (g. L⁻¹. h⁻¹)</i>	<i>Test (g. L⁻¹. h⁻¹)</i>
0-21	0.1	0.07
21-64	0.18	0.29
64-84	0.3	no consumption

As shown in Table 22, maximum glutamic acid consumption rate in the test culture was at 21-64 h period of fermentation, which was higher than that of the control. The maximum consumption rate of the control culture occurred in the 64-84 h period.

3.1.4.4. Effect of 10 mT magnetic field on total carbohydrate content of cultures of *B. licheniformis* in a pH-controlled STR system

Total carbohydrate content of the control and the test STR was measured during the runs to investigate the release of polysaccharides throughout the fermentation period.

Fig. 38 shows total carbohydrate content of the culture medium during the course of the runs. Results are presented as averages of triplicates. Error bars indicate the standard deviation between these readings.

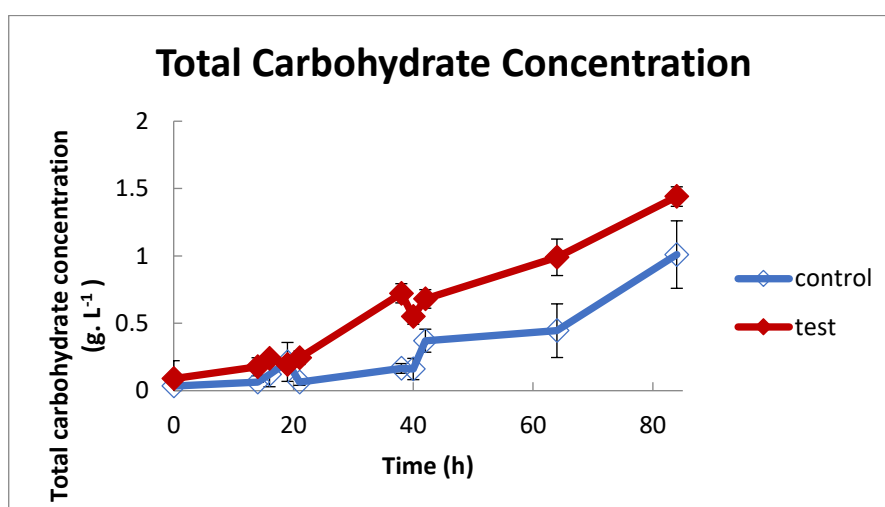


Figure 38. Total carbohydrate concentration profile in pH-controlled STRs of *B. licheniformis* with 10 mT MF exposure of the test STR.

Fig. 38 indicates that the change in the total carbohydrate concentration of the two STRS followed the same trend until the MF exposure was started at 16 h. Total carbohydrate concentration in the test culture decreased from 0.238 to 0.195 g. L⁻¹ after 3 h from the MFG start time. However, this concentration in the control culture increased from 0.120 to 0.195 g. L⁻¹ during these 3 h, which was then decreased to 0.63 g. L⁻¹. After 21 h of inoculation, the control culture was at the end of its first logarithmic growth phase. Following the start of diauxic growth in the control between 21-64 h, carbohydrates were released into the medium and the total carbohydrate concentration reached 0.445 g. L⁻¹. It then increased rapidly to 1.010 g. L⁻¹ during the stationary phase.

Total carbohydrate content in the test culture followed an overall increasing trend from 21 h (0.244 g. L⁻¹) until 64 h of incubation (0.990 g. L⁻¹).

The main increase in the total carbohydrate content of the two STRs started after the first logarithmic stage of growth at 21 h. Table 23 shows the rate of carbohydrate production in the two STRs in the following two stages. The negative value indicates the percentage difference of a lower carbohydrate production rate in the test as compared to the control culture.

Table 23. Total carbohydrate production rate in *B. licheniformis* 2 L STRs after the first logarithmic stage. The test was exposed to 10 mT MF.

<i>Time interval (h)</i>	<i>Control (g. L⁻¹. h⁻¹)</i>	<i>Test (g. L⁻¹. h⁻¹)</i>
21-64	0.009	0.018
64-84	0.028	0.021

According to Table 23, the rate of total carbohydrate production in the test culture was twice than that of the control during the diauxic growth stage. However, carbohydrate production rate of the control culture increased to 0.028 g. L⁻¹. h⁻¹, 27% higher than that of the test during the stationary phase.

3.1.4.5. Effect of 10 mT magnetic field on morphology of *B. licheniformis* cells in pH- controlled STRs

B. licheniformis is a rod-shaped robust bacterium. The effect of 10 mT MF on the morphology of the cells was in this system was investigated through SEM imaging.

Fig. 39 shows the images obtained from SEM system with two magnifications. These images were obtained from samples of both runs at late stationary phase of growth (64 h).

As shown in Fig. 39, *B. licheniformis* cells exposed to MF, developed some tumor-like shapes on their exterior.

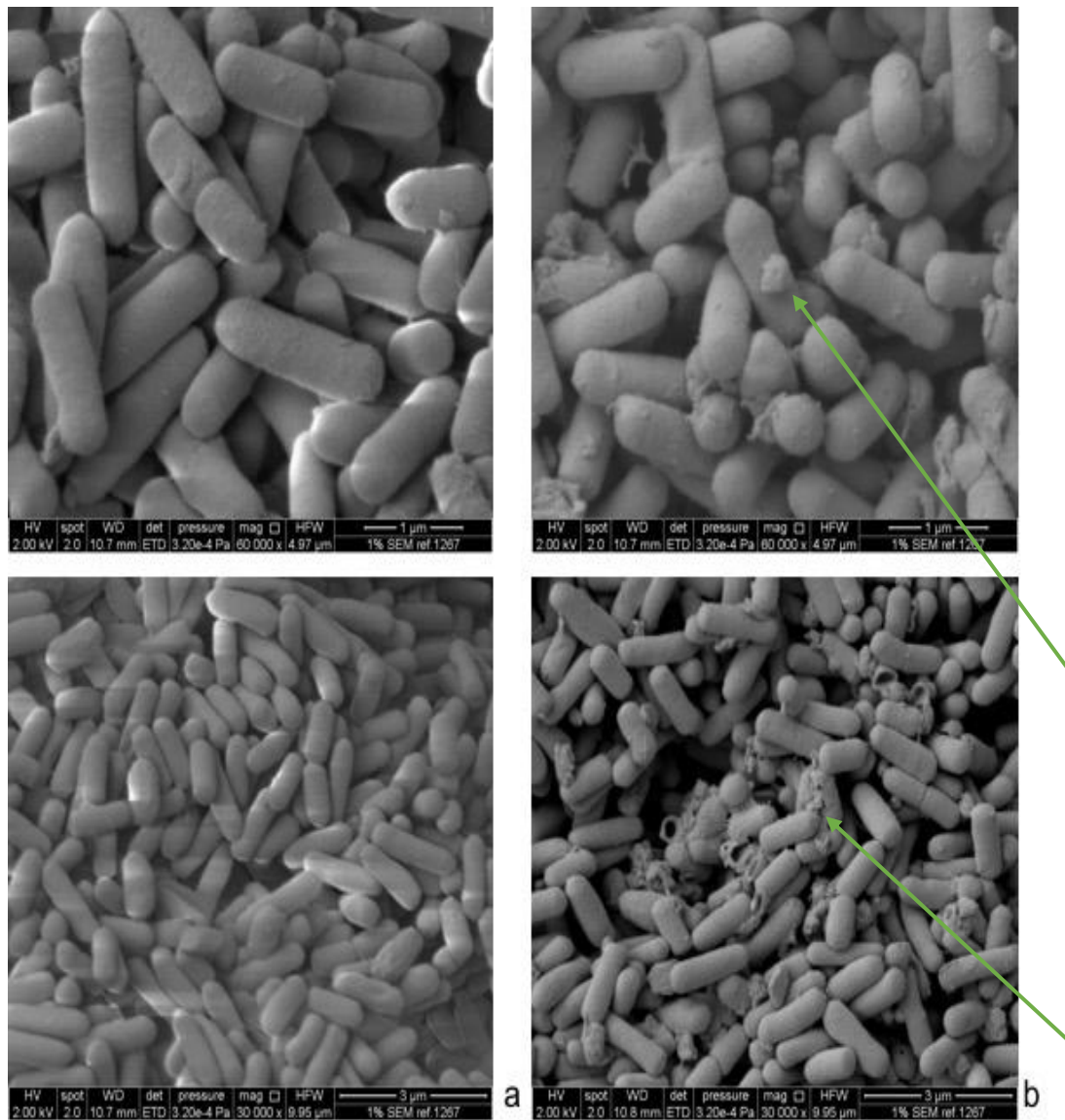


Figure 39. SEM images of *B. licheniformis* cells at the end of 2 L STR runs with pH control below 7. a) *B. licheniformis* cells in the control STR with 60K (top image) and 30K (bottom image) magnifications. b) *B. licheniformis* cells in the test STR under 10 mT magnetic field with 60k (top image) and 30k (bottom image). Arrows indicate the morphology changes to cells.

3.2. Studies on the effect of magnetic field on *Bacillus Subtilis*

After the studies on the effect of MF with two intensities on the Gram-positive *B. licheniformis* as antibiotic producer, the same STR set up was used to study effects of MF on another Gram-positive strain, *B. subtilis*, as a producer of biopolymers.

Two 2-L STRs (as described in materials and methods chapter) were ran in parallel with working volumes of 1.5 L, 10% inoculum, aeration rate of 1 vvm, agitation of 200 rpm, while DOT levels were kept at a minimum of 35%. Magnetic field exposure started immediately at the start of the run.

The MF intensity was set at 18, and 28 mT with the culture circulating through the MFG at a rate of 10 mL. min⁻¹. The MFG device was altered to reach intensity of 28 mT. This alteration changed the MF intensity range that could be obtained. Therefore, due to this technical difficulty, 18 mT was the lowest value to be used in these experiments.

Results of representative runs for each magnetic field intensity are reported in this chapter.

3.2.1. STR Batch fermentation of *B. subtilis* with magnetic field intensity of 18 mT

Bacillus subtilis cultures were cultivated in batch STRs. The test bioreactor was circulated through the MFG with magnetic field intensity of 18 mT.

Duration of the run was 73 h. During this time, 1.5 L of culture medium was circulated almost 30 times through the MFG.

3.2.1.1. Effect of 18 mT magnetic field on growth profile of *B. subtilis* in STR system

Results of OD₆₀₀ measurements presented in Fig. 40, are averages of duplicate readings from samples of STRs at each time point.

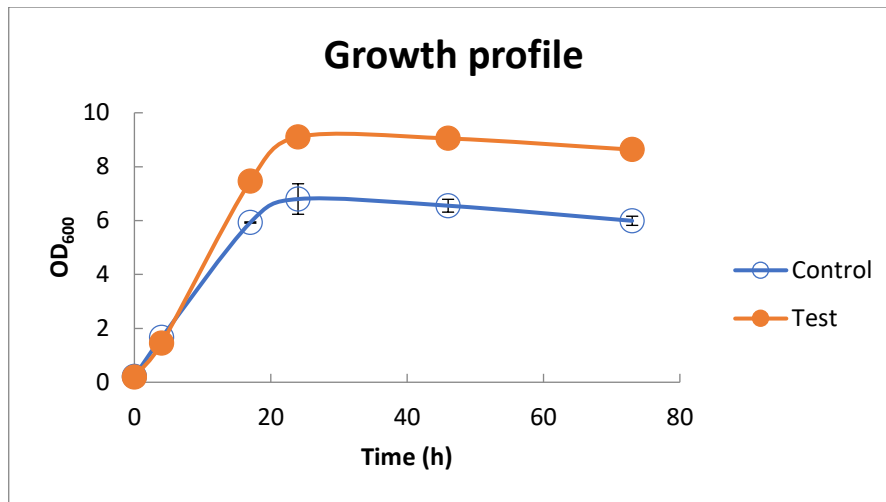


Figure 40. Growth profile of *B. subtilis* in the two 2 L STRs with test under 18 mT MF.

Fig. 40 shows the results of optical density measurements of the control and the test samples during the fermentation period. Error bars indicate standard deviations between duplicate readings. Both cultures reached maximum growth at 24 h with values of OD₆₀₀ at 6.8 and 9 in the control and the test, respectively.

Control OD₆₀₀ reached a maximum of 6.8, while the test culture reached 34% higher optical density value of 9.1.

The OD₆₀₀ of the test culture remained higher than that of the control throughout the stationary phase.

Growth profile of *B. subtilis* on logarithmic scale is shown in Fig. 41.

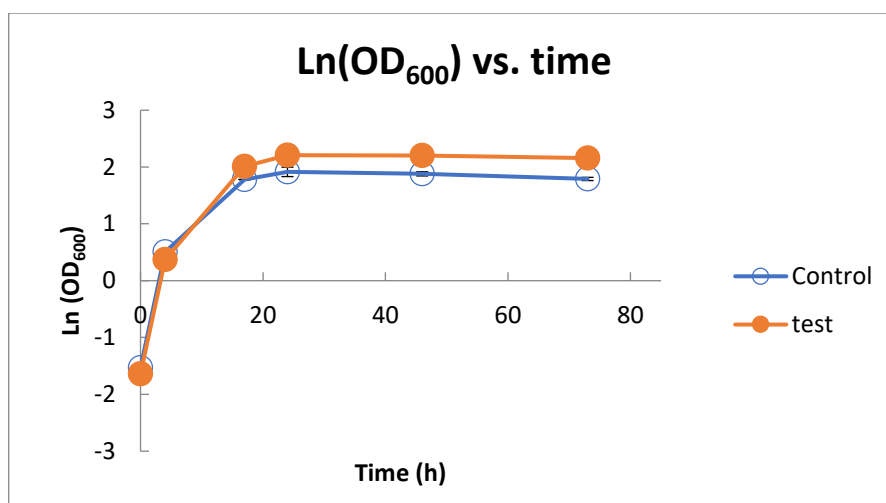


Figure 41. Growth profile of *B. subtilis* in 2 L bioreactors in logarithmic scale with test under 18 mT MF

Maximum growth rate and doubling time were calculated based on Fig. 41. Maximum growth rate was 0.19 h^{-1} in the control and 0.21 h^{-1} in the test STRs. Therefore, the doubling time was 3.6 h for the control and 3.2 h for the test cultures.

Results obtained from colony forming unit counts were also in line with the OD₆₀₀ profile. Number of viable cells in samples of the test culture at late logarithmic stage was higher than the control STR and remained higher until the end of the fermentation period.

Table 24. Colony counts in the Control and the Test STRs of *B. subtilis* under 18 mT MF

<i>Time interval (h)</i>	<i>Control</i> <i>10⁷ CFU. mL⁻¹</i>	<i>Test</i> <i>10⁷ CFU. mL⁻¹</i>
17	73	85
46	20	37

3.2.1.2. Effect of 18 mT magnetic field on formation, chemical characteristics and concentration of P(3HB) in *B. subtilis* cultures in STR system

Samples taken throughout the fermentations, were screened for P(3HB) by Nile red staining and visualisation of P(3HB) under fluorescence microscope.

This was confirmed against non-PHA producing strains of *Pseudomonas* spp. as control.

Fig. 42 shows the microscope image taken from samples of the STRs. P(3HB) inside the cells show fluorescence and can be observed under fluorescence microscope. These observations confirm the production of P(3HB) inside the cultures.

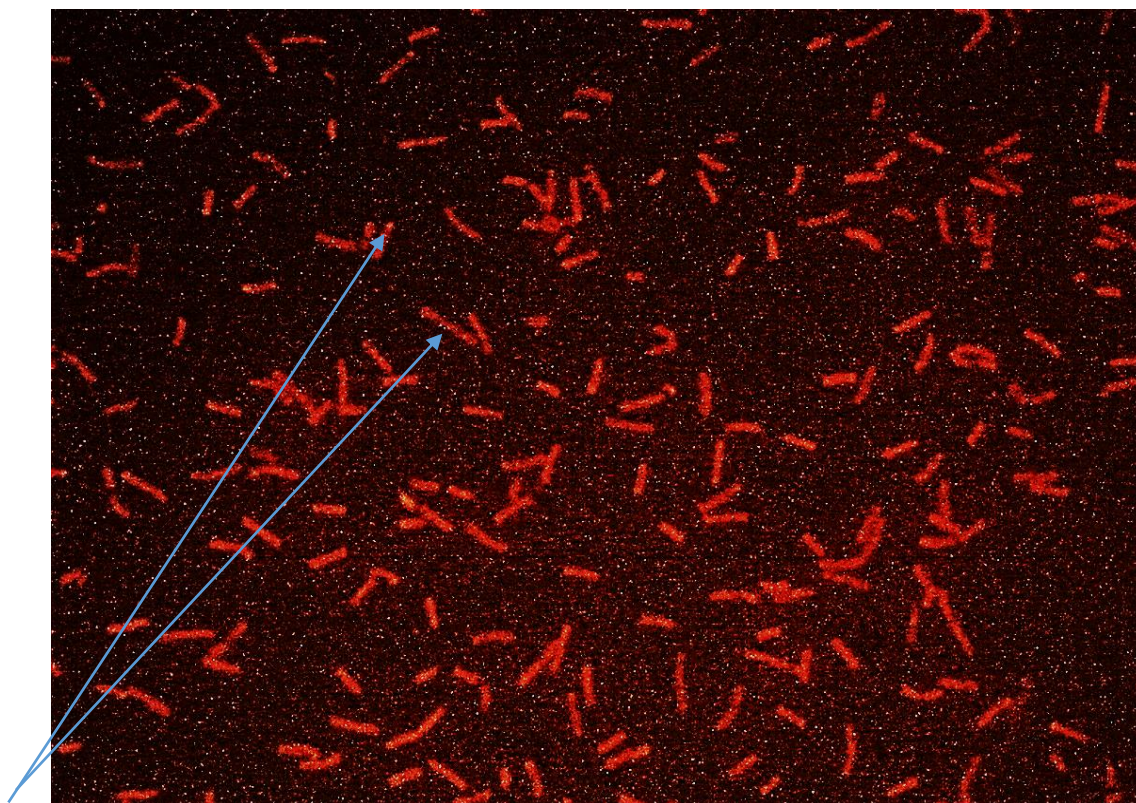


Figure 42. Microscopic image of *B. subtilis* culture taken from the control STR under 10 X magnification. The P(3HB) present as inclusion bodies inside the cells, were observed by their fluorescence. Arrows indicate these inclusion bodies.

Chemical characteristic of the produced biopolymers was assessed by FTIR. Biopolymers were extracted from the samples of both STRS and the bonds present in their structure were confirmed (Fig. 43)

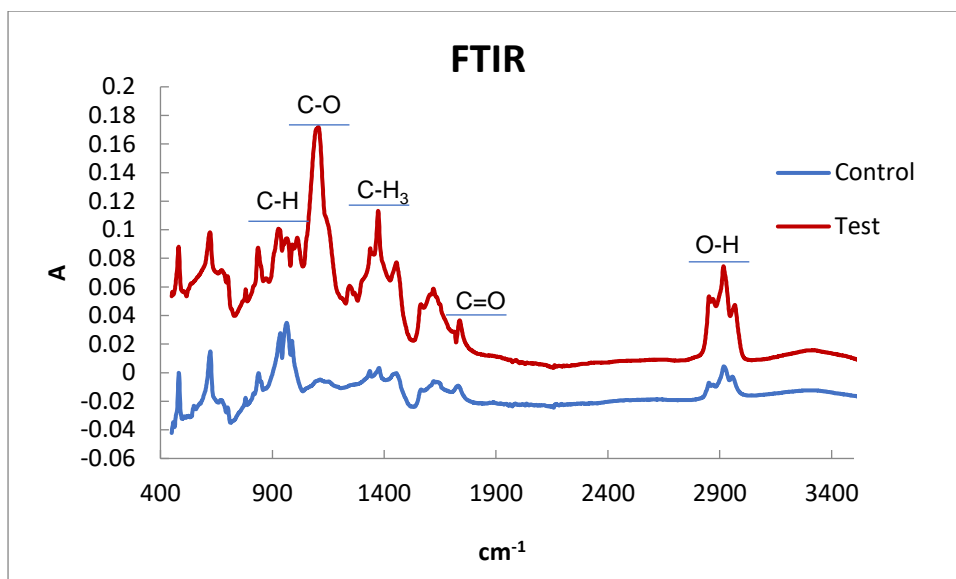


Figure 43. FTIR results of the control and the test P(3HB) from *B. subtilis* under 18 mT MF. Chemical structure of the polymer in both gave the same peaks. This confirms the structural similarity of the product between the two reactors.

As shown in Fig. 43, polymer produced in the test STR, had the same chemical structure as the control and MF did not cause any changes in the product's conformation.

After confirmation of P(3HB) production and chemical analysis of the produced polymer, the concentration of P(3HB) in each sample was quantified. Fig. 44 shows the PHB content of the STRs from the results of crotonic acid assay on the samples taken at different time points throughout the fermentation.

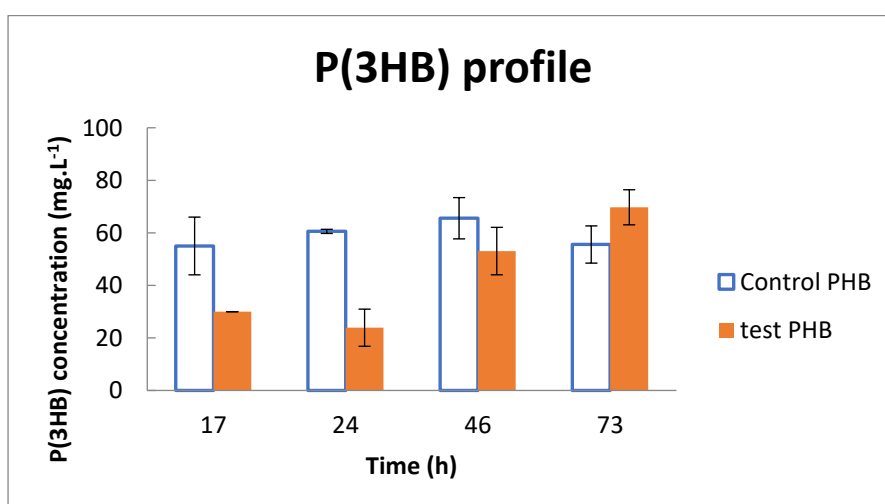


Figure 44. P(3HB) concentration change in *B. subtilis* STRs throughout the fermentation period in 2 L STRs with the test under 18 mT MF.

The results presented in Fig. 44 indicate that the concentration of P(3HB) in the control changed within the range of 55-66 mg. L⁻¹. The concentration of P(3HB) in the MF exposed culture increased within the range of 24 to 70 mg. L⁻¹.

Although the maximum P(3HB) production was 66 mg. L⁻¹ at 46 h in the control, the P(3HB) concentration of the test reached a maximum of 70 mg. L⁻¹ after the end of fermentation period (26% higher than the control P(3HB) content). This was achieved after 29 circulations of the medium through the MFG.

As presented in Table 25, the mg P(3HB) / g CDW at the fermentation end time, was almost the same.

Table 25. mg P(3HB)/ g CDW in the control and test (18 mT) STRs of *B. subtilis*

<i>Time(h)</i>	<i>Control Mg P(3HB)/g CDW</i>	<i>Test Mg P(3HB)/ g CDW</i>
17	16	16
24	22	14
47	23	21
73	20	19

3.2.2. STR Batch fermentation of *B. subtilis* with magnetic field intensity of 28 mT

Bacillus subtilis cultures were cultivated in batch fermentations with the test bioreactor circulating through the MFG with magnetic field intensity of 28 mT. The duration of the run was 77 h. During this time, 1.5 L culture was circulated almost 30 times through the magnetic field.

3.2.2.1. Effect of 28 mT magnetic field on growth profile of *B. subtilis* in STR system

As shown in Fig. 45, both cultures followed the same trend of growth during the fermentation period. The test fermenter reached maximum growth at 28 h

with OD₆₀₀ of 6.7, while the test culture reached its maximum of 5.9 after 22 h of incubation.

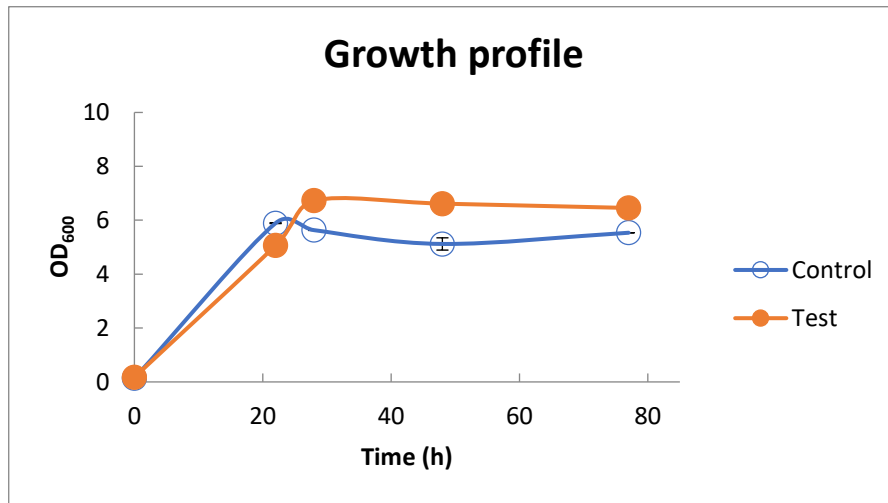


Figure 45. Growth profile of *B. subtilis* in 2 L STRs. The control and the test under 28 mT MF are shown

As indicated in this table OD₆₀₀ of the test culture was 19% higher than that of the control culture at its peak at 28 h. Negative percentage values indicate a lower OD₆₀₀ value of the test compared to the control.

Growth profile of both STRs on logarithmic scale is shown in Fig. 46.

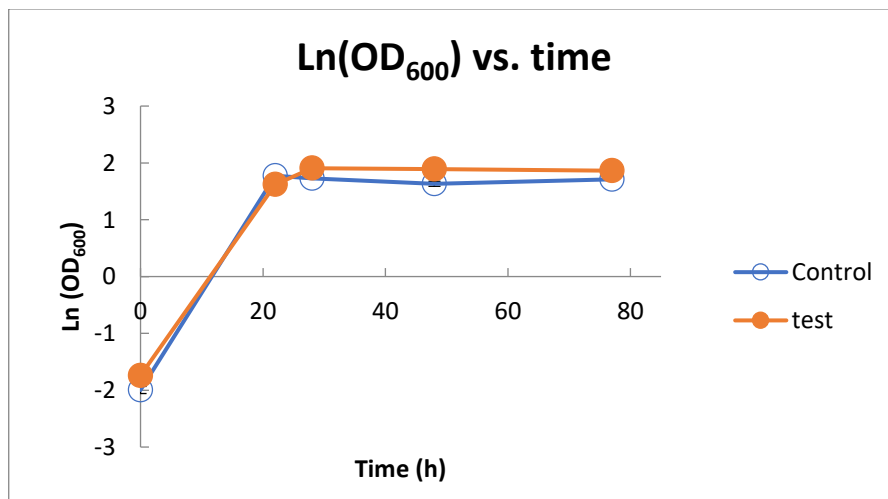


Figure 46. Growth profile of *B. subtilis* in two 2 L STRs in logarithmic scale. The control and the test under 28 mT are shown

Fig. 46 shows that maximum growth rate occurred between 0-22 h of incubation. The maximum growth rate was 0.17 and 0.15 h⁻¹ in the control and the test STRs, respectively. Consequently, the doubling time was calculated as 4 h in the control and 4.5 h in the test culture.

As presented in Table 26, mg P(3HB)/ g CDW at the fermentation end time, was 20% different.

Table 26. mg P(3HB)/g CDW in 2 L STRs of *B. subtilis* under 28 mT MF

<i>Time(h)</i>	<i>Control mg P(3HB)/ g CDW</i>	<i>Test P(3HB)/CDW</i>
22	20	26
28	21	16
48	24	18
77	18	15

Results obtained from the colony forming units of samples taken from the two STRs throughout the fermentation period were also in line with the OD₆₀₀ measurements.

Number of CFU per mL of culture was much higher in the test fermenter after 28 h of incubation. The number of viable cells then started to decrease in both bioreactors (Table 27).

Table 27. Colony count of *B. subtilis* in 2 L STRs with test under 28 mT MF

<i>Time (h)</i>	<i>Control (10⁶ CFU.mL⁻¹)</i>	<i>Test (10⁶ CFU.mL⁻¹)</i>
28	10	64
52	10	18

3.2.2.2. Effect of 28 mT magnetic field on morphology of *B. subtilis* cells in STRs

The effect of 28 mT MF on the morphology of *B. subtilis* cells was investigated through SEM imaging.

Fig. 47 shows the images obtained from SEM system with two magnifications.

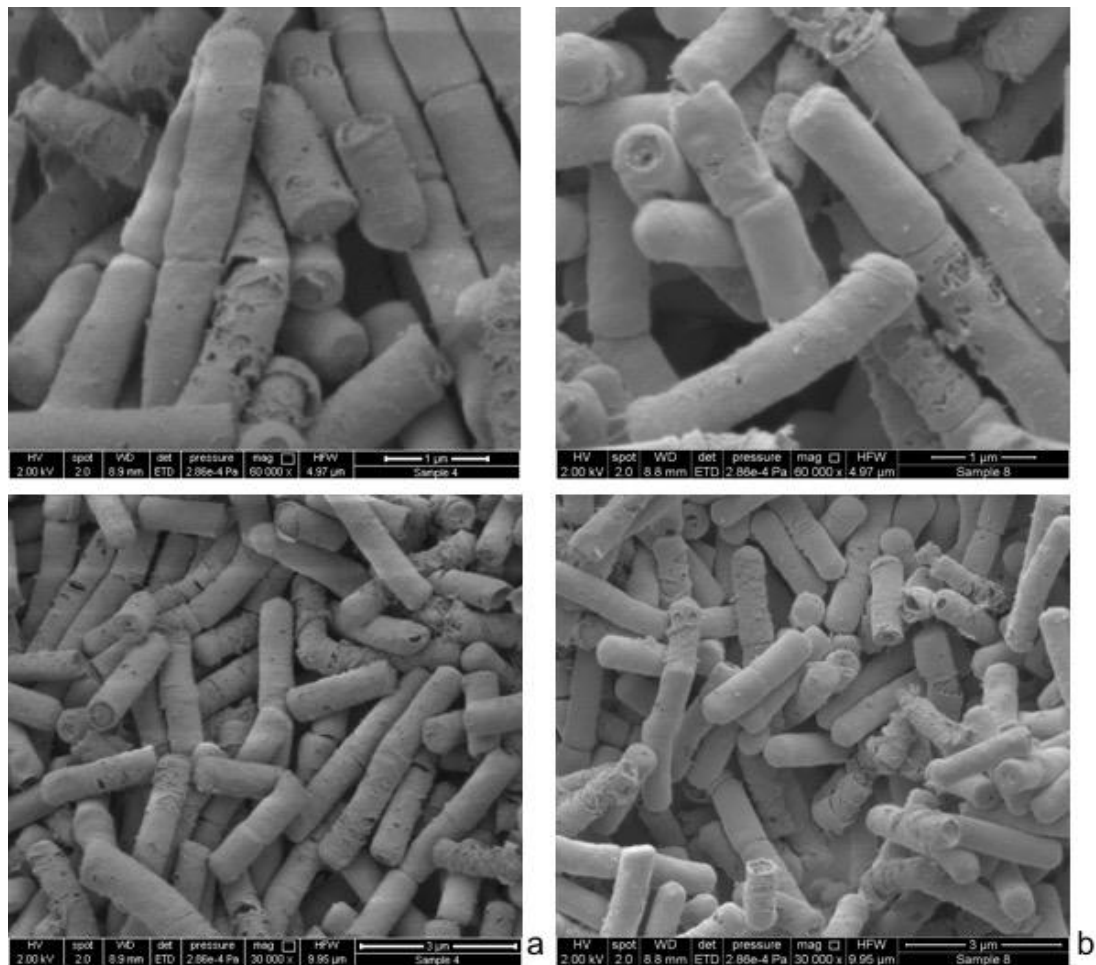


Figure 47. SEM images of *B. subtilis* cells. a) *B. subtilis* cells in the control STR with 60K (top image) and 30K (bottom image) magnifications. b) *B. subtilis* cells in the test STR exposed to 28 mT MF) with 60k (top image) and 30k (bottom image).

The images show that morphology of *B. subtilis* cells was not affected after exposure to 28 mT magnetic field.

3.2.2.3. Effect of 28 mT magnetic field on formation, chemical characteristics and concentration of P(3HB) in *B. subtilis* cultures in STR system

Samples from both STRs were screened for the presence of P(3HB) by Nile-red staining. Inclusion bodies containing PHB within the bacterial cells absorb the stain and can be observed under fluorescent microscope.

Fig. 48 shows images captured from the samples under fluorescent microscope, confirming the production of P(3HB).

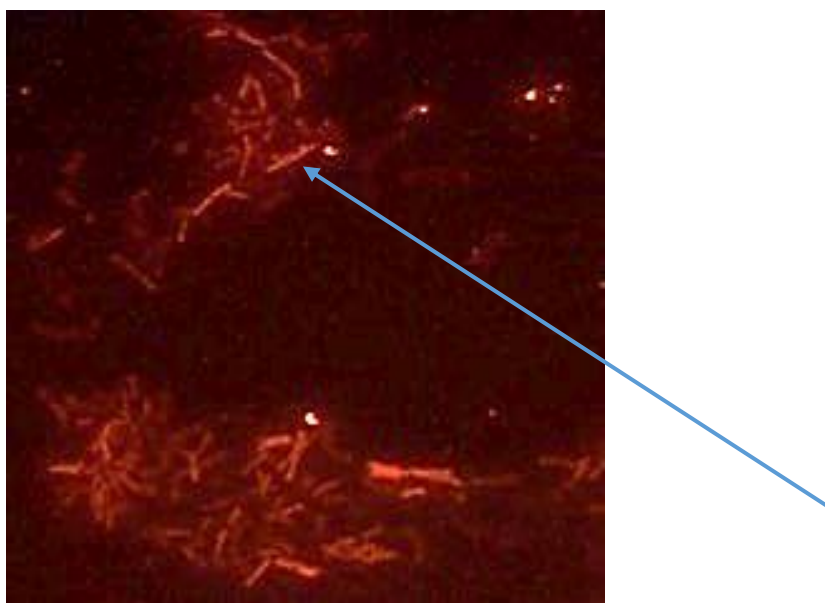


Figure 48. Microscopic image of *B. subtilis* in the control STR. P(3HB) present as inclusion bodies inside the cells was observed by fluorescence. The arrow indicates some of these inclusion bodies.

After confirmation of the production of P(3HB) inside bacterial cells, chemical structure of the products was analysed by FTIR. The FTIR peaks obtained from samples taken from the control and the test (presented in Fig. 49), confirmed that exposure of *B. subtilis* to 28 mT magnetic field did not change the polymer's chemical structure.

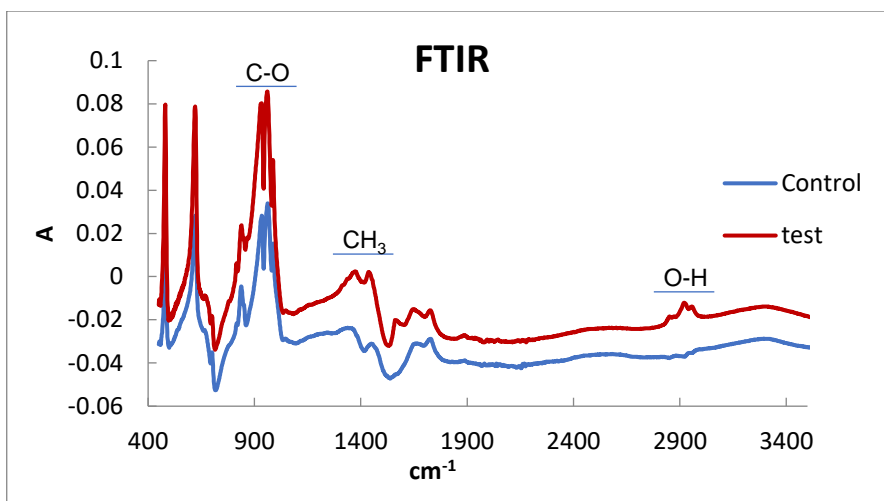


Figure 49. FTIR results of the control and the test P(3HB) by *B. subtilis* under 28 mT MF. Chemical structure of the polymer in both gave the same peaks. This confirms the structural similarity of the product between the two reactors.

The amount of PHB was quantified using crotonic acid assay. Results of this assay are presented in Fig. 50.

Once P(3HB) was extracted from the control and the test cultures using fluorescence microscope and chemical structure of the product obtained from both was confirmed through FTIR, the polymer was quantified and the concentration profile of P(3HB) throughout the fermentation period was detected.

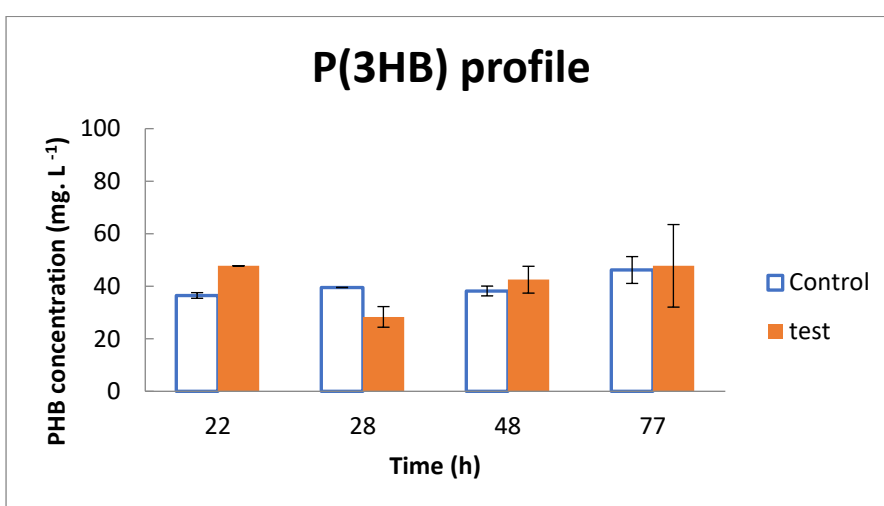


Figure 50. Concentration of P(3HB) during 2 L STR fermentation of *B. subtilis* with the test under 28 mT MF

Fig. 50 shows that the maximum P(3HB) content in the test culture was obtained after 22 h of incubation (48 mg. L⁻¹), when the culture medium had circulated through the MFG for 8 rounds. PHB concentration in the control culture at this time point was 36 mg. L⁻¹.

The maximum PHB content in the control STR (46 mg. L⁻¹) was observed after 77 h of incubation.

The maximum PHB content was 31% higher in the magnetic field exposed cultures after 22 h of incubation.

3.3. Studies on the effect of magnetic field on *Pseudomonas putida*

After the studies on the effect of magnetic field of two intensities on the Gram-positive *B. subtilis* as a biopolymer producer, the same STR set up was used to study these effects on a Gram-negative P(3HB) producing bacterium. To this end, *P. putida* KT2440 was chosen as the model strain for this study.

Two 2-L STR fermentations (as described in materials and methods chapter) were carried out in parallel. The fermentation specifications were: 1.5 L working volume, 10% inoculum, aeration rate of 1 vvm, agitation of 200 rpm, DOT (dissolved oxygen tension, air saturation) levels at a minimum of 35%.

Magnetic field exposure started immediately at the start of the run.

The magnetic field intensity was set at 18 and 28 mT with the culture circulating through the MFG at a rate of 10 mL.min⁻¹. These settings were consistent with those used for P(3HB) production by *B. subtilis* for comparison of the effect of MF based on the type of bacterium. Each run was performed in duplicates for biological repeatability.

Results of representative runs for each magnetic field intensity are reported in this chapter.

3.3.1. STR Batch fermentation of *P. putida* with magnetic field intensity of 18 mT

Pseudomonas putida culture was cultivated in batch fermentations with the test bioreactor circulating through the MFG at a rate of 10 mL. min⁻¹. Magnetic

field intensity was set at 18 mT. The duration of the run was 150 h. During this time, 1.5 L culture medium was circulated 60 times through the MFG.

3.3.1.1. Effect of 18 mT magnetic field on growth profile of *P. putida* in STR system

As shown in Fig. 51, the growth profile of the culture in the test bioreactor reached its maximum of 5.5 after 120 h of incubation. However, the control bioreactor reached its maximum OD₆₀₀ of 3.4 after 29 h of incubation, after which time it entered the stationary phase of growth.

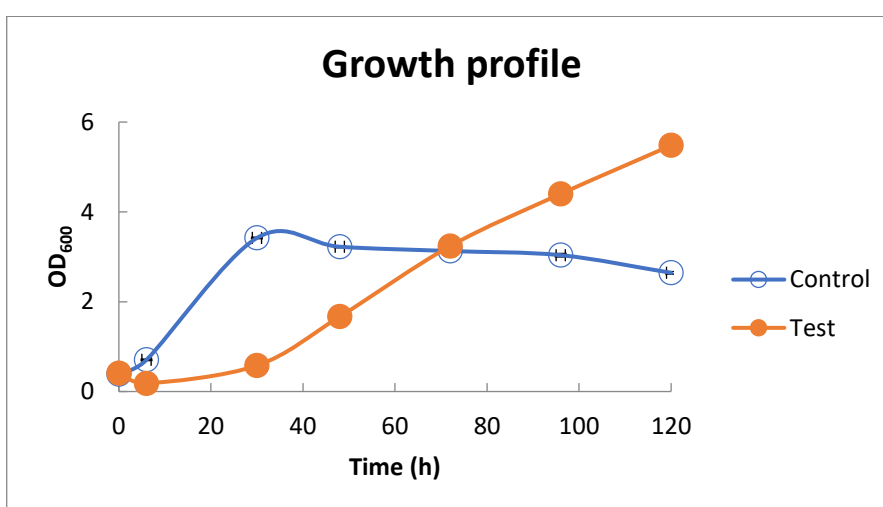


Figure 51. Growth profile of *P. putida* in 2 L STRs. The test was exposed to 18 mT MF

Fig. 52 shows the growth profile of *Pseudomonas putida* in the STRs on logarithmic scale.

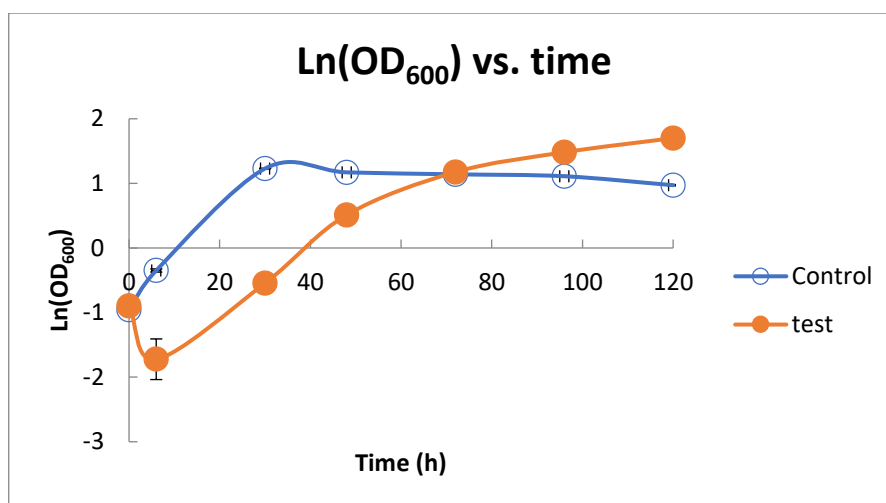


Figure 52. Growth profile of *P. putida* in 2 L STRs on logarithmic scale. The test was exposed to 18 mT MF.

Fig. 52, shows the different growth phases of the two STRs. Maximum growth rate of 0.05 h^{-1} was obtained between 6-30 h of incubation in both cultures. The doubling time in both STRs was 10.5 and 12 h for the control and the test, respectively.

The test culture showed a diauxic growth model as the cells continued growth after reaching their initial stationary phase at 29 h.

As shown in Table 28, the number of viable cells in the STRs followed the same trend as the OD_{600} measurements and the maximum CFU. mL^{-1} was reached towards the end of fermentation in the test culture, while it reached its maximum after 29 h in the control culture.

Table 28. CFU percentage change at different time points after the application of 18 mT magnetic field to 2 L STR of *P. putida*

<i>Time</i>	<i>Control</i> ($10^7 \text{ CFU. mL}^{-1}$)	<i>Test</i> ($10^7 \text{ CFU. mL}^{-1}$)
6	147	5
30	193	32
72	130	157
96	97	323

3.3.1.2. Effect of 18 mT magnetic field on morphology of *P. putida* cells in STRs

Scanning Electron Microscopic (SEM) images were obtained from the samples of the control and the test.

These images are presented in Fig. 53 below. The samples were taken towards the end of the fermentation period after 72 h. Rod cell of *P. putida* cells changed into a coin-like shape.

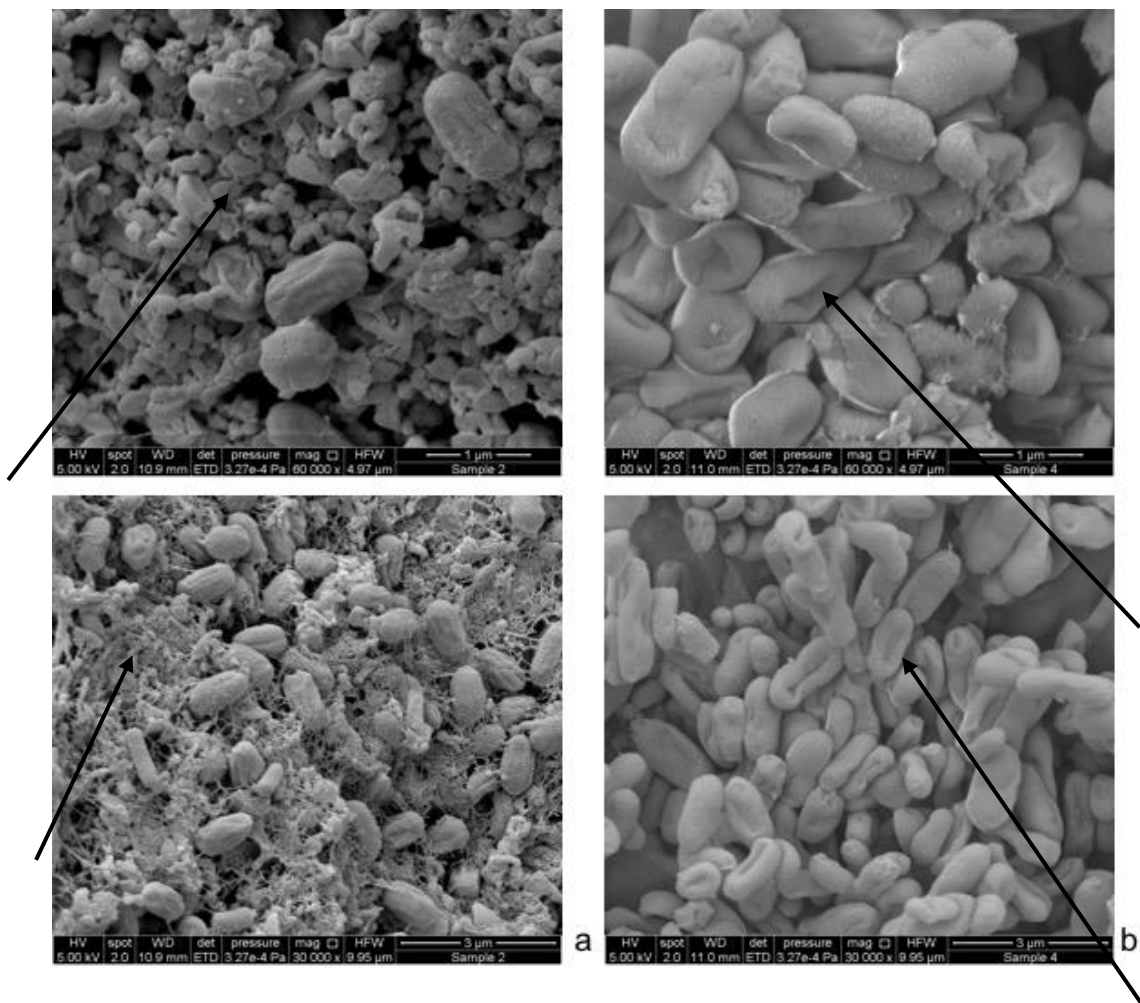


Figure 53. SEM images of cultures of *P. putida* (a) Control and (b) Test (18 mT). Top images were taken at 60k magnification; bottom images were taken at 30k magnification. Arrows on (a) images indicate web formation and the chain-like organisation of the cells. Arrows on the right images indicate morphological changes to the control culture's cells. Arrows on (b) images indicate the de-shaped cells of the test.

As indicated by arrows on the images of the test samples on the right, morphological change in *P. putida* under the magnetic field was confirmed.

Moreover, the cells were consolidated in a web shaped formation in the control sample. However, the test sample remained without the named formation.

3.3.1.3. Effect of 18 mT magnetic field on formation, chemical characteristics and concentration of biopolymer in *P. putida* cultures in STR system

Samples taken from the two SRTs were screened for the presence of PHB. Production of this biopolymer was confirmed through performing Sudan Black test on plates from the samples of both STRs.

Plated samples from the control and the test cultures after Sudan Black staining were observed. The colonies containing P(3HB) absorbed the black stain. These colonies were then observed in more detail under a 10X microscope.

The presence of P(3HB) was also observed through fluorescence microscopy of stained samples of both STRs (Fig. 54)

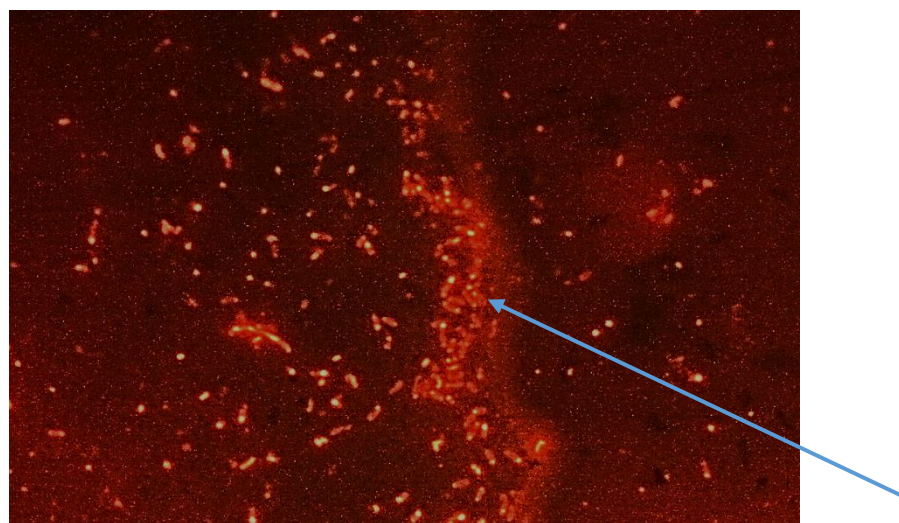


Figure 54. Image visualisation of *P. putida* cells containing P(3HB). These cells were stained with Nile red and visualised under fluorescence microscope. P(3HB) retains the Nile red colour, which was then observed under the microscope with 10 x magnification. Arrow indicates a floc of cells with inclusion bodies of P(3HB)

Cells containing P(3HB), obtained the fluorescent dye (Nile red) were visualised under the fluorescence microscope. The orange/red colour under this microscope is due to the presence of inclusion bodied of P(3HB) within the bacterial cells and confirms the production of this biopolymer.

The polymer extracted from samples of both STRs was also screened for its characteristics via FTIR. As presented in Fig. 55, chemical structure profile of samples obtained from FTIR, confirmed the biopolymer achieved in both STRs was the same and the magnetic field did not make structural changes to the produced P(3HB).

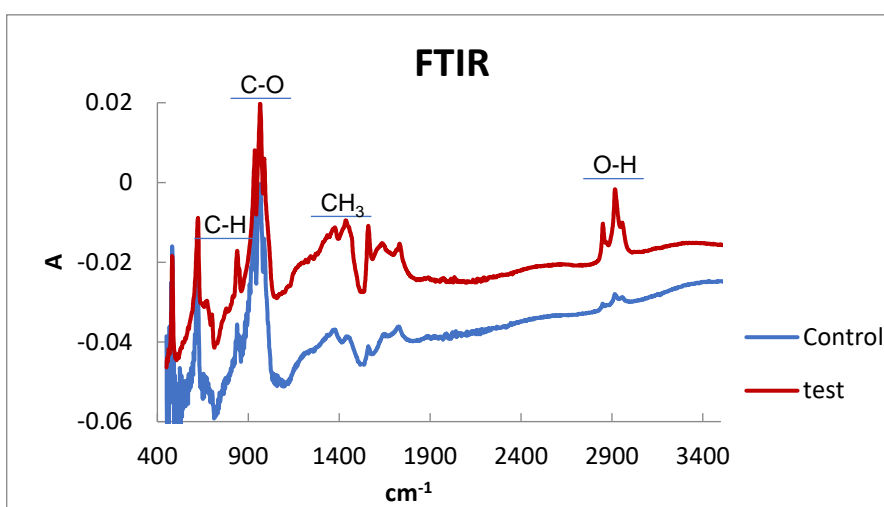


Figure 55. FTIR results of the control and the test (18 mT) PHAs from *P. putida* STR cultures. Chemical structure of the polymer in both gave the same peaks. This confirms the structural similarity of the product between the two reactors

After confirmation of P(3HB) production in the two STRs, the P(3HB) concentration in samples taken from both cultures was then quantified through crotonic acid assay.

The results of this assay are presented in Fig. 56.

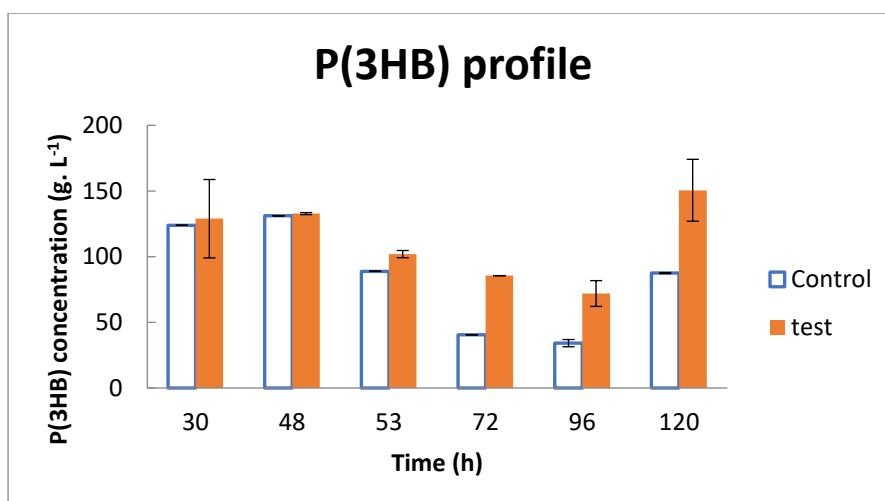


Figure 56. P(3HB) concentration profile during fermentation of *P. putida* under 18 mT magnetic field

As shown in Fig. 56, the concentration of P(3HB) followed the same trend in both bioreactors until 48 h of incubation, when the growth profile of the test was reached its first stationary phase and the control was at the stationary growth phase. From this point onwards, the PHB content decreased in both at the intervals of 53-96 h. after 96h, the concentration of PHB increased in both cultures with different rates.

The maximum P(3HB) concentration (150 mg. L⁻¹) was achieved after 120 h of incubation in the test culture while the lower maximum value of 131 mg. L⁻¹ was obtained after 48 h in the control.

The maximum biopolymer obtained from the MFG-exposed culture was therefore 15% higher than in the control.

P(3HB) production rate at different intervals within the two STRs is calculated in Table 29.

Table 29. P(3HB) production rate at different time intervals in *P. putida* 2 L STRs. The test was exposed to 18 mT MF

<i>Time interval (h)</i>	<i>Control production rate (mg. L⁻¹. h⁻¹)</i>	<i>Test production rate (mg. L⁻¹. h⁻¹)</i>
0-48	0.7	0.5
96-120	1	2

As shown in Table 29, the rate of P(3HB) production was twice higher in the test than that of the control between 96-120 h.

3.3.1.4. Effect of 18 mT magnetic field on glucose consumption of *P. putida* cultures in STR system

Glucose assay was carried out on samples taken from both STRs at different time intervals. This assay quantifies the concentration of glucose in the culture medium. Results of glucose assay are presented in Fig. 57.

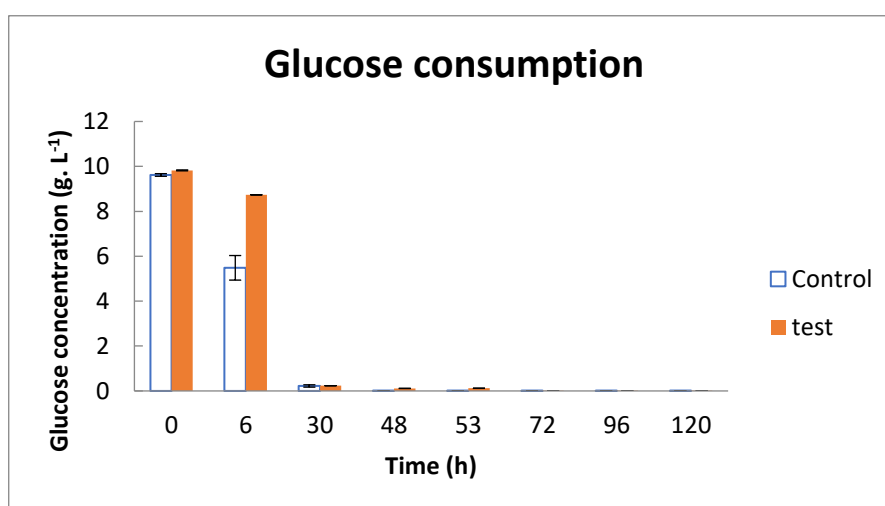


Figure 57. Glucose consumption profile in the control and test cultures of *P. putida* in 2 L STRs. The test was exposed to 18 mT MF

As shown in Fig. 57, glucose was consumed within the first 30 h of incubation in both STRs. The consumption rate of glucose was 0.29 and 0.33 g. L⁻¹.h⁻¹ in the control and the test STRs, respectively.

3.3.2. STR Batch fermentation of *P. putida* with magnetic field intensity of 28 mT

Pseudomonas putida culture was cultivated in batch fermentations with the test bioreactor circulating through the MFG with magnetic field intensity of 28 mT. The duration of the run was 120 h. During this time, the whole 1.5 L culture was circulated 48 times through the magnetic field.

3.3.2.1. Effect of 28 mT magnetic field on growth profile of *P. putida* in STR system

Fig. 58 shows the growth profile of the two STRs through optical density measurements at 600 nm (OD_{600}). The data in this Fig. show averages of duplicate readings. Error bars show standard deviation between these readings.

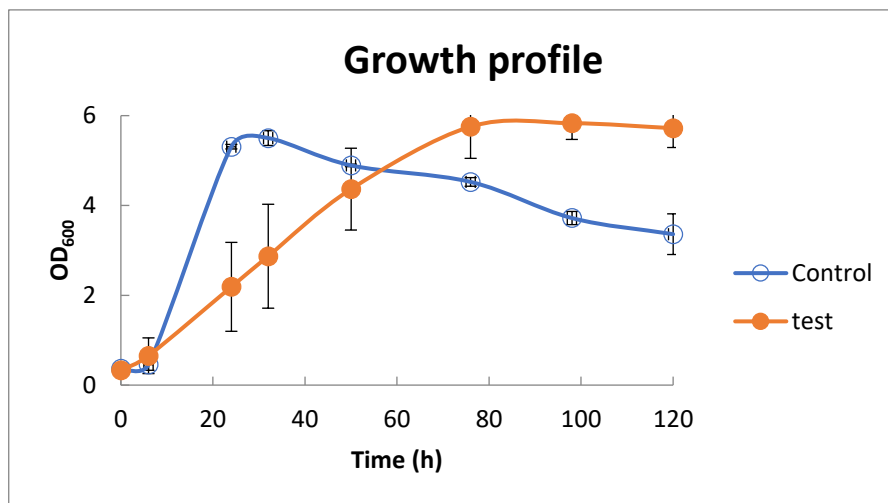


Figure 58. Growth profile of *P. putida* in 2 L STRs under 28 mT MF

As presented in Fig. 58, the growth profile of *P. putida* reached its maximum stage of 5.5 after 32 h of incubation in the control STR. The maximum OD_{600} of the test STR (5.8) was achieved after 76 h of incubation. At this point the culture medium had passed through the MFG for 30 rounds.

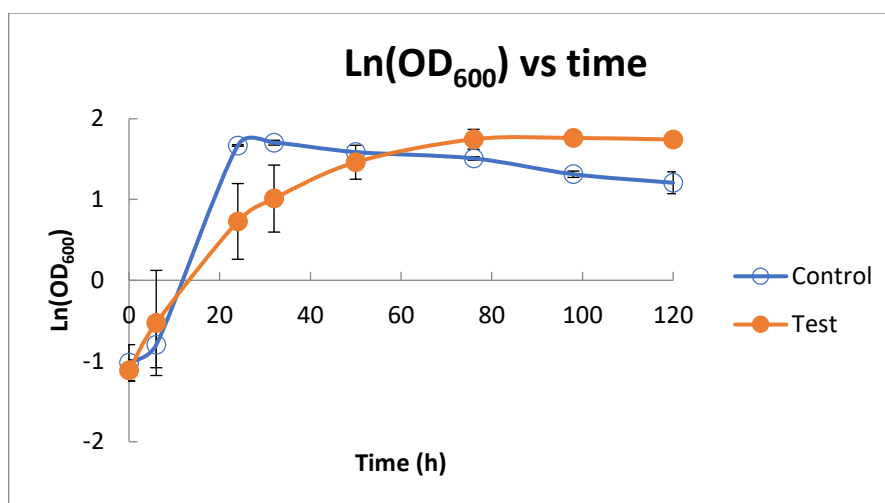


Figure 59. Growth profile of *P. putida* in 2 L STRs under 28 mT magnetic field on logarithmic scale

Fig. 59 shows the growth profile of the two cultures on logarithmic scale. The maximum growth rate occurred at 6-24 h interval in both STRs, with 0.14 h^{-1} in the control and 0.07 h^{-1} in the test. Doubling times in the two STRs were therefore calculated as 5 and 9.9 h in the control and the test, respectively. Table 30 shows the results of CFU counts in the two STRs.

Table 30. Colony Forming Units per mL of *P. putida* culture in 2 L STRs. The test was exposed to 28 mT magnetic field

<i>Time interval (h)</i>	<i>Control ($10^7 \text{ CFU. mL}^{-1}$)</i>	<i>Test ($10^7 \text{ CFU. mL}^{-1}$)</i>
0	12	14
32	257	123
50	208	203
76	211	398
98	135	355
120	20	200

According to the results obtained from colony forming unit counts (Table 30), number of viable cells in both cultures followed the same trend as the OD_{600} . The number of viable cells in the control culture increased until 32 h of incubation and declined afterwards. On the other hand, cell counts in the test cultures increase until 76 h.

3.3.2.2. Effect of 28 mT magnetic field on morphology of *P. putida* cells in STRs

In order to investigate the effect of 28 mT magnetic field on morphological properties of *P. putida*, SEM images were obtained from the samples of the control and the test.

These images are presented in Fig. 60 below. The samples were taken towards the end of the fermentation period at 98 h. Rod cell of *P. putida* cells changed into a coin-like shape.

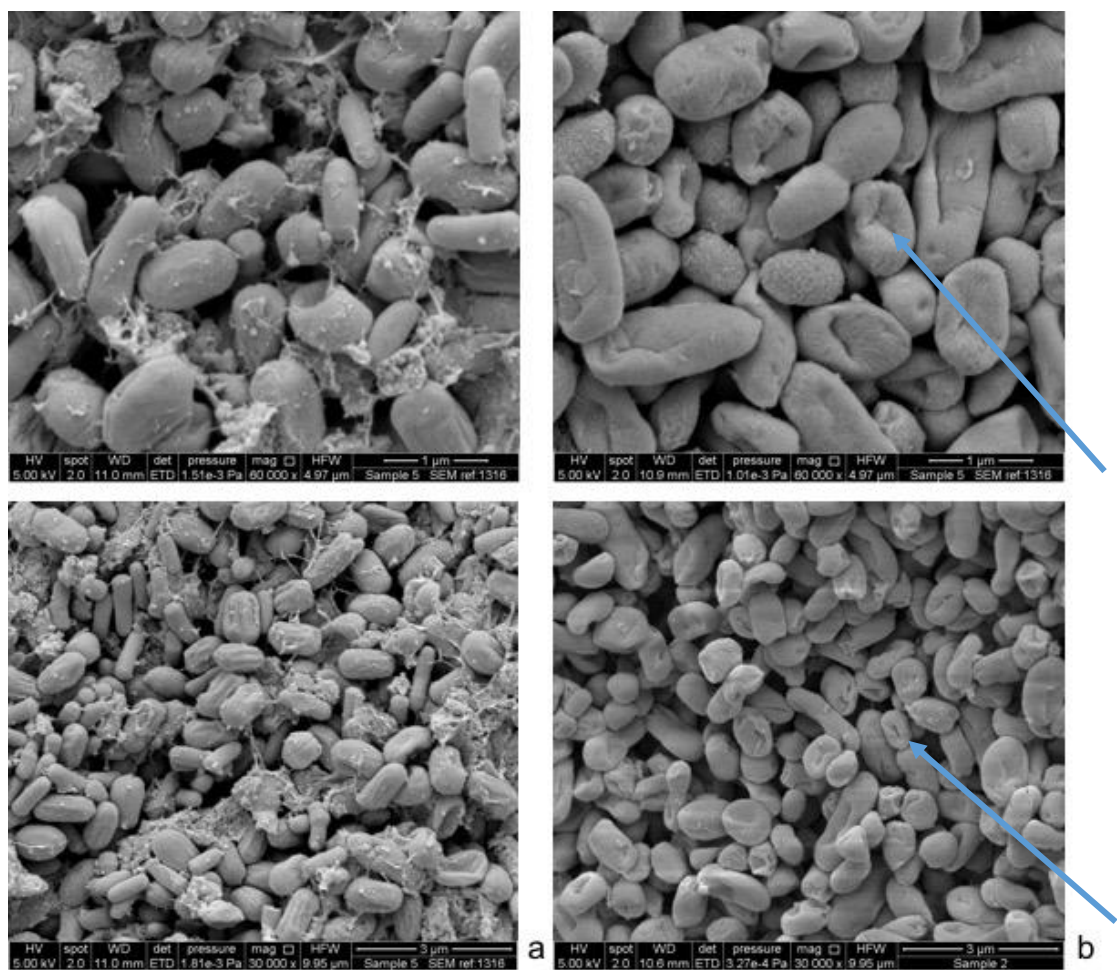


Figure 60. SEM images of samples of a: Control; b: The test culture of *P. putida* with 28 mT MF taken after 98 h of incubation. Top images were taken at 60k magnification; bottom images were taken at 30k magnification. Arrows indicate the de-shaped cells.

As indicated by arrows on the images of the test samples on the right, a conformation change of *P. putida* under the magnetic field was confirmed.

There was also less cell debris/extracellular polymeric substances present in the test as compared to the control samples.

3.3.2.3. Effect of 28 mT magnetic field on formation, chemical characteristics and concentration of P(3HB) in *P. putida* cultures in STR system

Samples taken from the two SRTs were screened for the presence of P(3HB). The production of this biopolymer was confirmed through performing Sudan Black test on plates from the samples of both STRs (Fig. 61).

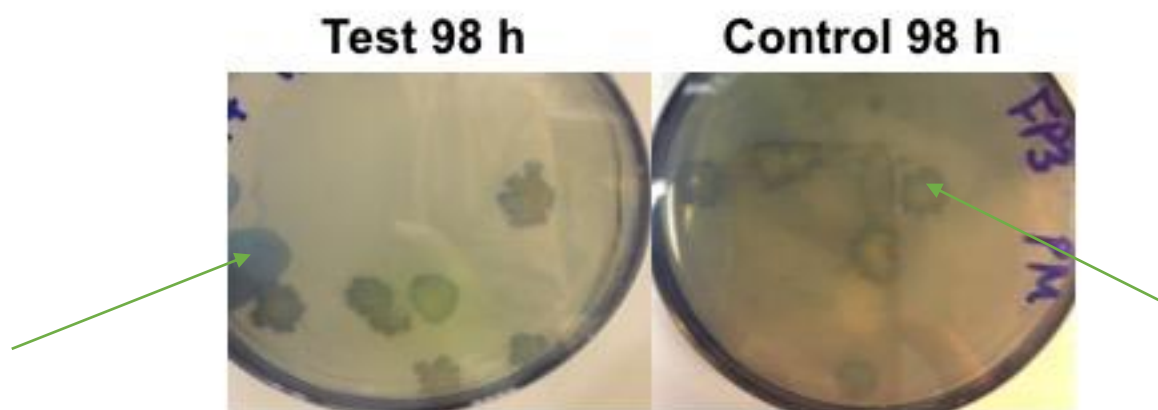


Figure 61. Sudan Black test on diluted samples (2×10^7 fold) of the control and the test (28 mT MF) STRs of *P. putida*. Arrows indicate the colonies containing P(3HB), which retained the black stain.

Samples were diluted and plated out on nutrient agar plates. The plates were incubated for 48 h and colonies were then stained by Sudan Black method after which time they were washed. Colonies retained the black stain, confirming the presence of PHB inside the cells (indicated by arrows in the image).

The polymer extracted from samples of both STRs was screened in FTIR. As presented in Fig. 62 the chemical structure profile obtained from FTIR, indicates the chemical structure of the biopolymer achieved in both STRs was the same and the magnetic field did not make structural changes to the P(3HB) produced.

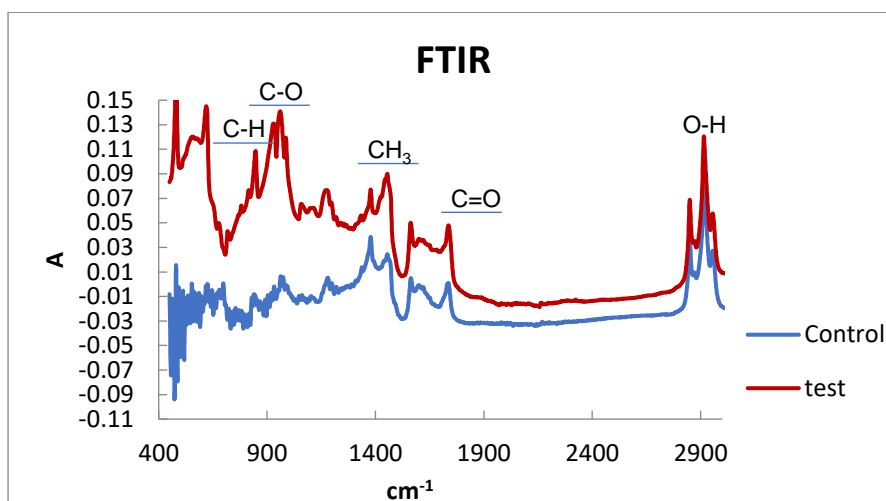


Figure 62. Confirmation of type of P(3HB) produced by *P. putida* in 2 L STRs . The test was exposed to 28 mT magnetic field

After confirmation of P(3HB) production in the two STRs, the P(3HB) concentration in samples taken from both cultures was then quantified through crotonic acid assay. Results of this assay are presented in Fig. 63.

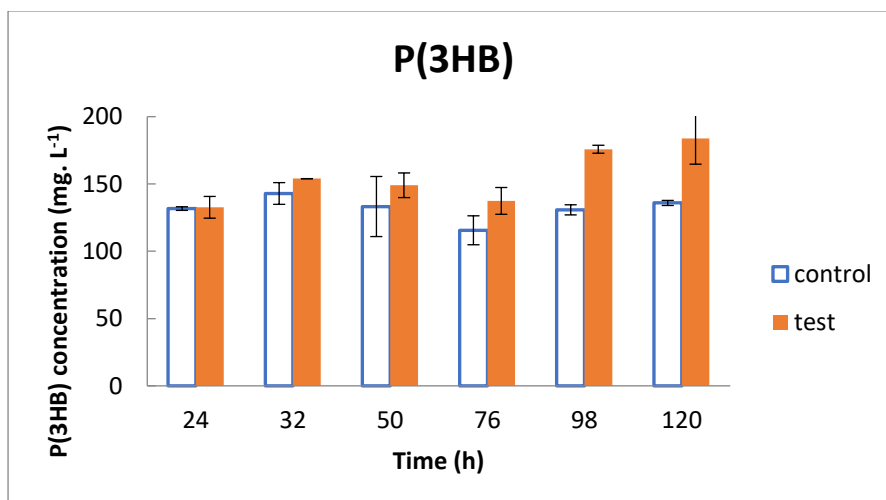


Figure 63. P(3HB) concentration profile at different time points of fermentation of *P. putida* in 2 L STRs . The test was exposed to 28 mT magnetic field

As shown in Fig. 63, the concentration of P(3HB) in samples taken at different time points of the fermentation, followed a slight increase towards the end of the fermentation period in both STRs. The P(3HB) content of the culture medium was higher in the test culture compared to the control, with the difference increasing at the end of the fermentation period.

Table 31 shows the concentrations of P(3HB) with percentage difference between the test and the control at each time point.

At 32 h, where maximum number of cells were present in the control STR, the P(3HB) content of the medium was also at its maximum of 143 mg. L⁻¹, approx. 8% lower than that of the test.

Although the test culture reached its maximum cell density at 76 h, the maximum P(3HB) content was obtained at the end of the fermentation period at 120 h, which was 35% higher than that of the control.

Table 31. P(3HB) concentration and the percentage difference between the control and the test STRs of *P. putida* under 28 mT MF at different time points

<i>Time interval (h)</i>	<i>Control P(3HB) (mg. L⁻¹)</i>	<i>Test P(3HB) (mg. L⁻¹)</i>	<i>Percentage difference</i>
24	132	133	0.7
32	143	154	7.7
50	133	149	11.8
76	116	137	18.9
98	131	176	34.4
120	136	184	35.2

3.3.2.4. Effect of 28 mT magnetic field on glucose consumption of *P. putida* cultures in STR system

Glucose concentration changes in the two STRs are shown in Fig. 64.

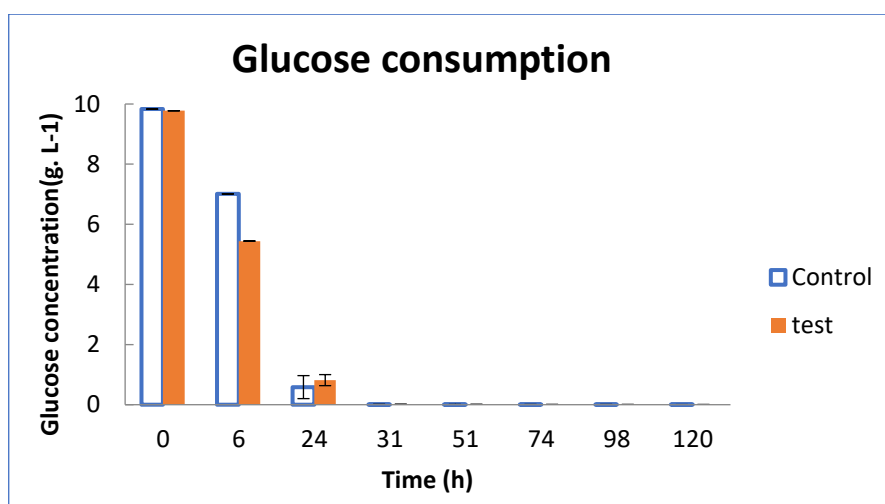


Figure 64. Glucose consumption of by *P. putida* in 2 L STRs. The test was exposed to 28 mT magnetic field

Glucose was consumed during the first 31 h of fermentation from its initial concentration of 10 g.L⁻¹. Fig. 64 shows the results obtained from glucose assay of samples taken throughout the course of this run.

As shown in Table 32, the consumption rate of glucose remained the same at both control and test STRs.

Table 32. Glucose consumption rate between different time points in *P. putida* cultures in 2 L STRs . The test was exposed to 28 mT magnetic field

<i>Time interval (h)</i>	<i>Control glucose consumption rate (g. L⁻¹. h⁻¹)</i>	<i>Test glucose consumption rate (g. L⁻¹. h⁻¹)</i>
0-31	0.34	0.34
0-24	0.38	0.39

Chapter 4

Discussion

4. Discussion

The main aim of this research was to investigate the potential effects of static magnetic field on production of microbial products. To this end, cultures of three bacterial strains including *Bacillus subtilis*, *Bacillus licheniformis* and *Pseudomonas putida* were monitored as producers of two industrially viable products; bacitracin and P(3HB).

Two members of *Bacillus* family (*Bacillus subtilis* and *Bacillus licheniformis*) were the candidates for this research due to the following reasons:

The selected strains are robust, and are ubiquitous in nature. They are classified as GRAS (Generally Regarded As Safe) by the Food and Drug Administration (FDA) (De Boer et al., 1994). Therefore, extensive research has been carried out on these *Bacillus* spp., which has led to a good understanding of their physiological and biochemical characteristics such as metabolic activity, genetic sequence and product characterisation. Also, *Bacillus* spp. are considered as workhorses in microbial product industry, and are the most used bacteria for large-scale production of valuable metabolites, antibiotics, enzymes, proteases, biofuels, biopolymers and bioremediation (Singh et al., 2009; Sukan, 2015).

Bacitracin as an antibiotic produced by *B. licheniformis*, and PHAs as biopolymers produced by *B. subtilis* were used as model products in this study. To test the introduced model system, a microbial product was required, which could be produced from both Gram-positive and Gram-negative microorganisms. PHAs were great candidates for this purpose as they are well-studied and produced by a range of Gram-positive and Gram-negative bacteria (Akaraonye et al., 2010; Anderson and Dawes, 1990; Getachew and Woldesenbet, 2016).

Pseudomonas putida was then selected as a Gram-negative model strain to study effects of magnetic field. This strain was selected due to two main reasons; Firstly, it is classified as one of the main PHA producers within the Gram-negative strains used for biopolymer production (Singh et al., 2009).

Therefore, the experimental set up could be used for the same product but from a Gram-negative producer. Secondly, *Pseudomonas* spp. are considered as a microbial work-horse of interest in microbial industry and a wealth of research is available on their cultivation and molecular biology. This is mainly due to their low maintenance requirements, high biomass yield, metabolic adaptability and ability to degrade various toxic compounds (Poblete-Castro et al., 2012).

The effect of magnetic field on growth, substrate uptake, cell morphology and product concentrations of each strain are discussed, and where relevant, compared with the literature. As a result of current available research, and capability of our MFG device, MF intensities 10, 18 and 28 mT were chosen.

4.1. Effect of magnetic field on *Bacillus licheniformis* NCIMB 8874

Effect of magnetic field on cultures of *B. licheniformis* was investigated in this study. To this end, two intensities of magnetic field were applied to the cultures of *B. licheniformis* (10 mT and 28 mT).

For simplification of this discussion, these experiments, described briefly in Table 33, are referred to as SF, STR 1, STR 2 and STR 3.

Table 33. Specification of designs used for studies on the effect of magnetic field on *B. licheniformis*

<i>Fermentation name</i>	<i>SF</i>	<i>STR 1</i>	<i>STR 2</i>	<i>STR 3</i>
Magnetic field intensity	28 mT	28 mT	10 mT	10 mT
Description	100 mL Shaken flasks	2 L STRs	2 L STRs	2 L STRs with pH control

4.1.1. Effect of magnetic field on growth profile of *B. licheniformis*

Growth profile of *B. licheniformis* was monitored in all four systems through OD₆₅₀ measurements and cell viability was monitored through CFU counts as reported in the results chapter of this thesis.

In general, doubling times of the control runs were different. Table 34 below shows a summary of these observations.

Table 34. Doubling time of *B. licheniformis* in the experiments carried out in this research

<i>Fermentation system</i>	<i>SF</i>	<i>STR 1</i>	<i>STR 2</i>	<i>STR 3</i>
Control t _d (h)	5.5	2.55	1.5	4.4
Test t _d (h)	5.6	2.8	1.3	3.1

In this section, results of the controls and the tests of the four systems are compared. The STR 1 and STR 2 systems were of the same setups with only two different variables: the inoculum (although incubated for the same period and under the same conditions) and the MF intensity. Therefore, the control cultures are compared and differences are discussed. On another hand, the difference between the controls of these two setups, and the control culture of STR 3, was the inoculum and pH control strategy.

Results of these experiments show that the doubling time of SF culture was almost twice that of STRs. This is mainly due to the controlled environment in bioreactors. While aeration is controlled in STRs through changes in impeller speed and air flow-rate, oxygen transfer rate in SF system is very limited and occurs only through the shaker rpm and the air-flow through sponges placed on top of shaken flasks and the gas liquid interface. The lower oxygen transfer in SF therefore leads to slower microbial growth due to rapid oxygen limitation. Small flasks allow minimum surface area, which further slows down cell growth (Sedletsy, 2007).

The control cultures of STR 1 and STR 2, did not have the same doubling time although all conditions were the same. This difference may be related to the

inoculum condition. Although the stock culture was the same, it is known that each fermentation culture has its own characteristic, which may lead to different profiles (Webb and Kamat, 1993). The possibility of contamination, if not totally rejected, can be reasonably ruled out. Appropriate measures to verify this were taken in the experiments. These include microscopic examination of the cultures in samples of different time points, plating out of the samples and confirmation of similarity of colony shapes and control of growth aspects (e.g. pH profile and %D.O.T.) throughout the fermentation period. Also, SEM images showed no contaminants present in the samples taken at the end of the runs.

STR 2 control and test cultures did not have a lag phase in contrast to STR 1 cultures, which can also be related to the inoculum condition. In a review article written by Swinnen et al. (2004), it was concluded that incubation conditions, cell physiological properties and inoculum size are the crucial factors affecting the lag phase of microbial growth at the start of incubation (Swinnen et al., 2004). Particular effort was made to ensure similarity of the culture conditions at the start of each run.

Higher doubling time of *B. licheniformis* in the control reactor of STR 3 system as compared to that in STR 2 and STR 1, is associated with the application of pH control. 1 M hydrochloric acid addition was started after 20 h of incubation in both control and test cultures. Although this pH control improved production of bacitracin and halted product degradation in the culture media, pH control system also triggered a second lag phase in the growth profile (Fig 34, page 84). The presence of this second lag phase shows a diauxic growth behaviour in both cultures between 20-42 h. Both the control and the test reached stationary phase after 42 h of incubation. The change in growth may be due to the effect of pH on the transportation of molecules through cell membrane in *B. licheniformis* cells. This is also in line with previous research on the effect of pH on physiological properties of *Bacillus* cultures. Abusham et al. (2009) investigated the effect of pH on protease activity and growth of *B. subtilis* and observed that protease activity was highly influenced by pH of the medium. As the cultures grew, pH levels and protease activity also increased (Abusham et

al., 2009). Moon and Parulekar (1991) reported that maximum production yield of protease by *B. firmus* was achieved through optimisation of process parameters including pH. They suggested that the effect of pH on production is related to transport of molecules through cell membrane leading to changes in cell metabolism (Abusham et al., 2009). In a study on the effect of pH on *B. licheniformis* fed-batch cultures, researchers have shown that pH values effect citrate uptake of the microorganism (Cromwick et al., 1996).

Results obtained from total carbohydrate content of the culture media were also in line with growth profile between the STR 1 and STR 2.

Carbohydrate production rate in STR 3 system was slower as compared to the fast-grown control culture of STR 2. In the test cultures however, these profiles followed similar trend. Total carbohydrate content of the test culture in STR 3 increased rapidly from the beginning to mid-stationary phase of growth in fermentation, which was similar to the test culture of STR 2 system.

In general, the impact of MF (10 and 28 mT) on growth of *B. licheniformis* was insignificant in the first three systems with an exception in STR 3. Therefore, it can be concluded that since the test culture in neither STR 1 nor STR 2 was much different from the control cultures of the respective STRs, the difference between growth profiles of the control and the test cultures in STR 3 was due to the combination of pH control and magnetic field application. Application of pH on its own led to slower growth (comparison of Control STR3 with other controls). However, cells grew to a higher density.

Growth of bacterial culture in the test STR 3 was faster than the control culture of STR3. This is in line with findings of Kamel et al. (2013) who reported changes in the cell membrane due to MF exposure leading to change of cell division. Transmembrane potential was increased through addition of mild acid. The increase in transmembrane potential can be obtained through ion addition (Bruhn et al., 1997). Theoretically, application of MF has a more pronounced effect in increasing transmembrane potential than the effect of presence of ions in the culture medium. This can result in changes in cell metabolism and enzymatic activities (Yadollahpour et al., 2014) leading to better substrate uptake and faster growth. However no reports seem to have

been published so far on the combined effect of pH control and magnetic field on microorganisms.

4.1.2. Effect of magnetic field on morphology of *B. licheniformis*

Based on proof of concept studies carried out within the research group of Professor Keshavarz at the University of Westminster, application of very low intensity magnetic field on *B. subtilis* OK2 resulted in release of some extracellular polymeric substances into the culture medium of an STR system (Sukan, 2015). To investigate similar changes in the experiments carried out in this thesis, SEM images were obtained from the samples of STR 1 and STR 3. This enabled the detection of morphological changes to the cells.

Magnetic field of 28 mT in STR 1 system ruptured *B. licheniformis* cells and severe damage in the form of holes was observed on cell surface of the MF-exposed culture. This cell damage was the possible cause of decreased biomass and bacitracin contents.

As shown in Fig. 39 of the results chapter, page 95, cell morphology profile was different in the STR 3 cultures. Lower intensity MF (10 mT) did not cause bacterial cell damage but resulted in extracellular entities attached to the cells of *B. licheniformis*.

The control cultures of STR 1 and STR 3 were not morphologically different according to the SEM images presented in the results chapter. This confirms that the extracellular entities in the STR 3 system are not just due to pH control but a combination of MF application (10 mT) and pH modification.

4.1.3. Effect of magnetic field on substrate uptake of *B. licheniformis*

The main carbon source in the growth medium of *B. licheniformis* in the systems presented in this thesis was glutamic acid (20 g. L⁻¹).

Results of glutamic acid consumption rate in the studies of all four systems were in line with the respective growth profiles. As expected, maximum substrate consumption occurred during the logarithmic growth phase and was halted once the cultures entered stationary phase.

In the SF system, glutamic acid was consumed during logarithmic growth phase in both the control and the test cultures until they reached stationary phase (0-48 h). The consumption stopped at this stage (48-74 h).

A total of approximately 9 g. L⁻¹ glutamic acid was consumed in the control SF within 48 h. In the test SF, glutamic acid consumption continued after reaching stationary phase and a total of 11 g. L⁻¹ glutamic acid was consumed.

In STR 1, around 6.5 and 8 g. L⁻¹ glutamic acid was consumed in the control and the test, respectively. This consumption occurred during the growth phase (between 0-42 h) and stopped afterwards.

As stated previously, both the control and the test cultures of STR 2 grew faster than their respective STR 1 cultures. Although logarithmic growth phase occurred over 0-20 h in STR 2, glutamic acid was consumed until the end of the fermentation period with the same trend in both the control and the test. A total of approximately 13 and 14 g. L⁻¹ was consumed in the control and the test, respectively.

As the growth profile of the STR 3 system suggests, *B. licheniformis* followed a diauxic growth curve. This was also associated with glutamic acid results. Glutamic acid uptake profile in STR 3 system can be divided into three sections: First logarithmic growth (0-21 h), second logarithmic growth (21-64 h) and stationary phase (64-84 h). It appears that glutamic acid consumption at the first logarithmic growth phase was very slow in both the control and the test cultures as compared to the consumption rates of both

cultures of STR 1 and STR 2 systems during their logarithmic growth phase. This suggests a shift in substrate uptake introduced by pH adjustments. The second carbon source present in the minimal M20 medium was citric acid (1 g. L⁻¹).

Based on glutamic acid profiles during the fermentation processes (as shown in Fig. 37 on page 91) , a possible explanation for biphasic growth of *B. licheniformis* could be that citric acid was the first carbon source consumed during the period of 0-24 h, contributing to the first logarithmic phase in both the control and the test in STR 3. After depletion of citric acid, the culture started metabolising glutamic acid instead. Table 35 summarises consumption rates of glutamic acid in all four systems used for bacitracin production in this thesis. This is explained as the possible cause of this behaviour since citric acid consumption profile was not obtained and further research will clarify this hypothesis.

Effect of pH on cultures of *B. subtilis* and the strain's response to acid and base stress factors has been reported in the literature. Wilks et al. suggested an adaptation of cells to moderate pH changes in the medium, while more extreme changes of pH value led to lower growth profiles (Wilks et al., 2009) . The findings of the present study are in agreement with Wilks et al's paper. pH of the medium affects transmembrane potential, which leads to a change of metabolism. The difference of glutamic acid consumption-rate between control cultures of STR 1 and STR 2 as compared to STR3, is probably due to pH adjustments.

Table 35. Summary of glutamic acid consumption rates in *B. licheniformis* experiments

<i>Fermentation system</i>	<i>SF</i>		<i>STR 1</i>	<i>STR 2</i>		<i>STR 3</i>		
	<i>0-48</i>	<i>48-74</i>	<i>0-40</i>	<i>0-36</i>	<i>36-64</i>	<i>0-21</i>	<i>21-64</i>	<i>64-84</i>
Control consumption rate (g. L ⁻¹ . h ⁻¹)	0.19	-	0.15	0.28	0.11	0.1	0.18	0.29
Test consumption rate (g. L ⁻¹ . h ⁻¹)	0.18	0.07	0.19	0.26	0.15	0.07	0.29	-
Phase of growth	Log	Stat	Log	Log	Stat	Log 1	Log 2	Stat

4.1.4. Effect of magnetic field on bacitracin production

Similar to most secondary metabolites of bacterial cultures, bacitracin is normally produced after the culture of *B. licheniformis* reaches its maximum biomass, at later stages of exponential phase (Reffatti, 2012).

However, bacitracin production in the experiments reported in this thesis started at early to mid-logarithmic growth phase. This observation was expected from these experiments as it was a result of the choice of growth medium in favour of early production. Minimal growth medium (M20) resulted in early production of bacitracin in these experiments (Murphy, 2008; Reffatti, 2012).

The initial experiments (referred to as SF in this report) were carried out in 100 mL shaken flask cultures of *B. licheniformis*. These experiments were designed in such a way that the test culture got exposed to the magnetic field throughout the run. For this reason, circulation-rate through the MFG was set at 10 mL. min⁻¹ in 20 mL working volume SFs. Magnetic field of 28 mT intensity was applied to these cultures.

One of the findings of this study was the faster bacitracin production-rate in obtaining maximum bacitracin content in the MF exposed cultures. Concentration of bacitracin in the culture exposed to MF reached its maximum (262 mg. L⁻¹) after 24 h. At this point, the culture medium had passed through the MFG for 720 rounds. In the control system, although production of the antibiotic started in mid-growth phase, highest level of bacitracin (342 mg. L⁻¹) was obtained after 48 h of incubation when the culture entered stationary growth phase.

Profiles of bacitracin concentration throughout the SF runs were different between the control and the test. Bacitracin production of the control culture started at mid-logarithmic growth phase (24 h), concentration increased until

the culture reached stationary growth phase at 48 h and declined afterwards. Production profile of the MF exposed culture followed a decreasing trend from after 24 h (mid-logarithmic growth phase) until the end of the fermentation period. The decline in bacitracin content in both cultures after 48 h, can be related to pH changes of the cultures into high alkaline conditions (pH=9.36). According to the literature, the optimum pH for bacitracin production lies within the range of 6-8. Under more alkaline conditions, bacitracin A is oxidised into its inactive form of bacitracin F (Konigsberg and Craig, 1962).

The change in fermentation time required for obtaining the maximum bacitracin concentration, was a result of exposure to 28 mT magnetic field. Although growth continued after 24 h, bacitracin production profile changed into degradation/transformation. As mentioned in Table 13 of the results section (page 70), bacitracin concentration per cell dry weigh of the control SF changed from almost 24% at 24 h to 28% at the end of the logarithmic growth phase at 48 h. However, the test culture showed a rapid decrease in product yield from mid to the end of the logarithmic growth phase when total carbohydrate content of the test culture increased after 24 h. It appears that MF exposure triggered a shift in cell metabolism leading to lower bacitracin production/higher bacitracin degradation and more release of by-products such as extracellular polymeric substances (EPS) with a subsequent increase in growth.

The research was then focused on fermentation in STRs to investigate the effect of magnetic field exposure on cultures of *B. licheniformis* under more controlled conditions.

MF exposure was initiated as soon as bacitracin production started. This was after 16 h of incubation.

The profile trend obtained from the control STR, was similar to the profile of the control SF system. Bacitracin production started at logarithmic growth phase. It reached its maximum as soon as the culture went into stationary growth phase followed by a slight decrease. This also was related to the pH

change of the STR culture at this stage since it became alkaline after this period. The alkalinity of the culture medium (>7.5) in the STR was not as severe as that of the SF culture (>8.5), hence the antibiotic was stable for a longer period in the STR in contrast to the rapid degradation in the SF (Murphy, 2008).

Unlike the MF exposed culture of the SF system, 28 mT magnetic field did not have a significant impact on bacitracin content of the STR culture. Total bacitracin content of both control and test cultures increased until reaching the stationary phase at 40 h and decreased from then on. However, at the end of stationary phase after 64 h, degradation rate of bacitracin A in the test culture was higher than that of the control. After more than 19 passages through the MFG, bacitracin content of the test culture decreased rapidly as compared to the control culture.

It seems from both SF and STR 1 experiments that continued exposure to MF of 28 mT causes a decrease in bacitracin content, which can be related to either a shift in cell metabolism or assisting degradation process of bacitracin A in the culture medium by magnetising the molecules. However, the effect of MF on bacitracin's molecular structure was not studied. Another plausible reason for the lower bacitracin content in the MF exposed culture compared to the control, is cell disruption caused by 28 mT MF. This assumption is made based on comparison of SEM images obtained from relevant samples of control and test STRs presented in Fig. 26 of results chapter on page 79.

Total carbohydrate content of the STRs fluctuated during the period of fermentation. Unlike the SF experiments, there was no shift in product formation profile of the STRs. Therefore, total carbohydrate content of the test culture was not expected to change as compared to the control. This was confirmed in Fig. 25 of results chapter (page 78).

There was a sudden increase in the total carbohydrate content of both control and test STRs between 20 to 42 h (mid logarithmic to early stationary phase of growth). This was possibly due to the release of EPS into culture medium.

The increase in carbohydrate concentration of the cultures continued throughout the stationary phase until 64 h. These findings were similar to those of Malick et al. (2017), who reported growth-independent release of EPS throughout fermentation of *B. licheniformis* and suggested that this was mainly because glycosidase catalytic activity of bacterial cells was kept intact even during stationary and death phase (Malick et al., 2017). Total carbohydrate concentration increased at a higher rate in the test STR compared to the control. This might have been associated with the effect of MF on metabolic activity of *B. licheniformis* cells during stationary and growth phases of growth.

Maximum bacitracin concentration achieved from the STR systems in both control and the test was lower than that of the SFs. These findings were also in agreement with literature. Murphy (2008) reported 30% higher bacitracin content in SF than that in STRs. They suggested that this was due to a higher doubling time for cultures of SFs as compared to STRs. The rapid increase in cell growth led to rapid pH change in the culture, which had an adverse effect on bacitracin A (Murphy, 2008). Schlatmann et al. (1993) reported a decrease in ajmalicine production through scale-up of *Catharanthus roseus* cell culture from shaken flask to bioreactors. Effect of aeration and shear force were suggested to be the main causes for this decrease (Schlatmann et al., 1993). In this study, aeration facilitated bacitracin production. However, effect of shear force through rapid agitation specially for adjustment of dissolved oxygen levels, could have led to a decrease in maximum product concentration. Potumarthi et al. (2007) have also reported inhibition of protease production by *B. licheniformis* as a result of high agitation rates (Potumarthi et al., 2007). Another point for consideration is the number of passes through the MFG. The SF culture media circulated through the MFG for at least 36 times more than the STRs. As the higher number of passes suggests lower bacitracin levels, the possible explanation is that the negative effect of larger scale was higher than the positive effect of number of circulations. Another possible reason for this finding is the addition of anti-foaming agent to STRs. Antifoams reduce oxygen transfer by coalescing air bubbles and assisting their breakage. This reduces surface area for aeration and hence prevents oxygen transfer (Lakowitz et al., 2017).

After the above observations, a lower intensity of the MF (10 mT) was used. This experiment is referred to as STR 2.

MF of 10 mT intensity application was started at mid-logarithmic growth phase of *B. licheniformis* at 16 h. Bacitracin production in both control and test started at the beginning of logarithmic growth phase at 12 h and increased from then on.

Bacitracin concentration increased until 40 h of incubation after reaching mid-stationary phase. Production changed into a degradation trend at this point, when pH of the culture had exceeded 8.5.

In this experiment cell metabolism occurred faster than other runs of *B. licheniformis* fermentation. This might have been due to inoculum condition. Even though higher levels of bacitracin were achieved in these runs compared to those with MF of 28 mT intensity, comparison of the control and the test show that 10 mT had a positive impact on bacitracin production and the maximum concentration of bacitracin released into the medium of the test culture was 25% higher than that of the control at its maximum at 40 h.

Since the results of the STR 2 showed an increase in the maximum product concentration under MF of 10 mT, the system was further optimised in favour of bacitracin production in STR 3. This was through pH control of the culture medium since pH is one of the main factors affecting bacitracin A production by *B. licheniformis*. Optimum pH levels for bacitracin have been reported in the literature as 6-7 (Murphy, 2008).

pH value of the medium was initially adjusted to 6. Metabolic activity of *B. licheniformis* was allowed to increase the pH up to 7 in both STRs and the pH was then kept at 7 by mild acid addition. As presented in Fig. 35 of the results chapter (page 89), acid addition started at 21 h. This caused changes in growth and bacitracin content profiles of both STRs as compared to the STR 3 system.

MFG was started after 16 h to mimic the same process of STR 2, when bacitracin production was started.

Main finding of this design was the confirmation of the effect of pH as main limiting factor in bacitracin production. In this system, the concentration of bacitracin in the culture medium continued to increase until the end of the fermentation period. This finding was in agreement with previous research on the effect of pH on bacitracin content of bioreactors (Murphy, 2008; Reffatti, 2012; Wilks et al., 2009).

pH control in this system proved to have multiple impacts. Although pH of the culture medium increased to higher than 7 in the control STRs of the STR 1 and STR 2 experiments, bacitracin production did not change into a degradation profile until it reached to values of higher than 8.5 in the control STR 1 and 7.5 in control STR 2.

After 43 h both the control and the test in STR 2 were at mid-stationary phase, when the maximum bacitracin concentration was obtained. However, this maximum was lower than that obtained from the STR 3 system (256.8 mg. L⁻¹ in the control and 309.6 mg. L⁻¹ in the test STR 3 vs. 227 mg. L⁻¹ in the control and 283 mg. L⁻¹ in the test culture in STR 2).

The maximum concentration was obtained at the end of the fermentation period at 84 h, at a concentration of 571 mg. L⁻¹ in both control and test cultures.

Another finding of this experiment was that although maximum bacitracin obtained from both control and MF exposed cultures was the same at 84 h, the fermentation could have stopped at 64 h. At this point, bacitracin of the test was 501 mg. L⁻¹, 50% higher than the control STR. There was a more rapid increase in concentration of bacitracin between 42-64 h in the test culture as compared to the control. After 64 h, the test culture had approximately 20 passages through the MFG. The sudden increase of bacitracin concentration was in line with an increase in the total carbohydrate content of the test culture

as compared to the control culture. These results suggest that 10 mT magnetic field in this system induced the release of bacitracin and secretion of extracellular polymeric substances.

Effect of MF on microbial cells has been associated with permeability of ionic channels in bacterial cell membranes, which can lead to changes in ion transport through the cell membrane. This changes the physiological and metabolic activities of the cell (Mousavian-Roshanzamir and Makhdoumi-Kakhki, 2017). Inhan-Garip et al. (2011) reported disintegration of cell wall, extrusion of cytoplasmic contents, retraction of the cytoplasmic membrane and blebbing caused by application of MF on both Gram-positive and Gram-negative bacterial strains. They suggested that electrostatic balance of membrane constituents was altered through application of MF. This alteration resulted in disintegration of cell material and inhibition of growth (Inhan-Garip et al., 2011). These findings can be related to the changes observed in the present study. Change of pH along with MF may have had an impact on the ionic channels of bacterium resulting in such changes.

Furthermore, profile of bacitracin concentration in the control culture of STR 2 system did not contain the initial lag phase observed in STR 1. Consequently, growth profile was shifted backwards with no lag time. Possible reason for this is the initial inoculum used in the STR 1 system. It appears that cells initiating the fermentation were not at the same growth stage at the time of inoculation.

4.2. Effect of magnetic field on *Bacillus subtilis* NCTC 3610

After the studies on the effect of MF on cultures of *B. licheniformis*, the experiments were expanded to study the effect of magnetic field on a product produced by both Gram-positive and Gram-negative strains. *B. subtilis*, as a Gram-positive, well-studied bacterium, was selected. This bacterium is known as one of the industrial workhorses for production of useful bio products. The model product used for these experiments was P(3HB), a biopolymer of PHA

group. This product can be obtained from Gram-negative models, providing good basis as model bacterium/product for the introduced system.

In the experiments reported in this section, two intensities of magnetic field were applied to the cultures of *B. subtilis*.

For simplification of this discussion, these experiments, described briefly in Table 36, are referred to as STR 4 and STR 5.

Table 36. Specification of designs used for studies on the effect of magnetic field on *B. subtilis*

<i>Fermentation name</i>	<i>STR 4</i>	<i>STR 5</i>
Magnetic field intensity	18 mT	28 mT
Description	2 L STRs	2 L STRs

4.2.1. Effect of magnetic field on cell growth and morphology of *B. subtilis*

Growth profiles of the control and the test cultures in STR 4 and STR 5 showed an increase in cell density of the MF exposed cultures. Interestingly, MF with 18 mT strength resulted in a 34% increase in cell density while increasing the MF to 28 mT, had a lower impact on cell density of *B. subtilis* and resulted in 20% increase.

As shown in Table 37, cell doubling time was faster in the 18 mT MF-exposed culture. Higher intensity of 28 mT however, delayed increased doubling time by 12.5%. Although the doubling time of *B. subtilis* culture exposed to 28 mT magnetic field was longer than the control, the maximum cell density obtained from these cultures was higher than that of the control culture.

Also, doubling time of the controls of STR 4 and STR 5 were not the same. This can be related to the initial inoculum conditions. The difference between the two control systems was around 10%.

Table 37- doubling time of *B. subtilis* in STR 18 and STR 28 cultures

<i>Fermentation system</i>	<i>STR 4</i>	<i>STR 5</i>
Control t_d (h)	3.6	4
Test t_d (h)	3.2	4.5

According to the results obtained from SEM images, morphology of *B. subtilis* cells remained intact after application of magnetic field. The robust strain did not show cell damage after exposure to MF.

4.2.2. Effect of magnetic field on P(3HB) production

As described earlier in the introduction chapter PHBs are intracellular polymers stored in cells at the presence of excessive carbon source. P(3HB) content of the culture medium in the control and the test of STR 4 and STR 5 was measured at different intervals to study the effect of MF.

MF of 28 mT induced early P(3HB) production after 22 h, while MF of 18 mT delayed the onset of P(3HB) production and maximum concentration in the test was achieved later than the control.

Maximum P(3HB) concentration was achieved after 48 h in the controls of both STR 4 and STR 5, when both cultures were at stationary phase. These results were in line with the existing literature, whereby the optimum fermentation period for maximum PHB content is reported as 48 h for cultures of *B. subtilis* (Getachew and Woldesenbet, 2016).

The results of STR 4 suggest that MF of 18 mT intensity delayed the production of P(3HB) by *B. subtilis*. The maximum concentration was obtained after 73 h of incubation (70 mg. L⁻¹) in the test culture of STR 4 as compared to that in the control (65 mg. L⁻¹) after 48 h. However, maximum P(3HB) was obtained after 22 h of incubation in the test culture of STR 5 (47 mg. L⁻¹), while

in the control (46 mg. L⁻¹) it continued to increase until 48 h. These are presented in Table 38 below.

Table 38. Maximum P(3HB) content in STR cultures of *B. subtilis*

<i>Fermentation system</i>	<i>STR 4</i>		<i>STR 5</i>	
<i>maximum P(3HB)</i>	<i>Time (h)</i>	<i>Concentration (mg. L⁻¹)</i>	<i>Time(h)</i>	<i>Concentration (mg. L⁻¹)</i>
Control	46	65	48	46
Test	73	70	22	47

Based on the above observations and the fact that number of viable *B. subtilis* cells was higher under MF of 18 mT compared to non-exposed culture, it is possible that cellular metabolism of *B. subtilis* changed under 18 mT MF resulting in lower P(3HB) content and possibly production of by-products. It can be concluded that the uptake of carbon source, sucrose (20 g. L⁻¹) and yeast extract (2.5 g. L⁻¹), contributed only to cell growth during logarithmic growth phase and the cells did not store excess carbon in the form of P(3HB) until they reached later stages of stationary phase.

During stationary phase of growth, the MF-exposed cultures of *B. subtilis* had lower production yields than the non-exposed cultures. Therefore, it can be concluded from these experiments that MF had an adverse effect on P(3HB) production.

4.2.3. Confirmation of chemical structure of P(3HB)

Nile red fluorescence microscope observations were used as an indication of the presence of P(3HB) inclusion bodies in *B. subtilis* cells.

Molecular structure of the P(3HB) (Fig. 65) produced in these experiments was confirmed through FTIR.

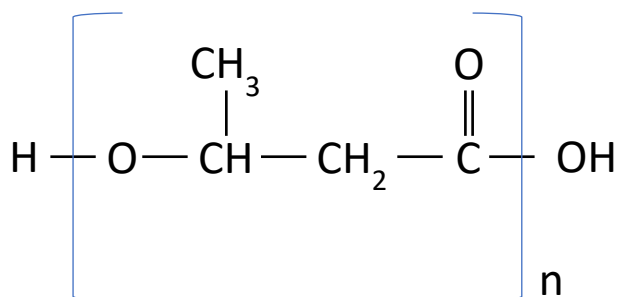


Figure 65. Molecular structure of P(3HB)

Therefore, functional groups to search for in FTIR peaks were C=O, OH (carboxylic acid), C-O and C-H. According to the results of these peaks and cross referencing these data with existing libraries for different functional groups (Bayari and Severcan, 2005; Torres et al., 2015), presence of these functional groups was confirmed. Table 39 summarises these findings.

Table 39. FTIR expected readings for different functional groups and results obtained from the control and the test STR 4 and STR 5

<i>Functional group</i>	<i>FTIR band in literature (cm⁻¹)</i>	<i>FTIR results of the experiments (cm⁻¹)</i>
C-O	900-1300	960-1120
C-H	1350-1480	1450-1465
C=O	1735-1750	1740-1757
O-H	2500-3000	2920-2955

FTIR spectroscopy results also confirmed that the chemical structure of the product was not affected by exposure to magnetic field. Neither of the two applied intensities changed the structure of the polymer. Both control and the tests in both experiments produced the same peaks. The functional peaks are presented in Fig. 66 and Fig. 67.

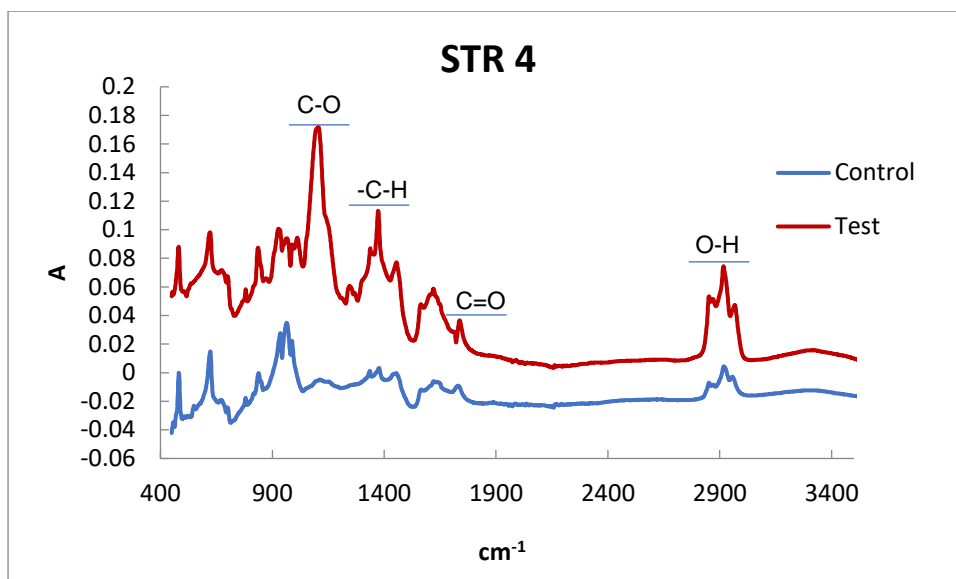


Figure 66. FTIR peaks obtained from STR 4

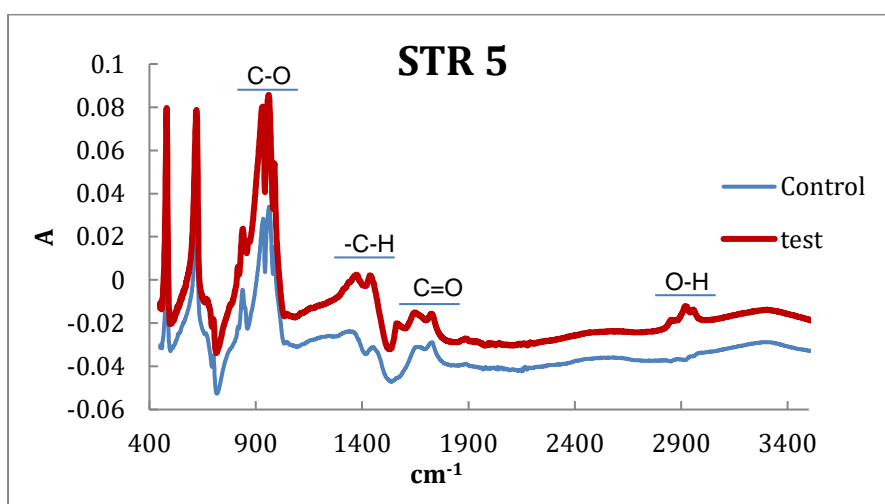


Figure 67. FTIR peaks obtained from STR 5

4.3. Effect of magnetic field on *Pseudomonas putida* KT 2440

Pseudomonas putida KT 2440 was used in this thesis as a Gram-negative P(3HB) producer. This bacterium is known as one of the industrial cell factories for production of useful bio products such as PHAs, phenol, Myxothiazol and aliphatic alcohols (Poblete-Castro et al., 2012).

In this section, STR 6 and STR 7 refer to the corresponding STR systems with application of 18 mT and 28 mT MF on *Pseudomonas putida* cultures, respectively (Table 40).

Table 40. Specification of designs used for studies on the effect of magnetic field on *P. putida* KT 2440

<i>Fermentation name</i>	<i>STR 6</i>	<i>STR 7</i>
Magnetic field intensity	18 mT	28 mT
Description	2 L STRs	2 L STRs

4.3.1. Effect of magnetic field on cell morphology of *P. putida* KT 2440

SEM images showed the effect of MF on morphology of *P. putida*. Both intensities resulted in notable changes in cell structure.

As presented in SEM results sections 3.3.1.2., Fig. 53 (page 111) and 3.3.2.2., Fig. 60 (page 118), cells in the control samples taken from STR 6 and STR 7 were embedded in a matrix of extra polymeric substances (EPS) in the culture medium. *Pseudomonas* spp. can synthesise a range of EPS, which assists with their resistance and survival in harsh environmental stress (Mann and Wozniak, 2012). The main constituents of *P. putida*'s EPS are exopolysaccharides such as alginates (Chang et al., 2007; Mann and Wozniak, 2012; Spiers et al., 2013), cellulose (Nilsson et al., 2011; Spiers et al., 2013), extracellular DNA (Jahn et al., 1999; Nilsson et al., 2011; Steinberger and Holden, 2005), proteins (Jahn et al., 1999), lipopolysaccharides (Nilsson et al., 2011) and random organic matter (Jahn et al., 1999). Pseudomonads biofilm also consists of polysaccharide levan as a nutrient storage molecule (Mann and Wozniak, 2012).

There is very limited published research on the effect of magnetic field on EPS formation of bacterial species. Bandara et al. (2015) reported a significant reduction in metabolic activity of *Pseudomonas aeruginosa* biofilm under the effect of magnetic field (Bandara et al., 2015). Furthermore, Di Bonaventura et al. (2014) observed that extremely low frequency magnetic

field (265 nT) was effective against biofilm formation. They anticipated this to be due to changes in ionic channels of bacterial cell membrane (Di Bonaventura et al., 2014). MF of 6-10 mT intensity was shown to increase EPS formation by *Bacillus cereus* CrA. What's more, application of MF with 7.4 mT intensity resulted in 20% decrease in negative charge of EPS as opposed to an increase in its negative charge when exposed to 10 mT MF (Xu et al., 2014).

The culture media of MF exposed *P. putida* cells in this study were free from EPS. It appears that MF either completely halted biofilm formation through changing ionic charge of EPS released into the medium, or induced biofilm dissolution process.

Biofilm dissolution is usually a result of carbon source starvation (Gjermansen et al., 2005), biofilm dispersing agents, bio surfactants, enzymes or other stress factors.

Another finding of these studies was the change in cell morphology of *P. putida* exposed to MF. Both MF-exposed cultures presented notable morphological changes. It appears that rod-shaped *P. putida* KT 2440 cells were compressed and developed a crinkly round shape rather than their original cylindrical form.

4.3.2. Effect of magnetic field on cell growth and P(3HB) production

Results obtained from the growth profiles presented in this thesis indicate a delay in growth of *P. putida* cells. Durner et. al reported different doubling times for the strain depending on the carbon source used in the growth medium (Durner et al., 2001). The cells grew much slower than expected in both cases. Table below shows a summary of the doubling times.

Table 41. Doubling time of *P. putida* in STR 6 and STR 7 cultures

<i>Fermentation system</i>	<i>STR 6</i>	<i>STR 7</i>
Control t_d (h)	10.5	5
Test t_d (h)	12	9.9

Doubling time in the control culture of STR 6 was double that of STR 7. This can be associated with the possible carry over of detergent in the inoculum shake flask, inferring stress on the strain. The possibility of this inconsistency being related to individual experiments is negligible since the parallel bioreactor settings of each run had similar trends.

Comparison of the two controls is presented in Fig. 68.



Figure 68. Growth profiles of the controls in STR 6 and STR 7

It can be concluded that although doubling times of the two cultures were different, they both followed the same profile and the reason for this difference can be due to the metabolic state of the initial inocula. Although every effort was made to mimic the same conditions for the inocula in all experiments including inoculation at the same optical density for all batches, different lag phases were observed due to the biological state of inoculum. The challenge of starting with a consistent inoculum and its effects on biomass growth and product formation have been pointed out in the literature (Jenzsch et al., 2006; Sen and Swaminathan, 2004). Sen and Swaminathan (2004) used two stage inoculum preparation for production of surfactin from *B. subtilis*. They reported the influence of inoculum size and age as main factors affecting surfactin concentration from *B. subtilis* (Sen and Swaminathan, 2004). According to Aehle et al. (2011), slight changes in the initial inoculum density can cause rather significant changes in growth profile of microorganisms (Aehle et al.,

2011). The difference in starting inocula was also expressed through behaviour of the microorganism in fermenters within the first 6 h of incubation. There was a lag time in growth of the control in STR 7, after which time cell density started increasing logarithmically. This was not the case in STR 6. No lag phase was detected in the growth profile of the control culture in STR 6 system. However, despite immediate growth, the maximum optical density obtained from this system was lower than that of the STR 7. The slower growth seen in STR 6 system, was in line with glucose consumption rates. Rate of consumption was higher in the control culture of STR 6 than STR 7 during the first 6 h of fermentation period. As cells were adapting to the fermenter conditions in STR 7, glucose uptake was slower resulting in the lag phase observed within this period. However, in the STR 7 system, cells started using glucose rapidly, contributing to their growth within 30 h and no lag was observed.

High glucose concentration in *P. putida* medium has shown to have inhibitory effect on cellular growth under nitrogen limiting conditions (Follonier et al., 2011). Another report on the effect of glucose concentration on growth of *P. putida* showed inhibitory effect on bacterial growth (Choi and Lee, 1997).

In this study, high glucose concentration led to decreased growth rate. The choice of medium was based on P(3HB) production.

Fig. 69 shows the difference between growth profiles of MF exposed cultures.

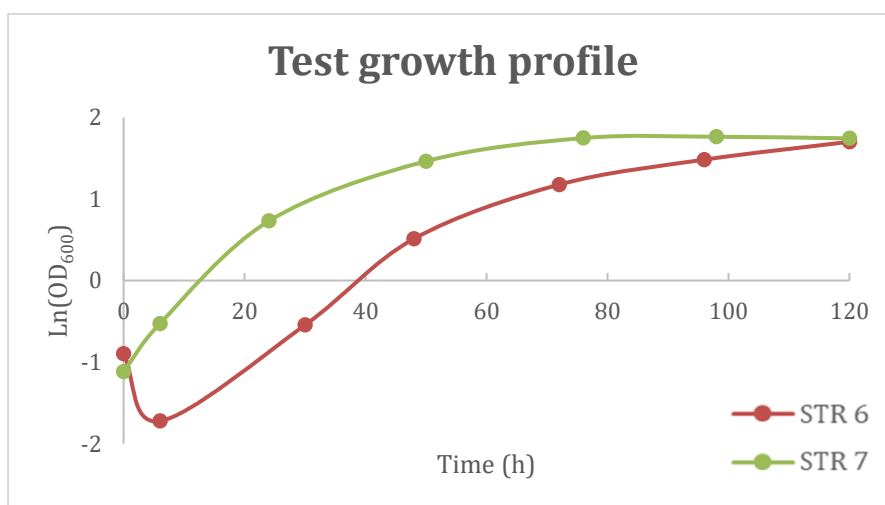


Figure 69. Growth profiles of the MF-exposed cultures in STR 6 and STR 7

It appears that the exposure to 18 mT MF resulted in a decline in cell density within the first 6h, which was then compensated, and logarithmic phase of growth started. During this period, glucose was not consumed in the test STR 6 and its concentration declined rapidly after this period until 24 h. However, glucose was consumed rapidly from the start and was depleted after 24 h in the test STR 7.

In general, magnetic field notably affected bacterial cell growth. Logarithmic growth was prolonged in the MF-exposed cultures and both reached stationary phase of growth later than the corresponding controls. The test culture in STR 7 reached stationary phase after 76 h, while the control reached stationary phase after 24 h of incubation. In the test culture of STR 6 system, cell density continued to increase until after 100 h. This difference might have been due to the initial lag phase of the test STR 6 system as compared to STR 7. The growth profile was shifted for a few hours in both control and test cultures of STR 6 compared to STR 7, which is related to the state of inoculum used. Both profiles followed the same trend in both test cultures.

Doubling time of the culture exposed to 18 mT was higher than that of 28 mT. This suggests an inverse correlation between MF intensity and cell growth of the *P. putida* cultures used in this study.

According to results obtained from the study of the effect of MF on *B. subtilis* and *P. putida*, P(3HB) production was very low at logarithmic phase of growth. Maximum amounts were obtained at stationary phase. This has been reported repeatedly in the literature (Gumel et al., 2014; Henderson and Jones, 1997; Kim, 2002; Sukan, 2015).

Table below shows the maximum P(3HB) concentrations obtained in these experiments.

Table 42. Maximum P(3HB) concentrations in STR 6 and STR 7 systems

<i>Fermentation system</i>	<i>STR 6</i>		<i>STR 7</i>	
<i>maximum P(3HB)</i>	<i>Time (h)</i>	<i>Concentration (mg. L⁻¹)</i>	<i>Time(h)</i>	<i>Concentration (mg. L⁻¹)</i>
Control	48	130	32	140
Test	120	150	120	180

From these results, it can be concluded that the effect of MF on P(3HB) production was associated with the intensity of MF. The higher intensity of 28 induced higher P(3HB) production. It is worth mentioning that although the control culture can be stopped after 48h with a maximum P(3HB) concentration of 130 mg. L⁻¹, the same concentration is obtained from the MF exposed cultures after this period. However, continuation of fermentation with application of MF, increases P(3HB) content by 15% under 18 mT intensity and by 28% under 28 mT intensity.

Another observation from P(3HB) profile was the trend of fluctuations in P(3HB) concentration. In both control and test cultures of the STR 6 system, P(3HB) concentration decreased after 48 h and increased again from 96 h until the end of the fermentation period. Glucose was depleted within 48 h of incubation, when the culture had completed its stationary phase. Therefore, this may be an indication that cells started utilising their stored carbon (P(3HB)) in the absence of glucose. Volova et al., 2013 also reported that the maximum P(3HB) content of *Ralstonia eutropha* occurred at stationary phase and after a decrease in production, P(3HB) utilisation started when the culture was at the end of stationary phase (Volova et al., 2013).

This was not the case in the control and test cultures of STR 7 system, which suggest that P(3HB) utilisation did not occur even at the starvation stage in the case of the control STR after the culture had reached its stationary phase. The test STR 7 however, continued to produce P(3HB) and maximum concentration was detected at the end of fermentation period. It appears that the MF stress prompted a survival mechanism on the cells, which lead to slower growth but increased product concentrations. Therefore, this decrease can be associated with other metabolic activities of cells at their stationary phase of growth and possible by-products made by these cells, which needs further investigation.

Chapter 5

Conclusion

5. Conclusion

The aim of this research was to investigate the effect of static magnetic field on microbial production of industrially viable microbial products. This was carried out on three bacterial strains (*Bacillus subtilis*, *Pseudomonas putida* and *Bacillus licheniformis*). P(3HB) and bacitracin were the two model industrially viable microbial products of interest from the named strains. In this chapter, the main conclusions obtained from the studies on each strain under the conditions chosen in this project including mode of operation (batch), MF type (Static from DC current) MF intensity (10, 18 and 28 mT), culture circulation rate (10 mL.min⁻¹) and scale of operation (SF or 2 L STR) are described.

5.1. Investigation of the effect of magnetic field on *Bacillus licheniformis* NCIMB8874

B. licheniformis NCIMB 8874 was used as a model strain for production of bacitracin. The experiments were carried out in two scales (20 mL in SFs and 1.5 L in STRs) and under 10 mT and 28 mT magnetic field. Another setting included pH adjustments to keep pH levels at an optimum level, which was combined with application of MF. In this concept, results were inconsistent under both MF strengths. It appears that MF was not effective in the enhancement of bacitracin production; although when coupled with pH control, bacitracin titres were enhanced. Therefore, there is a potential for increasing bacitracin production with MF in case of pH adjustment throughout the fermentation period and more scope for further investigations in this specific system. This is described in detail in the future work chapter.

Morphological changes caused by MF were also investigated and bacterial cell damage was observed under both 10 and 28 mT MF. The application of 10 mT with pH control resulted in development of tumor-like shapes on the cell surface.

5.2. Investigation of the effect of magnetic field on *Bacillus subtilis* NCTC 3610

B. subtilis NCTC 3610 was used as another model microorganism in this project. Production of P(3HB) by this Gram-positive producer was studied in the experiments carried out in 1.5 L working volume STR. Application of MF with 18 and 28 mT using the proposed system proved to have negative impact and not feasible for growth or enhancement of P(3HB) production.

In terms of morphological change, *B. subtilis* cells did not show any changes after application to MF of 10 and 28 mT.

5.3. Investigation of the effect of magnetic field on *P. putida* KT2440

P. putida KT2440 was used as a Gram-negative producer of P(3HB). This microorganism was used in 1.5 L working volume STRs and was exposed to 18 and 28 mT MF. Results obtained from this system showed notable changes in terms of P(3HB) production, growth profile and cell morphology.

The maximum P(3HB) concentration change was higher under MF of 28 mT (28% higher than the control) as compared to 18 mT (15% higher than the control)

SEM images obtained from samples of these experiments showed complete change in cell morphology.

Although results from exposure of Gram-positive *Bacillus* strains was not promising in terms of product enhancement, the Gram-negative *Pseudomonads* sp. used in this study showed very interesting changes. In this contest, there is scope for further studies on the cultures of *Pseudomonas putida* as detailed in the future work chapter.

Overall, this project arrives at the conclusion that there is no generic route to enhance production of microbial products through application of MF. The process depends on the microbial spp., strains, and strength of the MF applied

among other factors that remain to be explored. Some of the factors for further investigation are recommended in the next chapter (Future work).

Chapter 6

Future Work

6. Future Work

The experiments carried out in this research have provided a solid platform for wider investigations of the use of magnetic field in pharmaceuticals and biotechnology industries. This newly introduced concept, needs further research and investigation to find the exact mechanism of MF effect on microbial cultures.

Here, a novel bioreactor production technique was introduced, whereby a bioreactor was coupled with a magnetic field device while culture medium was circulated through the device. The properties of this system such as speed of circulation and intensity of the MF can be easily adjusted to optimum desired values.

Findings of this study confirmed that obtaining the desired results from this system and effect of MF on microbial product formation is strain-, and product-dependent. Results of each section have opened new doors to further research questions, which can lead to better understanding of engineering the process, and its optimisation for potential industrial use.

In this chapter, suggestions are made for further research to broaden the knowledge in this field and potentially taking the system to industrial level. These are categorised as short and long term research on the effects of MF on microorganisms.

6.1. Short term future work focus recommendations

Short term future work includes changes in operating parameters and can be described as below:

- Investigation of effect of other intensities of MF on Gram-positive and Gram-negative bacterial cultures
- Investigation of effect of non-static types of MF on Gram-positive and Gram-negative bacteria
- Investigation of the effect of residence time in the MFG on Gram-positive and Gram-negative bacteria

6.1.1. Different intensities of MF

The intensities used in this research were limited to 10, 18 and 28 mT. Changes were observed at 18 and 28 mT with regards to morphology, product formation and cell growth profiles.

Therefore, future studies can be focused on using the same system with more varied intensities of MF to provide better understanding of optimum MF values for better product formation.

6.1.2. Different types of MF

Static magnetic field was the focus of this study and use of other types of MF from alternating current was out of the scope of this research. Use of alternating MF in the same system would be a very good follow up on this study to obtain better range of options for optimisation of the process.

6.1.3. Different circulation rates through the MFG

Different circulation rate through the MFG would lead to different residence times and hence can be an important factor when optimising the system. The starting point in this research was 10 mL. min⁻¹ as circulation rate leading to 0.8 min residence time. Future work can also address the research question of whether different residence times inside the MFG would lead to different results and perhaps more product yields from Gram-positive and Gram-negative bacteria.

6.2. Long term future work recommendations

Longer term research on the effect of MF on microorganisms can be focused on growth and productivity related effects of MF. These include extensive research on the effect of MF on Gram-positive and Gram-negative bacteria at molecular, chemical and physiological levels. These include:

- Investigation of effect of MF at molecular and genetic level;

- Proteomics studies to investigate the effects of MF on cellular protein production;
- Investigation of effect of MF on product structure and stability;
- Investigation of the effect of MF on cells at a steady state physiological condition;
- Investigation of the effect of MF on diauxic growth, protein secretion and EPS composition
- Studies of the effect of MF on ionic channels of microbial cell membrane;
- Investigation of the effect of MF on extra polymeric substances (EPS) composition and production of by-products;
- Investigation of by-products produced through MF application and their structural integrity.

6.2.1. Molecular biology and proteomics investigation

According to the results obtained from this research, it was found that MF of 10 mT had a positive impact on bacitracin concentration in culture medium, while bacitracin concentration in cultures exposed to 28 mT decreased compared to the control culture. This decrease occurred simultaneously with an increase in total carbohydrate concentration in the medium. It was therefore concluded that an MF intensity dependent shift may have occurred in cellular metabolism from production of bacitracin to EPS.

The effect of MF on *B. subtilis* cultures was not significant. However, in *P. putida* cultures, growth profile changed notably under MF application. Therefore, further studies to investigate the effect of MF at molecular level would be beneficial to confirm these findings, and to reveal the reason for this shift of metabolism.

Genomics and proteomics studies will provide more information on the mechanism of the observed changes. For this purpose, experiments should involve protein extraction and quantification from fermentation samples of both control and the test via protein extraction kits and Bradford assay, respectively. Once the total protein content is separated and quantified, isoelectric focusing and SDS page can help separate different proteins based on their electric

charge and molecular weight, respectively. Proteomics can then be carried out by staining and image analysis on separated proteins and finally protein sequencing via LC-MS/MS mass spectrometers (Reffatti, 2012).

6.2.1. Investigation of the effect of MF on product structure

Based on the present study, the effect of MF on bacitracin production was dependent on the field strength. Bacitracin yield decreased at MF of 28 mT, in both SF and STR cultures. Rate of decrease in MF exposed cultures was higher than that of the controls. It was concluded that this could be a result of either bacitracin degradation prompted by MF exposure or a metabolic shift at cellular level. The direct effect of MF on bacitracin molecule should be further investigated as the peptide antibiotic's conformation might have changed due to MF exposure.

6.2.2. Investigation of the effect of MF on cells at a steady state physiological condition

The effect of MF on batch cultures of *B. subtilis*, *B. licheniformis* and *P. putida* was studied. As the application of MF on *B. licheniformis* and *P. putida* affected their growth profiles, steady state conditions of continuous culture can help confirm the effect of MF without growth-stage dependent changes during the course of batch fermentation. Continuous culture experiments in order to obtain a synchronised culture at production stage of growth (late exponential in the case of bacitracin and mid-stationary in the case of P(3HB)), will be another step forward to understanding the exact mechanism of MF effect on bacterial cultures.

The number of passes were different at different scales (SF and STR) so the exposure of the culture to MF on different stages of growth were different. Continuous culture will provide similar culture conditions for exposure to MF.

6.2.3. Investigation of the effect of MF on diauxic growth, protein secretion and EPS composition

The slimy appearance of *B. licheniformis* fermentation culture at the end of batch period implied the release of extracellular polymeric substances. The nature of these EPS products was potentially polysaccharides, the composition of which needs to be investigated in further studies.

The release of new proteins into the culture medium is also another parameter leading to better understanding of the system. This can be achieved through further analysis of fermentation samples including protein assay.

As citric acid was the only carbon source other than glutamic acid in the experiments on *B. licheniformis*, citric acid assay can lead to better understanding of the diauxic growth mechanism as well as an insight into the composition of EPS.

6.2.4. Investigation of the effect of MF on ionic channels of cell membrane

In the studies on *P. putida*, morphological changes were observed in the cell shape. Also, damaged cells of *B. licheniformis* were observed under SEM. Based on the observations in both cases, it has been suggested that these changes are related to changes to ionic channels of cellular membranes through MF exposure. Further investigation of membrane structure and integrity through TEM (transmission electron microscopy) analysis and atomic force microscopy (AFM) can therefore be another step forward in understanding of the mechanism of MF application affects.

6.2.5. Investigation of the effect of MF on production of by-products

An inverse correlation between MF intensity and cell growth of *P. putida* cultures was observed in these experiments. It appears that MF exposed cultures of *P. putida* triggered production of other products than P(3HB). The nature of these by-products and their molecular structure can be further investigated through further understanding of the proteomics along with transmission electron microscopy (TEM) analysis. Knowing which cellular mechanisms were activated, will give a presumption of what other products to look for.

Chapter 7

References

7. References

- Abusham, R.A., Rahman, R.N.Z.R., Salleh, A.B., Basri, M., 2009. Optimization of physical factors affecting the production of thermo-stable organic solvent-tolerant protease from a newly isolated halo tolerant *Bacillus subtilis* strain. *Rand. Microb. Cell Factories* 8, 20. <https://doi.org/10.1186/1475-2859-8-20>
- Aehle, M., Kuprijanov, A., Schaepe, S., Simutis, R., Lübbert, A., 2011. Increasing batch-to-batch reproducibility of CHO cultures by robust open-loop control. *Cytotechnology* 63, 41–47.
- Aftab, M.N., Haq, I., Baig, S., 2012. Systematic mutagenesis method for enhanced production of bacitracin by *Bacillus licheniformis* mutant strain UV-MN-HN-6. *Braz. J. Microbiol.* 43, 78–88.
- Agrawal, T., Kotasthane, A.S., Kushwah, R., 2015. Genotypic and phenotypic diversity of polyhydroxybutyrate (PHB) producing *Pseudomonas putida* isolates of Chhattisgarh region and assessment of its phosphate solubilizing ability. *3 Biotech* 5, 45–60.
- Akaraonye, E., Keshavarz, T., Roy, I., 2010. Production of polyhydroxyalkanoates: the future green materials of choice. *J. Chem. Technol. Biotechnol.* 85, 732–743.
- Al-Khaza'leh, K.A., Al-fawwaz, A.T., 2015. The Effect of Static Magnetic Field on *E. coli*, *S. aureus* and *B. subtilis* Viability. *J. Nat. Sci. Res.* 5, 153–157.
- Alvarez, D.C., Pérez, V.H., Justo, O.R., Alegre, R.M., 2006. Effect of the extremely low frequency magnetic field on nisin production by *Lactococcus lactis* subsp. *lactis* using cheese whey permeate. *Process Biochem.* 41, 1967–1973. <https://doi.org/10.1016/j.procbio.2006.04.009>
- Amin, M., Rakhisi, Z., Ahmady, A.Z., 2015. Isolation and identification of *Bacillus* Species from soil and evaluation of their antibacterial properties. *Avicenna J. Clin. Microbiol. Infect.* 2.
- Anderson, A.J., Dawes, E.A., 1990. Occurrence, metabolism, metabolic role, and industrial uses of bacterial polyhydroxyalkanoates. *Microbiol. Rev.* 54, 450–472.

- Angioi, A., Zanetti, S., Sanna, A., Delogu, G., Fadda, G., 1995. Adhesiveness of *Bacillus subtilis* strains to epithelial cells cultured in vitro. *Microb. Ecol. Health Dis.* 8, 71–77.
- Anjum, A., Zuber, M., Zia, K.M., Noreen, A., Anjum, M.N., Tabasum, S., 2016. Microbial production of polyhydroxyalkanoates (PHAs) and its copolymers: A review of recent advancements. *Int. J. Biol. Macromol.* 89, 161–174. <http://dx.doi.org/10.1016/j.ijbiomac.2016.04.069>
- Anzai, Y., Kim, H., Park, J.-Y., Wakabayashi, H., Oyaizu, H., 2000. Phylogenetic affiliation of the pseudomonads based on 16S rRNA sequence. *Int. J. Syst. Evol. Microbiol.* 50, 1563–1589.
- Aremu, M., Aransiola, E., Layokun, S., Solomon, B., 2011. Production of Polyhydroxybutyrate (PHB) by *Pseudomonas Putida* Strain KT2440 on Cassava Hydrolysate Medium. *Res J Chem Sci* 1, 67–73.
- Bajpai, I., Saha, N., Basu, B., 2012. Moderate intensity static magnetic field has bactericidal effect on *E. coli* and *S. epidermidis* on sintered hydroxyapatite. *J. Biomed. Mater. Res. B Appl. Biomater.* 100B, 1206–1217. <https://doi.org/10.1002/jbm.b.32685>
- Bandara, H., Nguyen, D., Mogarala, S., Osiniński, M., Smyth, H., 2015. Magnetic fields suppress *Pseudomonas aeruginosa* biofilms and enhance ciprofloxacin activity. *Biofouling* 31, 443–457.
- Bandyopadhyay, S.K., Majumdar, S., 1974. Regulation of the formation of alkaline phosphatase during neomycin biosynthesis. *Antimicrob. Agents Chemother.* 5, 431–434.
- Baptist, J., Werber, F., 1963. Molded product containing poly-beta-hydroxybutyric acid and method of making. US3107172 A.
- Baron, S. (Ed.), 1996a. *Medical Microbiology*, 4th ed. Galveston (TX): University of Texas Medical Branch at Galveston.
- Baron, S., 1996b. *Epidemiology--Medical Microbiology*. University of Texas Medical Branch at Galveston.
- Barrett, E.L., Solanes, R.E., Tang, J.S., Palleroni, N.J., 1986. *Pseudomonas fluorescens* biovar V: its resolution into distinct component groups and the relationship of these groups to other *P. fluorescens* biovars, to *P. putida*, and to psychrotrophic pseudomonads associated with food spoilage. *Microbiology* 132, 2709–2721.

- Bauman, R.W., 2012. Microbiology: With diseases by body system (3rd Edition), 3rd ed. Benjamin Cummings.
- Bayari, S., Severcan, F., 2005. FTIR study of biodegradable biopolymers: P(3HB), P(3HB-co-4HB) and P(3HB-co-3HV). J. Mol. Struct. 744, 529–534. <http://dx.doi.org/10.1016/j.molstruc.2004.12.029>
- Bhat, S., Paul, B.C., Jun, D., Dahms, T.E., 2012. Viscoelasticity in biological systems: a special focus on microbes. INTECH Open Access Publisher.
- Bond, G.C., Himelick, R., Macdonald, L.H., 1949. The stability of bacitracin. J. Pharm. Sci. 38, 30–34.
- Borlido, L., Azevedo, A.M., Roque, A.C.A., Aires-Barros, M.R., 2013. Magnetic separations in biotechnology. Biotechnol. Adv. 31, 1374–1385. <http://dx.doi.org/10.1016/j.biotechadv.2013.05.009>
- Brewer, G.A., 1981. Bacitracin, in: Florey, K. (Ed.), Analytical Profiles of Drug Substances. Academic Press, pp. 1–69.
- British plastics federation, 2016. The UK plastics industry: A strategic vision for growth (guide). British Plastics Federation, London.
- Bruhn, R., Pedrow, P., Olsen, R., Barbosa-Canovas, G., Swanson, B., 1997. Electrical environment surrounding microbes exposed to pulsed electric fields. IEEE Trans. Dielectr. Electr. Insul. 4, 806–812.
- Bugnicourt, E., Cinelli, P., Lazzeri, A., Alvarez, V.A., 2014. Polyhydroxyalkanoate (PHA): Review of synthesis, characteristics, processing and potential applications in packaging. EXPRESS Polym. Lett. 8, 791–808. <https://doi.org/10.3144/expresspolymlett.2014.82>
- Cabeen, M.T., Jacobs-Wagner, C., 2005. Bacterial cell shape. Nat. Rev. Microbiol. 3, 601–610.
- Canli, O., Kurbanoglu, E.B., 2012. Application of low magnetic field on inulinase production by *Geotrichum candidum* under solid state fermentation using leek as substrate. Toxicol. Ind. Health 28, 894–900. <https://doi.org/10.1177/0748233711425079>
- Catone, M.V., Ruiz, J.A., Castellanos, M., Segura, D., Espin, G., López, N.I., 2014. High polyhydroxybutyrate production in *Pseudomonas extremaustralis* is associated with differential expression of horizontally

- acquired and core genome polyhydroxyalkanoate synthase genes. *PLoS One* 9, e98873.
- Cellini, L., Grande, R., Di Campli, E., Di Bartolomeo, S., Di Giulio, M., Robuffo, I., Trubiani, O., Mariggio, M.A., 2008. Bacterial response to the exposure of 50 Hz electromagnetic fields. *Bioelectromagnetics* 29, 302–311.
- Chabay, R.W., Sherwood, B.A., 2015. *Matter and interactions*. John Wiley & Sons.
- Chang, W.-S., van de Mortel, M., Nielsen, L., de Guzman, G.N., Li, X., Halverson, L.J., 2007. Alginate production by *Pseudomonas putida* creates a hydrated microenvironment and contributes to biofilm architecture and stress tolerance under water-limiting conditions. *J. Bacteriol.* 189, 8290–8299.
- Cheirsilp, B., Jeamjounkhaw, P., Aran, H., 2009. Optimizing an alginate immobilized lipase for monoacylglycerol production by the glycerolysis reaction. *J. Mol. Catal. B Enzym.* 59, 206–211.
- Choi, J.I., Lee, S.Y., 1997. Process analysis and economic evaluation for poly(3-hydroxybutyrate) production by fermentation. *Bioprocess Eng* 17. <https://doi.org/10.1007/s004490050394>
- Chua, L.-Y., Yeo, S.-H., 2005. Surface bio-magnetism on bacterial cells adhesion and surface proteins secretion. *Colloids Surf. B Biointerfaces* 40, 45–49.
- Cohen, I., Cahan, R., Shani, G., Cohen, E., Abramovich, A., 2010. Effect of 99 GHz continuous millimeter wave electro-magnetic radiation on *E. coli* viability and metabolic activity. *Int. J. Radiat. Biol.* 86, 390–399.
- Cromwick, A.-M., Birrer, G.A., Gross, R.A., 1996. Effects of pH and aeration on γ -poly(glutamic acid) formation by *Bacillus licheniformis* in controlled batch fermentor cultures. *Biotechnol. Bioeng.* 50, 222–227. [https://doi.org/10.1002/\(SICI\)1097-0290\(19960420\)50:2<222::AID-BIT10>3.0.CO;2-P](https://doi.org/10.1002/(SICI)1097-0290(19960420)50:2<222::AID-BIT10>3.0.CO;2-P)
- De Boer, A.S., Priest, F., Diderichsen, B., 1994. On the industrial use of *Bacillus licheniformis*: a review. *Appl. Microbiol. Biotechnol.* 40, 595–598. <https://doi.org/10.1007/BF00173313>

- DeFlaun, M.F., Condee, C.W., 1997. Electrokinetic transport of bacteria. *J. Hazard. Mater.* 55, 263–277.
- Del Re, B., Garoia, F., Mesirca, P., Agostini, C., Bersani, F., Giorgi, G., 2003. Extremely low frequency magnetic fields affect transposition activity in *Escherichia coli*. *Radiat. Environ. Biophys.* 42, 113–118. <https://doi.org/10.1007/s00411-003-0192-9>
- Di Bonaventura, G., Pompilio, A., Crocetta, V., De Nicola, S., Barbaro, F., Giuliani, L., D'emilia, E., Fiscarelli, E., Bellomo, R.G., Saggini, R., 2014. Exposure to extremely low-frequency magnetic field affects biofilm formation by cystic fibrosis pathogens. *Future Microbiol.* 9, 1303–1317.
- Di Campi, E., Di Bartolomeo, S., Grande, R., Di Giulio, M., Cellini, L., 2010. Effects of extremely low-frequency electromagnetic fields on *Helicobacter pylori* biofilm. *Curr. Microbiol.* 60, 412–418.
- Doyle, M., 1989. Foodborne bacterial pathogens, Food Science and Technology. Marcel Dekker Inc., New York.
- Drahos, D., West, L., 2004. *Bacillus licheniformis* biofungicide. US 6824772 B2.
- Durner, R., Zinn, M., Witholt, B., Egli, T., 2001. Accumulation of poly [(R)-3-hydroxyalkanoates] in *Pseudomonas oleovorans* during growth in batch and chemostat culture with different carbon sources. *Biotechnol. Bioeng.* 72, 278–288.
- Faraday, M., 1833. Experimental researches in electricity. Fourth series. *Philos. Trans. R. Soc. Lond.* 123, 507–522.
- Fijałkowski, K., Żywicka, A., Drozd, R., Niemczyk, A., Junka, A.F., Peitler, D., Kordas, M., Konopacki, M., Szymczyk, P., El Fray, M., 2015. Modification of bacterial cellulose through exposure to the rotating magnetic field. *Carbohydr. Polym.* 133, 52–60.
- Fojt, L., Klapetek, P., Strašák, L., Vetterl, V., 2009. 50 Hz magnetic field effect on the morphology of bacteria. *Micron* 40, 918–922. <https://doi.org/10.1016/j.micron.2009.06.009>
- Fojt, L., Strašák, L., Vetterl, V., 2007. Effect of electromagnetic fields on the denitrification activity of *Paracoccus denitrificans*. *Bioelectrochemistry* 70, 91–95. <https://doi.org/10.1016/j.bioelechem.2006.03.023>

- Fojt, L., Strašák, L., Vetterl, V., Šmarda, J., 2004. Comparison of the low-frequency magnetic field effects on bacteria *Escherichia coli*, *Leclercia adecarboxylata* and *Staphylococcus aureus*. *Bioelectrochemistry* 63, 337–341. <https://doi.org/10.1016/j.bioelechem.2003.11.010>
- Follonier, S., Panke, S., Zinn, M., 2011. A reduction in growth rate of *Pseudomonas putida* KT2442 counteracts productivity advances in medium-chain-length polyhydroxyalkanoate production from gluconate. *Microb Cell Fact* 10. <https://doi.org/10.1186/1475-2859-10-25>
- Gao, M., Zhang, J., Feng, H., 2011. Extremely low frequency magnetic field effects on metabolite of *Aspergillus niger*. *Bioelectromagnetics* 32, 73–78.
- Gao, W., Liu, Y., Zhou, J., Pan, H., 2005. Effects of a strong static magnetic field on bacterium *Shewanella oneidensis*: An assessment by using whole genome microarray. *Bioelectromagnetics* 26, 558–563.
- Getachew, A., Woldesenbet, F., 2016. Production of biodegradable plastic by polyhydroxybutyrate (PHB) accumulating bacteria using low cost agricultural waste material. *BMC Res. Notes* 9, 509.
- Giordano, N., 2012. *College Physics: Reasoning and Relationships*, 2nd ed, Science Physics General. Cengage Learning, USA.
- Gjermansen, M., Ragas, P., Sternberg, C., Molin, S., Tolker-Nielsen, T., 2005. Characterization of starvation-induced dispersion in *Pseudomonas putida* biofilms. *Environ. Microbiol.* 7, 894–904.
- Gram, H.C.J., Friedlaender, C., 1884. Ueber die isolirte Färbung der Schizomyceten: in Schnitt-und Trockenpräparaten. Theodor Fischer's medicinischer Buchhandlung.
- Green, D.H., Wakeley, P.R., Page, A., Barnes, A., Baccigalupi, L., Ricca, E., Cutting, S.M., 1999. Characterization of Two *Bacillus* Probiotics. *Appl. Environ. Microbiol.* 65, 4288–4291.
- Gumel, A., Annuar, M., Heidelberg, T., 2014. Growth kinetics, effect of carbon substrate in biosynthesis of mcl-PHA by *Pseudomonas putida* Bet001. *Braz. J. Microbiol.* 45, 427–438.
- Gupta, R., Gupta, N., Rathi, P., 2004. Bacterial lipases: an overview of production, purification and biochemical properties. *Appl. Microbiol. Biotechnol.* 64, 763–781. <https://doi.org/10.1007/s00253-004-1568-8>

- Guru, B.S., Hiziroglu, H.R., 2004. Electromagnetic field theory fundamentals, 2nd ed, Science Physics General. Cambridge University Press, New York, USA.
- Haavik, H., 1974. Studies on the formation of bacitracin by *Bacillus licheniformis*: effect of glucose. *Microbiology* 81, 383–390.
- Haddar, H.O., Aziz, G.M., Al-Gelawi, M.H., 2007. Optimization of bacitracin production by *Bacillus licheniformis* B5. *Pak. J. Biol. Sci. PJB* 10, 972–976.
- Harris, S.-R., Henbest, K.B., Maeda, K., Pannell, J.R., Timmel, C.R., Hore, P., Okamoto, H., 2009. Effect of magnetic fields on cryptochrome-dependent responses in *Arabidopsis thaliana*. *J. R. Soc. Interface* 6, 1193–1205.
- Henderson, R.A., Jones, C.W., 1997. Physiology of poly-3-hydroxybutyrate (PHB) production by *Alcaligenes eutrophus* growing in continuous culture. *Microbiology* 143, 2361–2371.
- Hönes, I., Pospischil, A., Berg, H., 1998. Electrostimulation of proliferation of the denitrifying bacterium *Pseudomonas stutzeri*. *Bioelectrochem. Bioenerg.* 44, 275–277.
- Hunt, R.W., Zavalin, A., Bhatnagar, A., Chinnasamy, S., Das, K.C., 2009. Electromagnetic biostimulation of living cultures for biotechnology, biofuel and bioenergy applications. *Int. J. Mol. Sci.* 10, 4515–4558.
- Ignatyeva, T.A., Voyevodin, V.N., Goltsev, A.N., Kiroshka, V.V., Bovda, A.M., Kalynovskii, V.V., Velikodny, A.N., Kutsenko, P.A., Golub, V., Dzhedzheria, Y., 2014. Perspectives of constant gradient magnetic fields applications in biotechnology. *Am. J. Biosci. Bioeng.* 2, 72–77.
- Inhan-Garip, A., Aksu, B., Akan, Z., Akakin, D., Ozaydin, A.N., San, T., 2011. Effect of extremely low frequency electromagnetic fields on growth rate and morphology of bacteria. *Int. J. Radiat. Biol.* 87, 1155–1161.
- Insomphun, C., Chuah, J.-A., Kobayashi, S., Fujiki, T., Numata, K., 2016. Influence of hydroxyl groups on the cell viability of polyhydroxyalkanoate (PHA) scaffolds for tissue engineering. *ACS Biomater. Sci. Eng.*
- Iwata, T., 2015. Biodegradable and Bio-Based Polymers: Future Prospects of Eco-Friendly Plastics. *Angew. Chem. Int. Ed.* 54, 3210–3215.

- Jahn, A., Griebe, T., Nielsen, P.H., 1999. Composition of *Pseudomonas putida* biofilms: accumulation of protein in the biofilm matrix. *Biofouling* 14, 49–57.
- Jaspers, E., Overmann, J., 1997. Separation of bacterial cells by isoelectric focusing, a new method for analysis of complex microbial communities. *Appl. Environ. Microbiol.* 63, 3176–3181.
- Jendrossek, D., Selchow, O., Hoppert, M., 2007. Poly (3-hydroxybutyrate) granules at the early stages of formation are localized close to the cytoplasmic membrane in *Caryophanon latum*. *Appl. Environ. Microbiol.* 73, 586–593.
- Jenzsch, M., Gnoth, S., Kleinschmidt, M., Simutis, R., Lübbert, A., 2006. Improving the batch-to-batch reproducibility in microbial cultures during recombinant protein production by guiding the process along a predefined total biomass profile. *Bioprocess Biosyst. Eng.* 29, 315–321.
- Jiles, D., 2015. Introduction to magnetism and magnetic materials. CRC press.
- Johnson, B.A., Anker, H., Meleney, F.L., 1945. Bacitracin: A new antibiotic produced by a member of the *B. Subtilis* group. *Science* 102, 376–377. <https://doi.org/10.1126/science.102.2650.376>
- Justo, O.R., Pérez, V.H., Alvarez, D.C., Alegre, R.M., 2006. Growth of *Escherichia coli* under extremely low-frequency electromagnetic fields. *Appl. Biochem. Biotechnol.* 134, 155–163.
- Kamel, F.H., Saeed, C.H., Qader, S.S., 2013. The Effects of Magnetic Fields on Some Biological Activities of *Pseudomonas Aeruginosa*. *Diyala J. Med.* 5, 29–35.
- Kefeli, V., Blum, W.E., 2010. Mechanisms of landscape rehabilitation and sustainability, *Science Environmental Science*. Bentham Science Publishers.
- Keshavarz, T., Roy, I., 2010. Polyhydroxyalkanoates: bioplastics with a green agenda. *Curr. Opin. Microbiol.* 13, 321–326. <http://dx.doi.org/10.1016/j.mib.2010.02.006>
- Kim, B.S., 2002. Production of medium chain length polyhydroxyalkanoates by fed-batch culture of *Pseudomonas oleovorans*. *Biotechnol. Lett.* 24, 125–130.

- Kohno, M., Yamazaki, M., Kimura, I., Wada, M., 2000. Effect of static magnetic fields on bacteria: *Streptococcus mutans*, *Staphylococcus aureus*, and *Escherichia coli*. *Pathophysiology* 7, 143–148.
- Konigsberg, W., Craig, L.C., 1962. On Bacitracin F. *J. Org. Chem.* 27, 934–938. <https://doi.org/10.1021/jo01050a060>
- Konz, D., Klens, A., Schörgendorfer, K., Marahiel, M.A., 1997. The bacitracin biosynthesis operon of *Bacillus licheniformis* {ATCC} 10716: molecular characterization of three multi-modular peptide synthetases. *Chem. Biol.* 4, 927–937. [http://dx.doi.org/10.1016/S1074-5521\(97\)90301-X](http://dx.doi.org/10.1016/S1074-5521(97)90301-X)
- Lakowitz, A., Krull, R., Biedendieck, R., 2017. Recombinant production of the antibody fragment D1. 3 scFv with different *Bacillus* strains. *Microb. Cell Factories* 16, 14.
- Lancini, G., Demain, A.L., 2013. Bacterial Pharmaceutical Products, in: Rosenberg, E., DeLong, E.F., Lory, S., Stackebrandt, E., Thompson, F. (Eds.), *The Prokaryotes: Applied Bacteriology and Biotechnology*. Springer Berlin Heidelberg, Berlin, Heidelberg, pp. 257–280. https://doi.org/10.1007/978-3-642-31331-8_28
- Law, J.H., Slepecky, R.A., 1961. Assay of poly- β -hydroxybutyric acid. *J. Bacteriol.* 82, 33–36.
- Le Meur, S., Zinn, M., Egli, T., Thöny-Meyer, L., Ren, Q., 2012. Production of medium-chain-length polyhydroxyalkanoates by sequential feeding of xylose and octanoic acid in engineered *Pseudomonas putida* KT2440. *BMC Biotechnol.* 12, 53. <https://doi.org/10.1186/1472-6750-12-53>
- Lemoigne, M., 1926. Produit de déshydratation et de polymérisation de l'acide β -oxybutyrique. *Bull Soc Chim Biol* 8, 770–782.
- Lenz, R.W., Marchessault, R.H., 2005. Bacterial polyesters: biosynthesis, biodegradable plastics and biotechnology. *Biomacromolecules* 6, 1–8.
- Li, Q., Yan, Y., 2010. Production of biodiesel catalyzed by immobilized *Pseudomonas cepacia* lipase from *Sapium sebiferum* oil in microaqueous phase. *Appl. Energy* 87, 3148–3154.
- Lipiec, J., Janas, P., Barabasz, W., 2004. Effect of oscillating magnetic field pulses on the survival of selected microorganisms. *Int. Agrophysics* 18, 325–328.

- Loeschcke, A., Thies, S., 2015. *Pseudomonas putida*—a versatile host for the production of natural products. *Appl. Microbiol. Biotechnol.* 99, 6197–6214. <https://doi.org/10.1007/s00253-015-6745-4>
- Madigan, M., Martinko, J., 2005. *Brock biology of microorganisms*. (11th edn).
- Madslie, E., Rønning, H., Lindbäck, T., Hassel, B., Andersson, M., Granum, P., 2013. Lichenysin is produced by most *Bacillus licheniformis* strains. *J. Appl. Microbiol.* 115, 1068–1080.
- Mah, T.-F., Pitts, B., Pellock, B., Walker, G.C., Stewart, P.S., O'toole, G.A., 2003. A genetic basis for *Pseudomonas aeruginosa* biofilm antibiotic resistance. *Nature* 426, 306–310.
- Malick, A., Khodaei, N., Benkerroum, N., Karboune, S., 2017. Production of exopolysaccharides by selected *Bacillus* strains: Optimization of media composition to maximize the yield and structural characterization. *Int. J. Biol. Macromol.* 102, 539–549.
- Malmivuo, J., Plonsey, R., 1995. *Bioelectromagnetism: principles and applications of bioelectric and biomagnetic fields*. Oxford University Press, USA.
- Mandel, M., 1966. Deoxyribonucleic Acid Base Composition in the Genus *Pseudomonas*. *Microbiology* 43, 273–292.
- Mann, E.E., Wozniak, D.J., 2012. *Pseudomonas* biofilm matrix composition and niche biology. *FEMS Microbiol. Rev.* 36, 893–916.
- Manoliu, A., Oprica, L., Olteanu, Z., Neacsu, I., Artenie, V., Creanga, D.E., Rusu, I., Bodale, I., 2006. Peroxidase activity in magnetically exposed cellulolytic fungi. *J. Magn. Mater.* 300, e323–e326. <https://doi.org/10.1016/j.jmmm.2005.10.111>
- Martirosyan, V., Baghdasaryan, N., Ayrapetyan, S., 2013. Bidirectional frequency-dependent effect of extremely low-frequency electromagnetic field on *E. coli* K-12. *Electromagn. Biol. Med.* 32, 291–300. <https://doi.org/10.3109/15368378.2012.712587>
- Maxwell, J.C., 1865. A dynamical theory of the electromagnetic field. *Philos. Trans. R. Soc. Lond.* 155, 459–512.
- Mehrotra, R., 2009. *Principles of Microbiology*. Tata McGraw-Hill Education.
- Mhamdi, L., Mhamdi, N., Mhamdi, N., Lejeune, P., Jaffrezic, N., Burais, N., Scorretti, R., Pokorny, J., Ponsonnet, L., 2016. Effect of a static

- magnetic field on *Escherichia coli* adhesion and orientation. *Can. J. Microbiol.* 62, 944–952.
- Mitoi, M.E., Helepciuc, F.E., Brezeanu, A., Cornea, C.P., 2012. Characterization of the impact of *Bacillus licheniformis* and *Pseudomonas aeruginosa* against *Alternaria alternata* by phase contrast microscopy and transmission electron microscopy. *Analele Stiintifice Ale Univ. Al Cuza Din Iasi* 58, 5.
- Moon, S.-H., Parulekar, S.J., 1991. A parametric study of protease production in batch and fed-batch cultures of *Bacillus firmus*. *Biotechnol. Bioeng.* 37, 467–483. <https://doi.org/10.1002/bit.260370509>
- Moore, E.R., Tindall, B.J., Dos Santos, V.A.M., Pieper, D.H., Ramos, J.-L., Palleroni, N.J., 2006. Nonmedical: *pseudomonas*, in: *The Prokaryotes*. Springer, pp. 646–703.
- Moore, R.L., 1979. Biological effects of magnetic fields: studies with microorganisms. *Can. J. Microbiol.* 25, 1145–1151. <https://doi.org/10.1139/m79-178>
- Mousavian-Roshanzamir, S., Makhdoumi-Kakhki, A., 2017. The Inhibitory Effects of Static Magnetic Field on *Escherichia coli* from two Different Sources at Short Exposure Time. *Rep. Biochem. Mol. Biol.* 5, 112–116.
- Murphy, T., Parra, R., Radman, R., Roy, I., Harrop, A., Dixon, K., Keshavarz, T., 2007. Novel application of oligosaccharides as elicitors for the enhancement of bacitracin A production in cultures of *Bacillus licheniformis*. *Enzyme Microb. Technol.* 40, 1518–1523.
- Murphy, T.M., 2008. Elicitation studies for enhanced production of bacitracin A by *Bacillus licheniformis* cultures (PhD Thesis). University of Westminster, London.
- Nadeem, M., Qazi, J.I., Baig, S., 2010. Enhanced production of alkaline protease by a mutant of *Bacillus licheniformis* N-2 for dehairing. *Braz. Arch. Biol. Technol.* 53, 1015–1025.
- Nagy, P., 2005. The effect of low inductivity static magnetic field on some plant pathogen fungi. *J. Cent. Eur. Agric.* 6, 167–172.
- Nagy, P., Fischl, G., 2004. Effect of static magnetic field on growth and sporulation of some plant pathogenic fungi. *Bioelectromagnetics* 25, 316–318. <https://doi.org/10.1002/bem.20015>

- Nilsson, M., Chiang, W., Fazli, M., Gjermansen, M., Givskov, M., Tolker-Nielsen, T., 2011. Influence of putative exopolysaccharide genes on *Pseudomonas putida* KT2440 biofilm stability. *Environ. Microbiol.* 13, 1357–1369.
- Novák, J., Strašák, L., Fojt, L., Slaninová, I., Vetterl, V., 2007. Effects of low-frequency magnetic fields on the viability of yeast *Saccharomyces cerevisiae*. *Bioelectrochemistry* 70, 115–121.
- Novik, G., Savich, V., Kiseleva, E., 2015. An insight into beneficial *Pseudomonas* bacteria. *Microbiol. Agric. Hum. Health* 73–105.
- Obermeier, A., Matl, F.D., Friess, W., Stemberger, A., 2009. Growth inhibition of *Staphylococcus aureus* induced by low-frequency electric and electromagnetic fields. *Bioelectromagnetics* 30, 270–279.
- Oncul, S., Cuce, E.M., Aksu, B., Inhan Garip, A., 2016. Effect of extremely low frequency electromagnetic fields on bacterial membrane. *Int. J. Radiat. Biol.* 92, 42–49.
- Parlane, N.A., Gupta, S.K., Rubio-Reyes, P., Chen, S., Gonzalez-Miro, M., Wedlock, D.N., Rehm, B.H.A., 2017. Self-Assembled Protein-Coated Polyhydroxyalkanoate Beads: Properties and Biomedical Applications. *ACS Biomater. Sci. Eng.* 3, 3043–3057. <https://doi.org/10.1021/acsbiomaterials.6b00355>
- Parrado, J., Rodriguez-Morgado, B., Tejada, M., Hernandez, T., Garcia, C., 2014. Proteomic analysis of enzyme production by *Bacillus licheniformis* using different feather wastes as the sole fermentation media. *Enzyme Microb. Technol.* 57, 1–7.
- Pavli, V., Kmetec, V., 2001. Optimization of {HPLC} method for stability testing of bacitracin. *J. Pharm. Biomed. Anal.* 24, 977–982. [http://dx.doi.org/10.1016/S0731-7085\(00\)00569-0](http://dx.doi.org/10.1016/S0731-7085(00)00569-0)
- Pérez Medina, G., Zambrano, N., Salas Auvert, R., 2010. Effect of weak magnetic fields on bacterium *Staphylococcus aureus*. *REVECITEC URBE* 1, 77–83.
- Perez, V.H., Reyes, A.F., Justo, O.R., Alvarez, D.C., Alegre, R.M., 2007. Bioreactor Coupled with Electromagnetic Field Generator: Effects of Extremely Low Frequency Electromagnetic Fields on Ethanol

- Production by *Saccharomyces cerevisiae*. *Biotechnol. Prog.* 23, 1091–1094. <https://doi.org/10.1021/bp070078k>
- Philip, S., Keshavarz, T., Roy, I., 2007. Polyhydroxyalkanoates: biodegradable polymers with a range of applications. *J. Chem. Technol. Biotechnol.* 82, 233–247.
- Phillips, I., 1999. The use of bacitracin as a growth promoter in animals produces no risk to human health. *J. Antimicrob. Chemother.* 44, 725–728. <https://doi.org/10.1093/jac/44.6.725>
- Piatti, E., Albertini, M.C., Baffone, W., Fraternali, D., Citterio, B., Piacentini, M.P., Dachà, M., Vetrano, F., Accorsi, A., 2002. Antibacterial effect of a magnetic field on *Serratia marcescens* and related virulence to *Hordeum vulgare* and *Rubus fruticosus* callus cells. *Comp. Biochem. Physiol. B Biochem. Mol. Biol.* 132, 359–365. [http://dx.doi.org/10.1016/S1096-4959\(02\)00065-9](http://dx.doi.org/10.1016/S1096-4959(02)00065-9)
- Pillet, F., Formosa-Dague, C., Baaziz, H., Dague, E., Rols, M.-P., 2016a. Cell wall as a target for bacteria inactivation by pulsed electric fields. *Sci. Rep.* 6.
- Pillet, F., Formosa-Dague, C., Baaziz, H., Dague, E., Rols, M.-P., 2016. Cell wall as a target for bacteria inactivation by pulsed electric fields. *Sci. Rep.* 6, Article number: 19778.
- Plastics Europe, 2016. *Plastics - the Facts 2016* [WWW Document]. URL <http://www.plasticseurope.org/Document/plastics---the-facts-2016-15787.aspx?FoIID=2> (accessed 7.8.17).
- Poblete-Castro, I., Becker, J., Dohnt, K., Dos Santos, V.M., Wittmann, C., 2012. Industrial biotechnology of *Pseudomonas putida* and related species. *Appl. Microbiol. Biotechnol.* 93, 2279–2290.
- Potumarthi, R., Ch, S., Jetty, A., 2007. Alkaline protease production by submerged fermentation in stirred tank reactor using *Bacillus licheniformis* NCIM-2042: Effect of aeration and agitation regimes. *Biochem. Eng. J.* 34, 185–192. <http://dx.doi.org/10.1016/j.bej.2006.12.003>
- Priest, F.G., 1993. Systematics and ecology of *Bacillus*, in: *Bacillus Subtilis and Other Gram-Positive Bacteria*. American Society of Microbiology Press, Washington, DC, pp. 3–16.

- Prieto, A., 2016. To be, or not to be biodegradable... that is the question for the bio-based plastics. *Microb. Biotechnol.* 9, 652–657.
- Priya, K., Chadha, A., 2003. Synthesis of hydrocinnamic esters by *Pseudomonas cepacia* lipase. *Enzyme Microb. Technol.* 32, 485–490.
- Raddadi, N., Crotti, E., Rolli, E., Marasco, R., Fava, F., Daffonchio, D., 2012. The most important *Bacillus* species in biotechnology, in: *Bacillus Thuringiensis* Biotechnology. Springer, pp. 329–345.
- Rai, R., 2010. Biosynthesis of Polyhydroxyalkanoates and its Medical Applications (PhD Thesis). University of Westminster, UK.
- Ramon, C., Martin, J., Powell, M., 1987. Low-level, magnetic-field-induced growth modification of *Bacillus subtilis*. *Bioelectromagnetics* 8, 275–282.
- Re, B., Bersani, F., Agostini, C., Mesirca, P., Giorgi, G., 2004. Various effects on transposition activity and survival of *Escherichia coli* cells due to different ELF-MF signals. *Radiat. Environ. Biophys.* 43, 265–270. <https://doi.org/10.1007/s00411-004-0260-9>
- Reddy, C., Ghai, R., Kalia, V., 2003. Polyhydroxyalkanoates: an overview. *Bioresour. Technol.* 87, 137–146.
- Reffatti, P.F., 2012. Physiological response of *Bacillus licheniformis* NCIMB 8874 to oligosaccharide elicitors (PhD Thesis). University of Westminster, London.
- Rehm, B.H.A., 2009. *Pseudomonas* Applications, in: *Encyclopedia of Industrial Biotechnology*. John Wiley & Sons, Inc., pp. 1–15. <https://doi.org/10.1002/9780470054581.eib520>
- Rodriguez Justo, O., Haber Pérez, V., Chacon Alvarez, D., Monte Alegre, R., 2006. Growth of *Escherichia coli* under extremely low-frequency electromagnetic fields. *Appl. Biochem. Biotechnol.* 134, 155–163. <https://doi.org/10.1385/ABAB:134:2:155>
- Rogers, W.J., 2014. *Healthcare Sterilisation: Challenging Practices*. Smithers Information Ltd., Shropshire, UK.
- Ružič, R., Gogala, N., Jerman, I., 1997. Sinusoidal magnetic fields: effects on the growth and ergosterol content in mycorrhizal fungi. *Electro-Magnetobiology* 16, 129–142.

- Saint-Cricq, P., Deshayes, S., Zink, J., Kasko, A., 2015. Magnetic field activated drug delivery using thermodegradable azo-functionalised PEG-coated core-shell mesoporous silica nanoparticles. *Nanoscale* 7, 13168–13172.
- Sangkharak, K., Prasertsan, P., 2013. The production of polyhydroxyalkanoate by *Bacillus licheniformis* using sequential mutagenesis and optimization. *Biotechnol. Bioprocess Eng.* 18, 272–279.
- Schallmeyer, M., Singh, A., Ward, O.P., 2004. Developments in the use of *Bacillus* species for industrial production. *Can. J. Microbiol.* 50, 1–17. <https://doi.org/10.1139/w03-076>
- Schlatmann, J., Nuutila, A., Van Gulik, W., Ten Hoopen, H., Verpoorte, R., J Heijnen, J., 1993. Scaleup of ajmalicine production by plant cell cultures of *Catharanthus roseus*. *Biotechnol. Bioeng.* 41, 253–262.
- Sedletsy, J., 2007. Process Development and Scale-up from Shake Flask to Fermenter of Suspended and Immobilized Aerobic Microorganisms.
- Segatore, B., Setacci, D., Bennato, F., Cardigno, R., Amicosante, G., Iorio, R., 2012. Evaluations of the effects of extremely low-frequency electromagnetic fields on growth and antibiotic susceptibility of *Escherichia coli* and *Pseudomonas aeruginosa*. *Int. J. Microbiol.* 2012.
- Seletzky, J., 2007. Process Development and Scale-up from Shake Flask to Fermenter of Suspended and Immobilized Aerobic Microorganisms (PhD Thesis Biochemical Engineering). RWTH Aachen University, Germany.
- Sen, R., Swaminathan, T., 2004. Response surface modeling and optimization to elucidate and analyze the effects of inoculum age and size on surfactin production. *Biochem. Eng. J.* 21, 141–148. <https://doi.org/10.1016/j.bej.2004.06.006>
- Setchell, C.H., 1985. Magnetic separations in biotechnology—a review. *J. Chem. Technol. Biotechnol.* 35, 175–182.
- Shamala, T., Chandrashekar, A., Vijayendra, S., Kshama, L., 2003. Identification of polyhydroxyalkanoate (PHA)-producing *Bacillus* spp. using the polymerase chain reaction (PCR). *J. Appl. Microbiol.* 94, 369–374.

- Sharaf-Eldin, M., Elkholy, S., Fernández, J.-A., Junge, H., Cheetham, R., Guardiola, J., Weathers, P., 2008. *Bacillus subtilis* FZB24® Affects Flower Quantity and Quality of Saffron (*Crocus sativus*). *Planta Med.* 74, 1316–1320.
- Sharma, S.K., Mudhoo, A., 2011. *A Handbook of Applied Biopolymer Technology: Synthesis, Degradation and Applications*, Green Chemistry Series. Royal Society of Chemistry, Cambridge, UK.
- Silhavy, T.J., 2016. Classic spotlight: Gram-negative bacteria have two membranes. *J. Bacteriol.* 198, 201–201.
- Silva-Queiroz, S.R., Silva, L.F., Pradella, J.G.C., Pereira, E.M., Gomez, J.G.C., 2009. PHA MCL biosynthesis systems in *Pseudomonas aeruginosa* and *Pseudomonas putida* strains show differences on monomer specificities. *J. Biotechnol.* 143, 111–118. <http://dx.doi.org/10.1016/j.jbiotec.2009.06.014>
- Singh, M., Patel, S.K., Kalia, V.C., 2009. *Bacillus subtilis* as potential producer for polyhydroxyalkanoates. *Microb. Cell Factories* 8, 38. <https://doi.org/10.1186/1475-2859-8-38>
- Sivasubramanian, V. (Ed.), 2016. *Environmental Sustainability Using Green Technologies*. CRC Press, USA.
- Sliker, L., Ciuti, G., Rentschler, M., Menciassi, A., 2015. Magnetically driven medical devices: a review. *Expert Rev. Med. Devices* 12, 737–752.
- Souza, P.M. de, 2010. Application of microbial α -amylase in industry-A review. *Braz. J. Microbiol.* 41, 850–861.
- Spiers, A.J., Deeni, Y.Y., Folorunso, A.O., Koza, A., Moshynets, O., Zawadzki, K., 2013. Cellulose expression in *Pseudomonas fluorescens* SBW25 and other environmental pseudomonads. *Cellul.-Med. Pharm. Electron. Appl.* 1–26.
- Stanier, R.Y., Palleroni, N.J., Doudoroff, M., 1966. The aerobic pseudomonads a taxonomic study. *Microbiology* 43, 159–271.
- Steinberger, R., Holden, P., 2005. Extracellular DNA in single-and multiple-species unsaturated biofilms. *Appl. Environ. Microbiol.* 71, 5404–5410.
- Stone, K.J., Strominger, J.L., 1971. Mechanism of Action of Bacitracin: Complexation with Metal Ion and C55-Isoprenyl Pyrophosphate. *Proc. Natl. Acad. Sci.* 68, 3223–3227.

- Strašák, L., Vetterl, V., Šmarda, J., 2002. Effects of low-frequency magnetic fields on bacteria *Escherichia coli*. *Bioelectrochemistry* 55, 161–164. [https://doi.org/10.1016/S1567-5394\(01\)00152-9](https://doi.org/10.1016/S1567-5394(01)00152-9)
- Strasak, L., Vetterl, V., Smarda, J., 1998. The effect of low-frequency electromagnetic fields on living organisms. *Sborník Lékařský* 99, 455.
- Sukan, A., 2015. Dual Biopolymer Production and Separation from Cultures of *Bacillus* spp. (PhD Thesis). University of Westminster, UK.
- Swinnen, I., Bernaerts, K., Dens, E.J., Geeraerd, A.H., Van Impe, J., 2004. Predictive modelling of the microbial lag phase: a review. *Int. J. Food Microbiol.* 94, 137–159.
- Terpe, K., 2006. Overview of bacterial expression systems for heterologous protein production: from molecular and biochemical fundamentals to commercial systems. *Appl. Microbiol. Biotechnol.* 72, 211. <https://doi.org/10.1007/s00253-006-0465-8>
- The International Pharmacopoeia, Sixth Edition, 2016.
- Tokiwa, Y., Jarerat, A., 2003. Microbial degradation of aliphatic polyesters. Presented at the Macromolecular Symposia, Wiley Online Library, pp. 283–290.
- Torres, M.G., Muñoz, S.V., Rosales, S.G.S., Carreón-Castro, M. del P., Muñoz, R.A.E., González, R.O., González, M.R.E., Talavera, R.R., 2015. Radiation-induced graft polymerization of chitosan onto poly(3-hydroxybutyrate). *Carbohydr. Polym.* 133, 482–492. <http://dx.doi.org/10.1016/j.carbpol.2015.07.032>
- Tsuruo, T., Oh-hara, T., Iida, H., Tsukagoshi, S., Sato, Z., Matsuda, I., Iwasaki, S., Okuda, S., Shimizu, F., Sasagawa, K., 1986. Rhizoxin, a macrocyclic lactone antibiotic, as a new antitumor agent against human and murine tumor cells and their vincristine-resistant sublines. *Cancer Res.* 46, 381–385.
- van Dijk, J.M., Hecker, M., 2013. *Bacillus subtilis*: from soil bacterium to super-secreting cell factory. *Microb. Cell Factories* 12, 3–3. <https://doi.org/10.1186/1475-2859-12-3>
- van Heijenoort, J., 2001. Formation of the glycan chains in the synthesis of bacterial peptidoglycan. *Glycobiology* 11, 25R–36R.

- Varsha, Y., Savitha, R., 2011. Overview on polyhydroxyalkanoates: A promising biopol. *J. Microb. Biochem. Technol.* 3, 99–105.
- Velizarov, S., 1999. Electric and magnetic fields in microbial biotechnology: possibilities, limitations, and perspectives. *Electro Magnetobiology* 18, 185–212.
- Visakh, P., 2014. Polyhydroxyalkanoates (PHAs), their Blends, Composites and Nanocomposites: State of the Art, New Challenges and Opportunities, in: *Polyhydroxyalkanoate (PHA) Based Blends, Composites and Nanocomposites*, RCS Green Chemistry. The Royal Society of Chemistry, UK, pp. 1–17.
- Volova, T.G., Zhila, N.O., Kalacheva, G.S., Brigham, C.J., Sinskey, A.J., 2013. Effects of intracellular poly(3-hydroxybutyrate) reserves on physiological–biochemical properties and growth of *Ralstonia eutropha*. *Res. Microbiol.* 164, 164–171. <https://doi.org/10.1016/j.resmic.2012.10.008>
- Wang, X.-H., Diao, M.-H., Yang, Y., Shi, Y.-J., Gao, M.-M., Wang, S.-G., 2012. Enhanced aerobic nitrifying granulation by static magnetic field. *Bioresour. Technol.* 110, 105–110. <https://doi.org/10.1016/j.biortech.2012.01.108>
- Webb, C., Kamat, S.P., 1993. Improving fermentation consistency through better inoculum preparation. *World J. Microbiol. Biotechnol.* 9, 308–312. <https://doi.org/10.1007/BF00383069>
- Weinberg, E., 1967. Bacitracin, in: Gottlieb, D., Shaw, P. (Eds.), *Mechanism of Action, Antibiotics*. Springer Berlin Heidelberg, pp. 90–101.
- Westers, L., Westers, H., Quax, W.J., 2004. *Bacillus subtilis* as cell factory for pharmaceutical proteins: a biotechnological approach to optimize the host organism. *Biochim. Biophys. Acta BBA-Mol. Cell Res.* 1694, 299–310.
- Wiener, M.C., Horanyi, P.S., 2011. How hydrophobic molecules traverse the outer membranes of Gram-negative bacteria. *Proc. Natl. Acad. Sci.* 108, 10929–10930. <https://doi.org/10.1073/pnas.1106927108>
- Wilks, J.C., Kitko, R.D., Cleeton, S.H., Lee, G.E., Ugwu, C.S., Jones, B.D., BonDurant, S.S., Slonczewski, J.L., 2009. Acid and base stress and

- transcriptomic responses in *Bacillus subtilis*. *Appl. Environ. Microbiol.* 75, 981–990.
- Williams, C.D., Markov, M.S., Hardman, W.E., Cameron, I.L., 2001. Therapeutic electromagnetic field effects on angiogenesis and tumor growth. *Anticancer Res* 21, 3887–3892.
- Williams, S.F., Martin, D.P., 2005. Applications of polyhydroxyalkanoates (PHA) in medicine and pharmacy. *Biopolym. Online* 4.
- Williams, S.F., Martin, D.P., Horowitz, D.M., Peoples, O.P., 1999. PHA applications: addressing the price performance issue: I. Tissue engineering. *Int. J. Biol. Macromol.* 25, 111–121.
- Wittekindt, E., Broers, D., Kraepelin, G., Lamprecht, I., 1990. Influence of non-thermic AC magnetic fields on spore germination in a dimorphic fungus. *Radiat. Environ. Biophys.* 29, 143–152.
- Xu, Y., Hou, M., Ruan, J., Qu, M., Sun, H., Xu, J., Zhou, S., 2014. Effect of magnetic field on surface properties of *Bacillus cereus* CrA and its Extracellular Polymeric Substances (EPS). *J. Adhes. Sci. Technol.* 28, 2196–2208.
- Xu, Z., Chen, H., Wu, H., Li, L., 2010. 7mT static magnetic exposure enhanced synthesis of poly-3-hydroxybutyrate by activated sludge at low temperature and high acetate concentration. *Process Saf. Environ. Prot.* 88, 292–296. <http://dx.doi.org/10.1016/j.psep.2010.03.009>
- Yadollahpour, A., Jalilifar, M., Rashidi, S., 2014. Antimicrobial effects of electromagnetic fields: A review of current techniques and mechanisms of action. *J Pure Appl Microbio* 8, 4031–4043.
- Young, F.K., Kastner, J.R., May, S.W., 1994. Microbial production of poly-beta-hydroxybutyric acid from D-xylose and lactose by *Pseudomonas cepacia*. *Appl Env. Microb* 60.
- Young, K.D., 2006. The Selective Value of Bacterial Shape. *Microbiol. Mol. Biol. Rev.* 70, 660–703. <https://doi.org/10.1128/MMBR.00001-06>
- Zhang, W., 2011. *Genomics of Foodborne Bacterial Pathogens*. Springer New York, New york.
- Zinn, M., Witholt, B., Egli, T., 2001. Occurrence, synthesis and medical application of bacterial polyhydroxyalkanoate. *Adv. Drug Deliv. Rev.* 53, 5–21.

Chapter 8

Appendices

8. Appendices

This chapter includes standard curves obtained from experiments carried out in this research, results of a control run (SF or STR) without external circulation into the MFG and one example experiment showing average values with standard deviations (error bars) of biological replicates (control and test, e.g. growth curves).

8.1. Appendix 1

This section includes all calibration and standard curves used in the experiments.

8.1.1. Bacitracin concentration standard curve

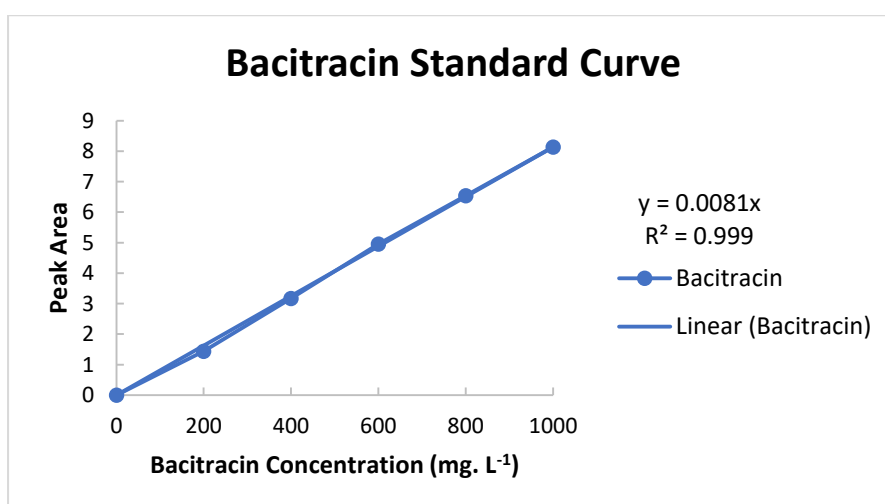


Figure 70. Standard bacitracin concentration against peak area obtained from HPLC used for measurement of bacitracin concentration in *B. licheniformis* experiments

8.1.2. P(3HB) concentration standard curve

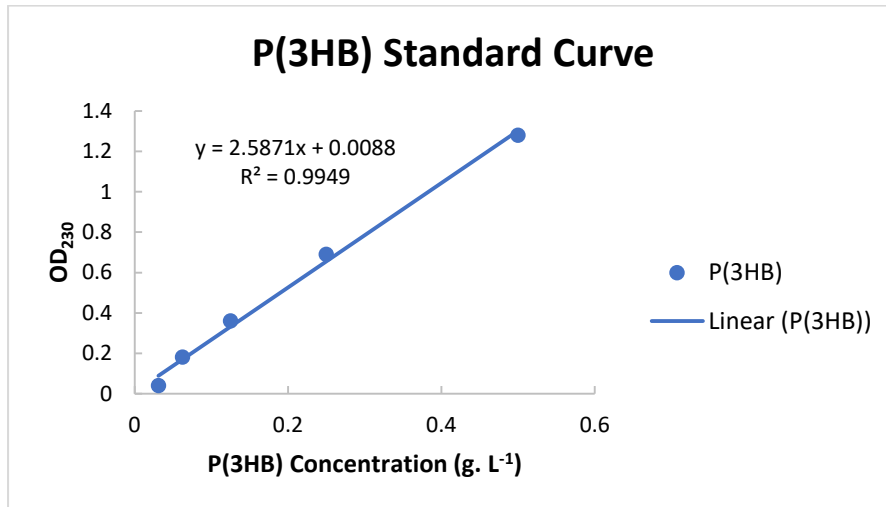


Figure 71. Standard curve obtained from crotonic acid assay on P(3HB) standards

8.1.3. Glutamic acid assay calibration curve

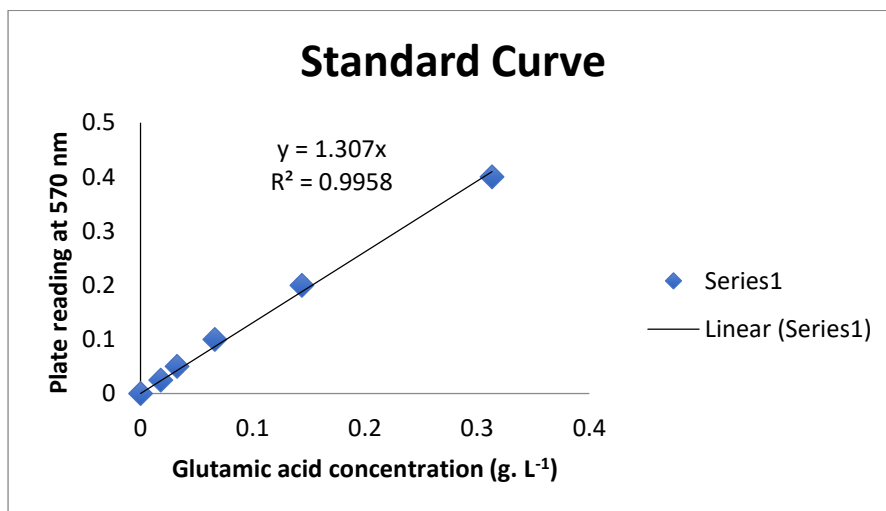


Figure 72. Glutamic acid assay standard curve. The curve was obtained from absorbance reading of assayed glutamic acid standards at 570 nm.

8.1.4. Total carbohydrate concentration calibration curve

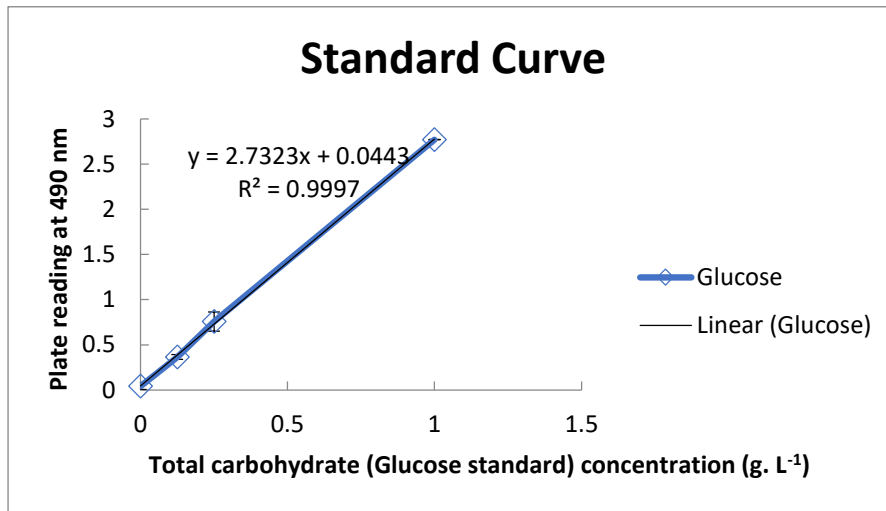


Figure 73. Total carbohydrate assay standard curve. The curve was obtained by reading absorbance of assayed glucose standards at 490 nm

8.1.5. Glucose concentration of glucose assay calibration curve

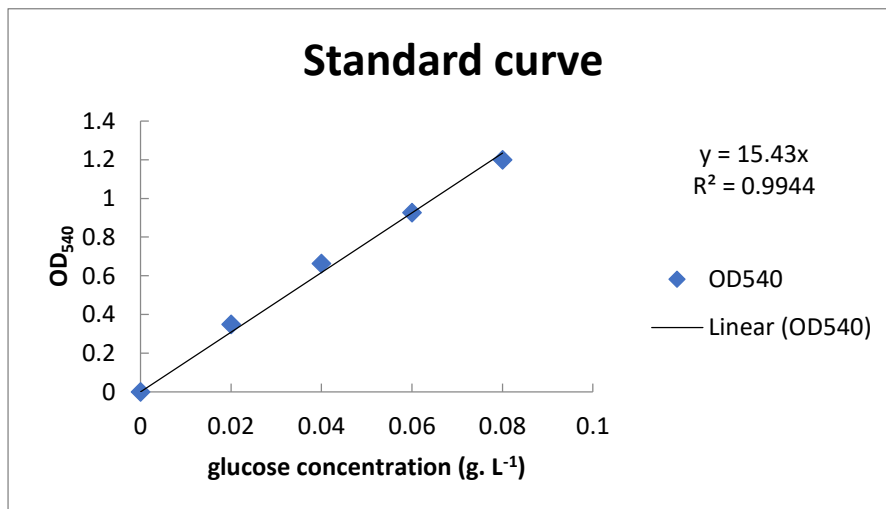


Figure 74. Standard glucose concentration against peak area obtained from HPLC used for measurement of bacitracin concentration in *B. licheniformis* experiments

8.1.6. Flow rate calibration curve of peristaltic pump

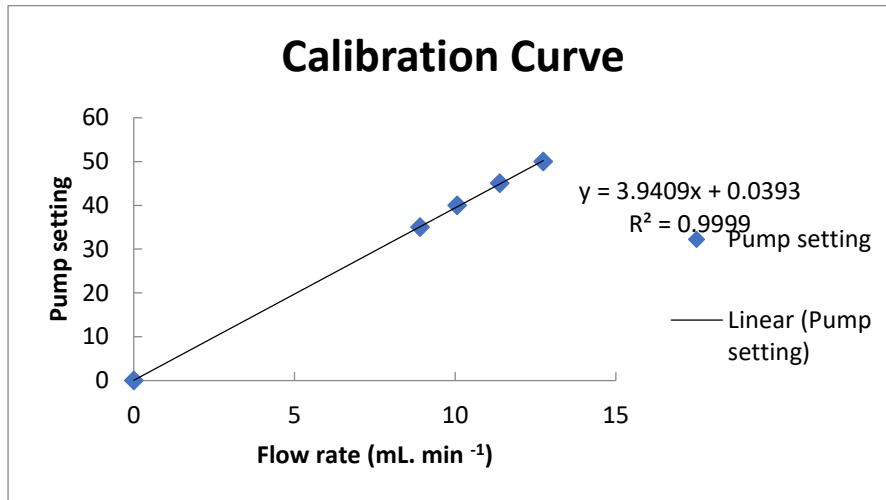


Figure 75. Calibration curve for flow rate of liquid circulation through the MFG

8.2. Appendix 2

This section includes a control run of *B. licheniformis* in STR without external circulation

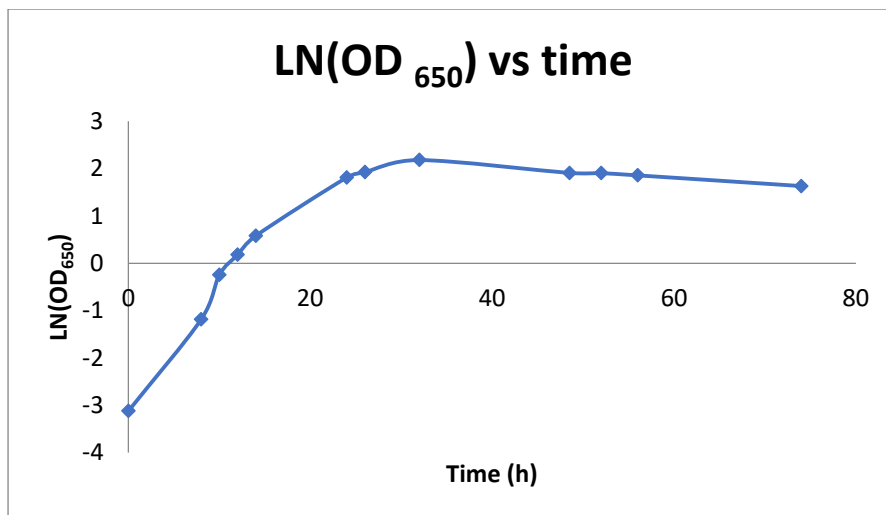


Figure 76. Growth profile of *B. licheniformis* in a 2 L STR without outside circulation

8.3. Appendix 3

This section includes the growth profile of *P. putida* in 2 L STRS as an example experiment showing average values of biological replicates with error bars showing standard deviation of biological replicates in both control and the test runs. The test STRs were exposed to 28 mT magnetic field.

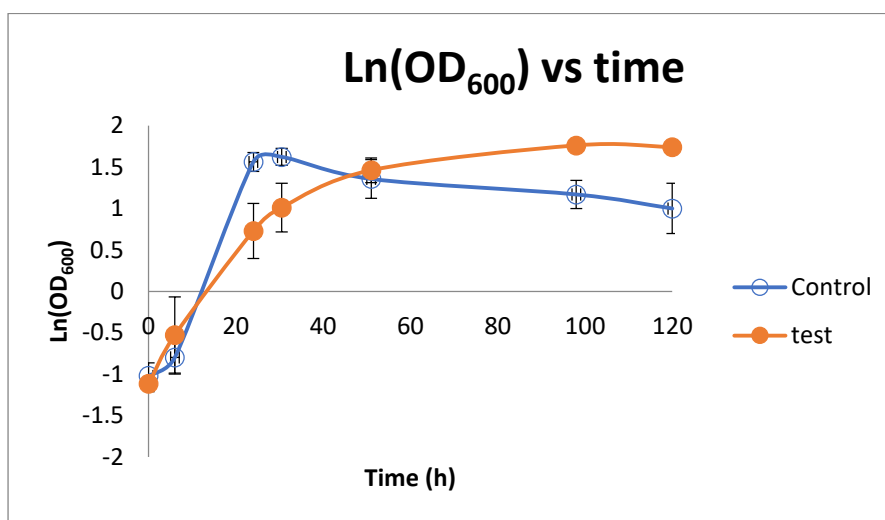


Figure 77. Growth profile of *Pseudomonas putida* 2 L STRs. The control and the test STR under 28 mT magnetic field are shown. Data points are average values of biological replicate runs with error bars showing standard deviations.